

**The effects of copper, manganese and mercury,
alone and in combinations, in an *ex vivo* model of
coagulation**

by

Maxine Janse van Rensburg

11107139

Dissertation submitted in partial fulfilment of the requirements for the
degree of

MASTER OF SCIENCE

in the

FACULTY OF HEALTH SCIENCES

Department of Anatomy

University of Pretoria

2017

Acknowledgments

I would first like to thank my supervisor Dr HM Oberholzer of the department of Anatomy at the University of Pretoria. The door to her office was always open whenever I ran into a problem or if I had any questions about my research or writing. She constantly allowed this paper to be my own work, but steered me in the right direction whenever she thought I needed it.

I would also like to thank my co-supervisor, Prof MJ Bester, also of the department of Anatomy at the University of Pretoria, for her guidance, experience and wisdom. Her profound knowledge helped me with complex problems I faced in my project.

I would also like to acknowledge Dr M van Rooy of the department of Physiology at the University of Pretoria as my co-supervisor of this research project and dissertation. I am gratefully indebted to her for her valuable comments on this dissertation.

I would also like to acknowledge various other individuals for the different roles they played within my research project. I would like to thank Ms C Venter, an Anatomy PhD student who works at the Microscopy and Microanalysis lab at the University of Pretoria for her assistance in the use of the scanning electron microscope and the thromboelastography[®]. I would like to thank Ms June Serum of the department of Anatomy of the University of Pretoria for helping me in the laboratory, answering my questions and also for helping me with my statistics of my results and helping me to understand them better. I would also like to thank my fellow Cell Biology students, Ms R Stanley and Ms B Maseko, for their helping hands in the laboratory. I would also like to thank Dr C Grobbelaar and Dr P Soma of the department of Physiology at the University of Pretoria, with their assistance with the phlebotomy, Prof E Pretorius of the department of Physiology at the University of Stellenbosch for the use of the thromboelastography[®] machine, all the volunteers that generously donated blood required for this study and the National Research Foundation for their financial support.

Finally I must express my very profound gratitude to my parents, Anton and Rosa Janse van Rensburg and to my boyfriend, Ockert Draper, for providing me with unfailing support and continuous encouragement throughout my years of study and through the process of researching and writing this dissertation. This accomplishment would not have been possible without everyone's contributions. A great and sincere thank you goes out to all of you.

**The effects of copper, manganese and mercury,
alone and in combinations, in an *ex vivo* model of
coagulation**

by

MAXINE JANSE VAN RENSBURG

SUPERVISOR: Dr HM Oberholzer

CO-SUPERVISOR: Dr M van Rooy

CO-SUPERVISOR: Prof MJ Bester

DEGREE: MSc in Anatomy with specialisation in Cell Biology

Abstract

Pollution is increasing rapidly due to anthropogenic activities and daily contact with metals is a reality. Metals at certain levels can have a negative effect on the health of an individual and can cause alterations in the coagulation system, which may result in cardiovascular system complications. The aim of this project was to investigate the effects of copper, manganese and mercury, alone and in combinations, using an *ex vivo* model of coagulation by using the haemolysis assay, scanning electron microscopy and thromboelastography[®]. These metals were chosen as there is an increase in exposure to these metals by the general public, but more specifically individuals living in rural areas, of South Africa due to pollution. The concentrations used were based on the World Health Organisation safety limit for each respective metal; e.g. copper X100 indicates the blood is exposed to a copper level that is 100 times greater than that of the safety limit set out for the metal according to the World Health Organisation. This investigation was conducted at the cell biology laboratory and the Unit of Microscopy and Microanalysis at the University of Pretoria.

The various constituents of blood showed different sensitivities to different metal groups. Manganese and mercury showed the highest haemolytic effects at higher concentrations. Synergism was only observed between the double combination groups of manganese and mercury (X100) and manganese and copper (X1000) as well as in the triple combination group (X100). Copper caused haemoglobin precipitation at higher concentrations. At low concentrations copper and copper combinations induced met- and sulfhaemoglobin formation, especially the copper and manganese combination at X10 concentration which increased met- and sulfhaemoglobin by about 5 – 10%. The degree of echinocyte formation was greatest in copper, but the combination of manganese and copper had the greatest impact on erythrocyte morphology. Activation and necrosis of platelets were most evident at the highest mercury concentration. All double metal combinations caused platelet interactions and aggregation. Novel findings indicated that at X1, manganese caused the formation of net-like structures of thin fibres and sticky masses of thick fibres with fused areas. In combination with copper and mercury, a similar effect was observed, however, in the triple combination group a lesser effect was observed. No statistically significant changes were observed in the measured coagulation parameters for thromboelastography[®], however, trends were observed compared to the control. These were a decrease in reaction time, a decrease in kinetics, an increase in angle, an increase in maximum amplitude, an increase in maximum rate of thrombus generation, an increase in thrombus generation and either increased or reduced time to maximum rate of thrombus generation. These trends indicate a

more hypercoagulable state of blood. All the metals, in their own way, had an effect on the coagulation system, resulting in an increase in the likelihood of thrombosis which will contribute to cardiovascular diseases.

Declaration

I, Maxine Janse van Rensburg, hereby declare that this dissertation entitled: “**The effects of copper, manganese and mercury, alone and in combinations, in an ex vivo model of coagulation**”, which I hereby submit for the degree at the University of Pretoria, is my own work and has not previously been submitted by me for a degree at this or any other tertiary institution. I understand what plagiarism is and am aware of the University’s policy in this regard. Where other people’s work has been used (either from a printed source, internet or any other source), this has been properly acknowledged and referenced in accordance with departmental requirements. I have not used work previously produced by another student or any other person to hand in as my own.

Ethics statement: The author, Maxine Janse van Rensburg, has obtained, for the research described in this work, the applicable research ethics approval. The author declares that she has observed the ethical standards required in terms of the University of Pretoria’s Code of ethics for researchers and the Policy guidelines for responsible research.

.....
SIGNATURE

.....
DATE

Department of Anatomy, School of Medicine, Faculty of Health Sciences

University of Pretoria

South Africa

Table of Contents

CHAPTER 1: Introduction	15
CHAPTER 2: Literature Review	16
2.1 Introduction.....	16
2.2 Copper	16
2.2.1 Sources.....	16
2.2.2 Absorption, distribution, metabolism and excretion (ADME)	17
2.2.3 Toxicity.....	19
2.3 Manganese.....	22
2.3.1 Sources.....	22
2.3.2 ADME	23
2.3.3 Toxicity.....	24
2.4 Mercury	25
2.4.1 Sources.....	25
2.4.2 ADME	26
2.4.3 Toxicity.....	26
2.5 Specific metal targets	28
2.5.1 Erythrocytes	28
2.5.2 The coagulation system	29
2.6 Aim.....	31
2.7 Objectives.....	32
2.8 Funding	32
2.9 Ethical considerations.....	32
2.9.1 Volunteer recruitment.....	33
2.10 Study design.....	33
CHAPTER 3: The haemolytic effects of copper, manganese and mercury, alone and in combination	34
3.1 Introduction.....	34
3.2 Materials and methods	35
3.2.1 Metal preparations	35
3.2.2 Blood collection	36
3.2.3 Sample preparation.....	36
3.2.4 Statistical analyses.....	38

3.3 Results	38
Table 3.1: MDR values and the type of interactions between metal combinations.....	40
3.4 Discussion	45
3.4.1 Cu, Mn and Hg alone	46
3.4.2 Cu, Mn and Hg in combination	49
3.5 Conclusion.....	52
CHAPTER 4: The effects of copper, manganese and mercury, alone and in combinations, on erythrocyte, platelet and fibrin network morphology	53
4.1 Introduction.....	53
4.2 Materials and methods	54
4.2.1 Metal preparations	54
4.2.2 Blood collection	54
4.2.3 Sample preparation	54
4.3 Results	55
4.5 Conclusion.....	77
CHAPTER 5: The quantitative effects of copper, manganese and mercury, alone and in combinations, on coagulation parameters.....	78
5.1 Introduction.....	78
5.2 Materials and methods	79
5.2.1 Heavy metal preparations	79
5.2.2 Blood collection	80
5.2.3 Sample preparation	80
5.2.4 Statistical analyses.....	80
5.3 Results	80
5.4 Discussion.....	85
5.5 Conclusion.....	89
CHAPTER 6: Concluding Discussion	90
6.1 Summarised results	90
6.2 Limitations and future prospective	92
CHAPTER 7: References.....	93
Appendix.....	102
Ethical Clearance	103
Participant information leaflet and consent form	104
Declaration of originality	107

List of Figures

Figure 2.1: Copper distribution of a healthy individual.	18
Figure 2.2: Induction of platelet shape change.	27
Figure 2.3: Discocyte, echinocyte and spherocyte shaped erythrocytes.	27
Figure 2.4: The mechanism of the coagulation pathway.	31
Figure 2.5: Flow diagram explaining the methodologies used for the different blood constituents being investigated.	33
Figure 3.1: A comparison of metal-induced haemolysis (%) of erythrocytes.	38
Figure 3.2: The comparison of supernatant colours of varying samples.	41
Figure 3.3: A comparison of the percentage (%) of haemoglobin precipitate formed.	42
Figure 3.4: A comparison of haemoglobin distribution (%) of various forms of haemoglobin within erythrocytes.	43
Figure 3.5: A comparison of the fold change of MetHb and SulfHb.	45
Figure 4.1: Scanning electron micrographs of whole blood without thrombin showing erythrocyte morphology.	58
Figure 4.2: Scanning electron micrographs of whole blood without thrombin showing platelet morphology.	64
Figure 4.3: Scanning electron micrographs of whole blood with thrombin showing fibrin network formation together with erythrocytes.	71
Figure 5.1: The graphical waveform representation of a normal signature TEG [®] tracing.	79
Figure 5.2: The graphical waveform representation of TEG [®] tracings and V-curves.	82

List of Tables

Table 2.1: Erythrocyte processes observed in an acute Cu sulphate poisoning case.	20
Table 2.2: The absorption, distribution and excretion of the different forms of Hg.	26
Table 2.3: Safety limits of the singular metals under investigation.	28
Table 3.1: The MDR values and the interaction type between the metal combinations.	40
Table 4.1: A summary of the changes observed in erythrocyte morphology of the different exposed groups.	56
Table 4.2: A summary of the changes observed in platelet morphology of the different exposed groups.	62
Table 4.3: A summary of the changes observed in whole blood with added thrombin in the different experimental groups.	69
Table 5.1: Description of the various whole blood parameters measured by the TEG [®]	79
Table 5.2: Summary of the effects of Cu, Mn and Hg, alone and in combinations, at the X1 concentration.	83
Table 5.3: Summary of the effects of Cu, Mn and Hg, alone and in combinations, at the X10 concentration.	84
Table 5.4: Data representing the changes of the various parameters measured of the metal exposed whole blood, as compared to the control.	85

List of Abbreviations, Symbols and Chemical Formulas

°C	Degrees Celsius
%	Percentage
α	Alpha
A	Absorbance
ADME	Absorption, distribution, metabolism and excretion
ASGM	Artisanal and small-scale gold mining
ATOX1	Antioxidant 1 (copper chaperone)
ATP	Adenosine triphosphate
Ca²⁺	Calcium (II) ion
cAMP	Cyclic adenosine monophosphate
CMT1	Copper membrane transporter 1
CO₂	Carbon dioxide
Cu	Copper
CuSO₄	Copper (II) sulphate
CuSO₄.5H₂O	Copper sulphate pentahydrate
CVD	Cardiovascular disease
CVS	Cardiovascular system
deoxyHb	Deoxygenated haemoglobin
dH₂O	Distilled water
DNA	Deoxyribonucleic acid
e.g.	Example
EtOH	Ethanol
Ev	Effect value
EVAC	Vacuum extraction
FA	Formaldehyde
Fe	Iron
Fe²⁺	Ferrous iron
Fe³⁺	Ferric iron
Fp	Fibrinopeptides
g	G-force

G-6-PD	Glucose-6-phosphate dehydrogenase
GA	Glutaraldehyde
GIT	Gastrointestinal tract
GR	Glutathione reductase
GSH	Glutathione
H₂O₂	Hydrogen peroxide
Hb	Haemoglobin
Hg	Mercury
HgCl₂	Mercuric chloride
HMDS	Hexamethyldisilazane
i.e.	That is
iso	Isotonic
K	Kinetics (clotting time)
K⁺	Potassium ion
KCl	Potassium chloride
kg	Kilogram
L	Litre
LDL	Low density lipoprotein
MA	Maximum amplitude
MetHb	Methaemoglobin
mg	Milligram
min	Minute(s)
mL	Millilitre
mM	Millimolar
M	Molar
Mn	Manganese
MnCl₂	Manganese (II) chloride
MRTG	Maximum rate of thrombus generation
Na⁺	Sodium
Na₂HPO₄	Disodium phosphate
NAC	N-Acetylcysteine
NaCl	Sodium chloride

NADPH	Nicotinamide adenine dinucleotide phosphate
NADH	Nicotinamide adenine dinucleotide
NaH₂PO₄	Monosodium phosphate
NC	Negative control
nm	Nanometer
NRF	National Research Foundation
O₂	Oxygen
OCS	Open canalicular system
OH	Hydroxide
OH•	Hydroxyl radical
Ov	Observed value
oxyHb	Oxygenated haemoglobin
PAI-1	Plasminogen activator inhibitor type 1
PBS	Phosphate buffered saline
PC	Positive control
ppm	Parts per million
PS	Phosphatidylserine
R	Reaction time
RCF	Relative centrifugal force
ROS	Reactive oxygen species
rpm	Revolutions per minute
RT-PCR	Reverse transcription-polymerase chain reaction
SDS	Sodium dodecyl sulphate
SEM	Scanning electron microscopy / microscope
SulfHb	Sulfhaemoglobin
TEG[®]	Thromboelastography [®]
TF	Tissue factor
TFPI	Tissue factor pathway inhibitor
TMRTG	Time to max rate of thrombus generation
t-PA	Tissue-type plasminogen activator
TTG	Final clot strength
µg	Microgram

μL	Microlitre
μm	Micrometre
μM	Micromolar
u-PA	Urokinase-type plasminogen activator
V-curve	Thrombus velocity curve
v/v	volume over volume
WHO	World Health Organisation

CHAPTER 1: Introduction

According to the Water for Growth and Development in South Africa document version 6, much of the water supplied to the mining sector is from the Vaal River System and water is supplied to the coal fields and gold, iron (Fe), manganese (Mn) and diamond mines as well as to the industry [1]. Although the quality of the water effluent from these activities is tightly regulated, water becomes contaminated with toxins including metals. Rural settlements often do not have access to clean water and use river water for drinking, washing and agricultural purposes, such as subsistence farming. If water sources are contaminated with metals, these communities are the most exposed and vulnerable to health complications.

South Africa's largest power source, coal mining, and other anthropogenic activities used in industries and manufacturing results in an increase of copper (Cu), Mn and mercury (Hg) in the water, atmosphere, and soil. Individuals mainly affected are industrial workers, but the general population is also at risk. Although a lot is known about the toxicity of Hg, essential metals such as Cu and Mn also pose a potential health risk, at certain concentrations. These metals can also accumulate within the body and possibly only manifest their toxic effects during later onset of life. These metals can act as catalysts resulting in the formation of reactive oxygen species (ROS), inhibiting enzyme activity or depleting essential biomolecules. In the environment exposure is usually not to a single metal but rather to mixtures of metals. In addition the concentration of each metal and the duration of exposure can vary and certain cells, tissues and organs are more susceptible to the toxic effects of these metals.

Environmental-based studies measure metal levels in the blood but little is known on how these metals affect the blood vascular system such as erythrocyte and leukocyte functioning, clotting and endothelial structure and integrity. Some metals are associated with the development of thrombo-embolic stroke, anaemia, hypertension, myocardial infarction and thrombo-emboli [2 – 4]. Central to most of these conditions is the disruption of haemostasis and the associated development of thrombosis. As in South Africa the incidence of these diseases are increasing worldwide [5].

The aim of this study was to investigate the effect of Cu, Mn and Hg alone and in combination on components of the coagulation system using an *ex vivo* blood model. In the following literature review (chapter 2) the sources and known cellular target effects of Cu, Mn and Hg with specific focus on the effect of these metals on the coagulation pathway will be reviewed.

CHAPTER 2: Literature Review

2.1 Introduction

In Africa, over the last decade there has been a large increase in pollution due to an increase in industrial activities and urbanisation. These anthropogenic sources can be divided into primary sources and secondary sources. A primary anthropogenic source is of geological origin, which becomes released into the environment as either an unintentional by-product or an intentional by-product e.g. coal and oil combustion. A secondary anthropogenic source is a source that intentionally uses the metal in some process e.g. during the extraction of ore [6].

Increased anthropogenic activities, such as mining and manufacturing, have led to an increase in the release of various wastes (solid, liquid or gaseous state), including metals, into the environment [7]. South Africa is in the top five largest coal producers in the world and approximately 90% of electricity demands are met by coal-burning power plants as it is an inexpensive form of energy [8, 9]. Coal contains a number of elements, some of which can cause health and environmental problems, such as: Cu, Mn and Hg. Copper and Hg coal levels (mean: Cu 13 parts per million (ppm) and Hg 0.22 ppm) of South African coal are lower than the world average whilst Mn is higher (mean: Mn 106 ppm) [10]. Scientific studies usually involve the measurement of blood levels of these metals or investigate the effects of individual metals or occasionally two metal combinations in animal or cell models [11 - 15, 16 - 19]. Very few studies investigate the effects of these metals as part of mixtures [7].

As in the rest of the world cardiovascular disease (CVD) in Africa is increasing and includes conditions such as myocardial infarction, stroke and venous thrombo-emboli. Central to disease development are changes in blood haemostasis [4, 5]. Metal pollutants such as Cu, Mn and Hg, alone and in combinations, may induce erythrocyte damage, alter coagulant factor activation and increase platelet aggregation, thereby increasing the risk of thrombosis [2].

2.2 Copper

2.2.1 Sources

Copper is a naturally occurring transition metal and is an essential nutrient needed in trace amounts by humans and animals [20 – 22]. Essential metals play important roles within biological processes and are required to maintain life. Levels of Cu are controlled and

regulated through absorption, storage and excretion within certain limits by metal ion transporters [23]. In a healthy 70 kg human Cu stores can reach 110 mg although Cu storage is dependent on several factors such as genetics, age, gender and environmental distribution [21, 22]. Copper is essential due to its ability to alter between oxidation states, cycling between Cu^+ [Cu (I)] and Cu^{2+} [Cu (II)] ions, referred to as cuprous and cupric ions respectively, and playing a role as an electron donor or recipient [20]. Both forms of Cu are found in the human body although the second oxidation form is the predominant form [22, 23]. Copper has a low redox potential (easily interchange between states) and acts mainly as a catalytic co-factor in enzymes that perform redox reactions, e.g. in the family of proteins known as ceruloplasmin – various types with different functioning [20, 23]. Ceruloplasmin contains approximately 95% of Cu found in serum [23]. Copper also plays a role in haemoglobin (Hb) production, as an electron transporter and is a strong antioxidant within the oxidant defence system [20, 21, 23].

Humans' Cu requirements are approximately 1 mg of Cu per day. Although an essential nutrient, it is a contaminant of water and at high concentrations is toxic. Copper is used in the manufacture of plumbing pipes, valves and fittings and can also be found in metal alloys and coatings. Copper sulphate pentahydrate ($\text{CuSO}_4 \cdot 5\text{H}_2\text{O}$) is also used as an algacide for surface water [24]. The main sources of Cu are through water and diet. The World Health Organisation (WHO) guideline for Cu in water is 2 mg/L but in drinking water it can range from 0.005 to 30 mg/L due to corrosion of plumbing pipes [21, 24]. The limit that is associated with adverse effects is 430 – 860 $\mu\text{g}/\text{kg}/\text{day}$ for an average 70 kg human [20]. Dietary Cu is absorbed through the gastrointestinal tract (GIT) especially the small intestine, transported via blood and stored by hepatocytes [21, 23]. Copper is transported in the blood by albumin, transcuprein and ceruloplasmin to peripheral tissues [21].

2.2.2 Absorption, distribution, metabolism and excretion (ADME)

2.2.2.1 Absorption

On average the human GIT can absorb between 30 – 40% of the total Cu that is consumed through Cu-containing foods and water. Copper plasma concentrations could be higher in older individuals due to a decrease in the functioning of mechanisms that keep Cu at acceptable homeostatic levels. Copper concentrations within blood may also be higher in females, due to physiological differences. Supplements containing minerals, such as zinc and Fe, may reduce Cu absorption, whilst Cu absorption can be increased by a diet high in fibre, proteins and soluble carbohydrates. Although consumed vegetables have a higher Cu percentage the GIT absorbs Cu more efficiently from proteins in meat, especially cooked meat [25]. Copper is absorbed differently in different species, but in mammals it is

predominantly absorbed through the stomach and small intestine. In humans maximal absorption of Cu is believed to occur in the stomach and upper small intestine. Absorption can range between 15 – 97% depending on how much Cu and the type of Cu present in the diet. Studies have shown that with an increase in Cu intake, there is a decrease in the absorption. The enzymes that are responsible for this process are the metallothioneins, which become activated and bind to metals (cadmium, zinc and Cu) to ensure homeostasis. Metallothionein will bind to Cu ions at their absorption site and remove them from enterocytes, when present in excess [26].

2.2.2.2 Distribution

The dietary Cu that is absorbed is then added to the pre-existing Cu stores within the body (4 – 5 mg). Most of the Cu returns to the circulation and the liver. Lower amounts of Cu are then distributed to the heart, muscles and brain. The Cu that is absorbed is transported via protein carriers, ceruloplasmin, albumin and transcuprein [27]. Firstly Cu is distributed from the GIT to the liver and kidneys, mainly by albumin, and then is transported from the liver to other organs and tissues [27, 28]. Ceruloplasmin plays the most important role in transportation of Cu from the liver to other organs and is also thought to help with transportation of Cu amongst bodily fluids such as: the fluid surrounding the brain and entire nervous system, bile and amniotic fluid. Figure 2.1 shows the distribution and amounts (mg) of Cu found within various organ systems [27].

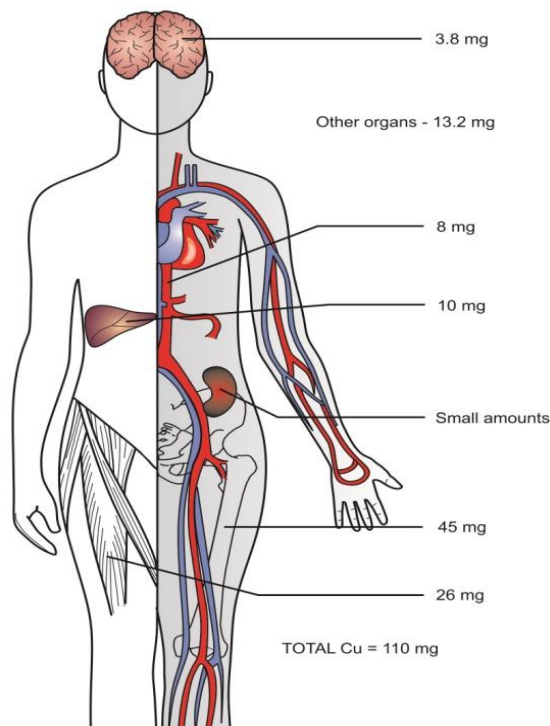


Figure 2.1: Copper distribution of a healthy individual. Image adapted from [27].

2.2.2.3 Metabolism

Not only does absorption of Cu require a balance between Cu and other minerals, e.g. Mn, zinc and Fe, but metabolism of Cu is also dependant on this homeostasis. Metabolism of Cu includes all reactions that occur within living cells, from absorption to excretion. Cellular metabolism of Cu is highly regulated. The Cu membrane transporter 1 (CMT1) of the small intestine transports the Cu inside the cells, where Cu becomes bound to metallothionein and some is carried by a chaperone protein for the enzymes adenosine triphosphate (ATP) 7A and ATP7B, known as the antioxidant 1 (ATOX1) copper chaperone protein. With a rise in Cu concentrations, ATP7A releases Cu into the portal vein to be transported to the liver. The transporter protein CMT1 allows Cu to be transported into the hepatocytes of the liver, where metallothioneins and ATOX1 bind to Cu [28].

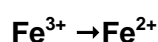
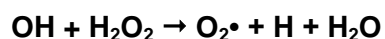
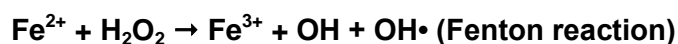
2.2.2.4 Excretion

Metallothioneins are thought to play a role in the main excretion of Cu, via bile [29]. Cells can also remove excess Cu via the ATPase's. The enzyme ATP7B binds Cu to ceruloplasmin to be released into the bloodstream. Mutations in the transport enzymes cause diseases linked with Cu toxicity, namely Wilson's disease (ATP7B mutation) and Menke's disease (ATP7A mutation). Metalloenzymes require Cu as an electron donor/acceptor and when Cu is in excess, the redox cycling of Cu can result in the formation of hydroxyl radical ($\text{OH}\cdot$) damage (see reaction below) to macromolecules such as protein and deoxyribonucleic acids (DNA) and this can result in cellular and tissue damage. Excretion of Cu is slow at a rate of 3.3% per day, thus excessive dosages are easily achieved through a high Cu-containing diet and environmental exposure [28].

2.2.3 Toxicity

Wilson's disease is an autosomal recessive disorder associated with a mutation of the ATP7B gene. The ATP7B mutation alters the structure of the Cu transporting ATPase 2 enzyme, reducing its capacity to bind Cu. This results in a Cu overload and Cu toxicity. Ceruloplasmins are Cu oxidases that also utilises Cu in oxidative reactions. Copper overload can result in cell death due to ROS formation. Copper acts as a catalyst in the Fenton and Haber-Weiss reactions. Cupric Cu-bound to ceruloplasmin oxidises ferrous iron (Fe^{2+}) to ferric iron (Fe^{3+}) with the formation of cuprous Cu [22]. Intracellular effects are due to cuprous ion and membrane transport effects are due to cupric ion. Cupric ions are found on the membrane surface where sulphhydryl groups act as the reducing agent [23].

The Fenton and Haber-Weiss reactions work together to form radical species. The Fenton reaction is a process whereby hydrogen peroxide (H₂O₂), a by-product of aerobic respiration, oxidises Fe²⁺ to Fe³⁺ and this in turn produces hydroxide (OH) and a OH• [30]. The OH• then interacts with H₂O₂ and a superoxide ion (O₂•). The O₂• then reacts again with H₂O₂ and forms OH and a OH•, in the Haber-Weiss reaction. Superoxide ion also reduces Fe³⁺ back to Fe²⁺ [31]. The nett reaction is as follows:

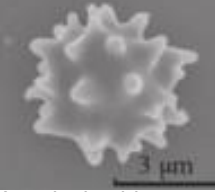


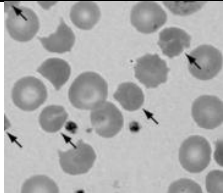
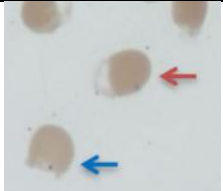
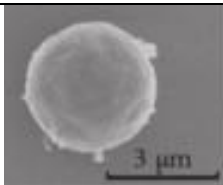
Copper also has the potential to cause damaging free radicals through the Fenton-like reaction, whereby cuprous Cu is oxidised to cupric Cu in the presence of H₂O₂. However, instead of a OH• being formed, a higher state of Cu is formed – Cu³⁺. This form of Cu reacts slower than the OH•, but is a very strong oxidant [32].

Ceruloplasmin (ferroxidase I and II) oxidises Fe³⁺ for the use in erythrocytes (Fe metabolism and formation of erythrocytes) [22]. Hypercupremia is associated with severe anaemia, haemochromatosis and myocardial infarction. There are contradictory results regarding Cu and CVD, however, some researchers have shown an increase in Cu to be correlated with an increase in atherosclerosis. High serum Cu levels are associated with an increased risk in CVD, but the exact mechanisms or causative effects are unknown [22]. Copper plays a role in the development of atherosclerosis as the unbound Cu and Cu ions have been shown to cause *in vitro* low density lipoprotein (LDL) oxidation, which is associated with atherosclerotic plaque formation [22, 23].

These biochemical events lead to changes in erythrocyte functioning and morphology as shown in Table 2.1. Little is known regarding the effect of Cu on other processes such as platelet aggregation and clot formation.

Table 2.1: Erythrocyte morphology in a case of acute copper (II) sulphate poisoning.

PROCESS	MORPHOLOGY
Echinocytosis: An echinocyte is an erythrocyte that has induced outward spikes [33].	 <p>A typical echinocyte [34].</p>

<p>Pyknocytosis: A pyknoocyte is an irregularly distorted, dense and contracted erythrocyte [35].</p>	 <p>Pyknoocytes (arrows) [35].</p>
<p>Blister and bite/degmacyte erythrocytes [36 – 38].</p>	 <p>Blister (red arrow) and bite erythrocyte (blue arrow) [36].</p>
<p>Microspherocytosis: Spherical erythrocytes with smaller diameter [34, 39].</p>	 <p>A typical spherocyte [34].</p>
<p>Hb precipitation [39].</p>	<p>N/A</p>
<p>Haemoglobinaemia: Loss of Hb [39].</p>	<p>N/A</p>
<p>Methaemoglobinaemia: A conversion of Hb to methaemoglobin (MetHb) through oxidation due to oxidative stress, which is unable to carry oxygen [39].</p>	<p>N/A</p>

Copper²⁺ in copper sulphate (CuSO₄) is a potent oxidant that inhibits the pentose phosphate pathway through inhibition of glucose-6-phosphate dehydrogenase (G-6-PD). This results in a lack of energy being provided to erythrocytes and thus the sodium-potassium (Na⁺-K⁺) ATPase pump becomes inhibited resulting in an increase in cell membrane permeability. Copper sulphate also indirectly inhibits glutathione reductase (GR), an antioxidant enzyme that protects erythrocytes against oxidative damage by causing a decrease in nicotinamide adenine dinucleotide phosphate (NADPH) production by G-6-PD. Inhibition of GR causes accumulation of ROS and an increase is associated with oxidative damage to erythrocytes [39 – 41]. Copper can trigger the sphingomyelinase enzyme, which results in the production of ceramide. Ceramide triggers the process of eryptosis and erythrocytes are positive for the presence of phosphatidylserine (PS), an indicator of eryptosis – a form of apoptosis for erythrocytes or more specifically the removal of damaged erythrocytes [42 – 44].

Copper toxicity results in free ionic Cu, which via the Fenton reaction results in the OH• formation which causes oxidative damage and the displacement of other essential metals

from metalloenzymes. Oxidative damage has an adverse effect on erythrocyte function and causes LDL oxidation contributing to atherosclerotic plaque formation [22, 23, 31, 32]. The effect of Cu on the coagulation system is unknown.

2.3 Manganese

2.3.1 Sources

Manganese is an abundant earth element that is categorised as a transition metal. Manganese has various valence states but the most common species of Mn are Mn^{2+} , which is mainly bound to albumin and Mn^{3+} , which is the more reactive and toxic species is bound to transferrin [45, 46]. The Mn^{2+} form is the dominant ion that exists within organ systems of humans [45]. Manganese is an essential trace element for human health and is a co-factor and regulator of many enzymes necessary for gluconeogenesis, maintenance of nerve and immune cell function and regulation of vitamins [45, 46]. A deficiency is rare but can result in bone deformation and remodelling while high Mn levels are toxic [46].

Environmental sources of Mn include eroded rock, soil and decomposing plants. Anthropogenic activities have increased environmental levels of Mn [45]. Ground water generally has the highest amount of Mn while surface water near mines also have high Mn levels. The main route for Mn exposure is through dietary ingestion whilst inhalation is the second most common route of exposure, although the latter is the main route of occupational exposure. Daily intake of a typical Western diet has approximately 2.3 – 8.8 mg of Mn, but these levels can be higher due to environmental contamination. Water can easily be contaminated and levels can exceed the WHO limit of 500 $\mu\text{g/L}$. In developing countries high water Mn levels is common [45]. Occupational exposure can occur in Mn dioxide mines and in smelting, welding and battery manufacturing industries [46]. Occupational workers are the main population exposed to Mn and recent studies have shown that even Mn levels, lower than occupational standards have damaging health effects [45]. Although there has been an increase in awareness of occupational Mn poisoning, over-exposure to airborne Mn still occurs. Blood Mn concentrations of exposed workers can range between 3 – 36 $\mu\text{g/L}$ as compared to 0.5 – 1.2 $\mu\text{g/L}$ in healthy subjects [46].

2.3.2 ADME

2.3.2.1 Absorption

Occupational exposure to Mn is mainly through inhalation. Exposure of the general population to Mn is via contaminated food and water and inhalation of polluted air [46]. Little is known about the exact mechanisms of Mn absorption, however dietary Mn is absorbed by the small intestine and by the lungs from polluted air [45, 47]. Various studies, have reported that human dietary absorption of Mn is approximately 5%. To determine the factors which may affect Mn absorption, clinical as well as animal and cell studies have been undertaken [48]. Identified factors include, the amount of other minerals such as Fe, calcium and phosphorous present in the food source, Mn levels in the dietary food source, consumption of animal protein, certain types of carbohydrates as well as the presence of phytate. High dietary Fe and phytate has been shown to decrease the amount of Mn absorbed [47, 48]. Manganese levels in tea may be high but as this Mn is not bio-available, compared to the bio-availability of Mn in meat it does not have any toxic effects [47].

2.3.2.2 Distribution

Once Mn enters the bloodstream, from either the small intestines or lungs, it is quickly distributed and mainly accumulates within tissues throughout the body [45 – 47]. The total Mn content of the average man (70 kg) is 15 mg [47]. The highest Mn concentrations are found in the thyroid, pituitary and adrenal glands, pancreas, kidneys, brain, liver and bone. The main sites of accumulation are the brain, kidney and bone [45, 47]. The elimination half-life of Mn from the blood is about two hours, while for the entire human body it can be up to 74 days. Due to bio-accumulation in the body, blood levels do not provide an accurate measure of Mn levels. Manganese can cross the blood-brain barrier and accumulate within the brain, thus its toxicity has been implicated in degenerative neurological disorders [46].

2.3.2.3 Excretion

The liver regulates Mn through the biliary system via excretion of bile, thus the main excretion route is through faecal hepatobiliary excretion [45, 47]. If the primary excretory route is blocked or overloaded, Mn can also be excreted through the ductal system of the pancreas [47]. Urinary excretion, sweat and milk excretion is low. Excretion of Mn-containing molecules such as protein occurs via a different route than that identified for ionic Mn [45].

2.3.3 Toxicity

Factors that contribute to Mn toxicity are age, sex, race, route of exposure, genetic factors and pre-existing medical conditions. Younger animals and humans have a greater degree of intestinal absorption and have a lesser biliary excretion capability. Generally, Mn levels in women are higher than men. Metabolic differences due to genetic polymorphisms can also play a role in Mn metabolism. Pre-existing medical conditions can make individuals more susceptible to the effects of Mn exposure. Occupational exposure is an acute form of exposure whilst environmental exposure of the general population is a chronic form of exposure, which can extend over many years [45].

Blood and urine Mn levels are used to monitor exposure. Whole blood is the most commonly used in human and animal studies. However, using blood as a biomarker yields results with wide ranges and large variations among individuals and this may be due to identified factors that affect Mn absorption and distribution [45].

Manganese toxicity mainly affects the nervous system, but other organ systems are also affected. In animal studies, Mn overexposure has toxic effects on the CVS. Manganese was found to inhibit the Ca^{2+} channels resulting in damage to heart muscle [46]. Few studies have investigated the effects of Mn on the human CVS, but clinical studies have shown that Mn exposure causes an increase in heart rate as well as hypotension, due to vasodilation of occupationally exposed workers. The exact mechanism of cardiac dysfunction by Mn is unknown. In cells the distribution of Mn is mainly to the nucleus and then the cytoplasm, followed by the mitochondria. Erythrocytes do not have nuclei or mitochondria, so Mn would accumulate in the cytoplasm after intracellular distribution by transferrin and a divalent metal transporter. In a rat study, blood Mn levels eventually reached a steady-state concentration. Normal human blood Mn levels range between 4 and 15 $\mu\text{g/L}$ [45].

Only 3 – 4% of Mn is absorbed through dietary intake. Manganese absorption is not well regulated and is independent of its concentration within the human body. Manganese deficiency results in depressed vitamin K-dependant clotting factors and therefore is a modulator of vascular biochemical processes. An imbalance in these processes can play a role in the pathophysiology of vascular diseases due to altered blood clotting, platelet aggregation and vessel permeability, associated with CVD. This effect of Mn is possibly due to its effect on the enzymes of the coagulation cascade [49]. Manganese is known to increase levels of plasminogen activator inhibitor type-1 (PAI-1), thus reducing fibrinolysis and also increases tissue factor (TF)-induced coagulation. Manganese also decreases Fe absorption, which can result in anaemia and a low platelet count [50 – 53]. Little is known

regarding the direct effects of Mn on erythrocyte membranes, platelet aggregation and clot formation.

2.4 Mercury

2.4.1 Sources

Mercury is a widespread environmental and industrial pollutant [54]. It is typically present in the earth's crust, sea and fresh water and in the air [55]. It has a high toxicity and it can bioaccumulate within the environment making exposure to dangerous Hg levels a prevalent health and environmental concern [6, 8]. The increase in Hg is mainly due to an increase in anthropogenic activities [8]. The primary anthropogenic sources for Hg include Hg mining, coal and oil combustion, steel, cement and non-ferrous metals production. Secondary anthropogenic sources for Hg include industrial processes, including artisanal and small-scale gold mining (ASGM) [6]. The ASGM mainly occurs in African, Asian and South American countries and it accounts for 20 – 30% of the world's gold production. South Africa has been identified as the second highest Hg emitting country, primarily through coal combustion for power and heat and secondly through ASGM for gold production [6]. Other anthropogenic sources include municipal incinerators, and chemical industries [54]. Mercury is the most dangerous of all the heavy metals and can modify the distribution and retention of other heavy metals. Mercury has no known physiological role in human metabolism and as it is not readily excreted, it accumulates in the human body [55].

Mercury exists in three basic forms namely elemental, inorganic and organic. Dental amalgams are the most common source for elemental Hg vapours. Inorganic Hg, a divalent compound, is the toxic species found in human tissue after the conversion from other forms. Organic Hg in the form of methyl and ethyl Hg is primarily from fish, sea mammals, and thimerosal vaccines [55]. Mercuric chloride (HgCl_2) was one of the first mercuric compounds to be used in drug preservation and in cosmetics, but due to its toxic effects it is no longer used [56]. Some uses of Hg include manufacturing of electrical equipment, scientific instruments, chemicals, explosives and the electrolytic production of chlorine and alkali. Exposure to Hg may primarily be through ingestion and/or inhalation [56].

Dental amalgams use to be the primary cause of Hg exposure but exposure through fish is increasing [55]. It is known that fatty fish, due to its high omega-3 fatty acids, reduces the risk for CVD. However, in some countries it has been noted that CVD is increasing where there is an increase in fish consumption and this is possibly due to increased Hg levels. Methyl Hg rapidly accumulates in fish and attains its highest concentration in the larger fish [54]. Selenium and fish containing omega-3 fatty acids antagonize Hg toxicity, but Hg

diminishes the protective effect of fish and omega fatty acids [55]. People living near gold mines can also be exposed to Hg [54]. It is harmless in the insoluble form, but the vapour or soluble form such as inorganic or methyl Hg can be extremely toxic. Inhaled Hg rapidly accumulates in erythrocytes and undergoes oxidation to mercuric ions by catalase. Orally absorbed methyl Hg is preferentially distributed to erythrocytes and slowly turns into mercuric ions through demethylation [54]. Measurement of Hg levels provide an accurate indication of Hg exposure as methyl Hg and elemental Hg is converted to mercuric ions in the body [54].

2.4.2 ADME

The absorption, distribution and excretion of the different forms of Hg are summarised in Table 2.2 below.

Table 2.2: The absorption, distribution and excretion of the different Hg forms [58, 59].

ABSORPTION		
Elemental Hg	Inorganic Hg	Methyl Hg
GIT: Poor absorption (0.01%) unless GIT is defective, which can increase the bio-availability. Dermal: Limited. Lungs: Main absorption (80%) via inhalation.	GIT: About 7 – 15%. Skin: Possible via the sweat and sebaceous glands and hair follicles.	GIT: About 95% via foodstuffs.
DISTRIBUTION		
Elemental Hg	Inorganic Hg	Methyl Hg
Blood: Rapid diffusion. Brain: Main site as well as the central nervous system. Kidneys: Found after some time following exposure.	Kidneys: Main target organ.	Liver: Site of accumulation. Small portion is converted to inorganic Hg.
EXCRETION		
Elemental Hg	Inorganic Hg	Methyl Hg
Urine and faeces: Main excretion route. Dose-dependent and bi-phasic. Half-life is approximately 30 to 60 days.	Urine and faeces: Main excretion route. Dose-dependent and bi-phasic. Half-life is approximately 60 days.	Bile: Main excretion route and is reabsorbed by the GIT and returns to the liver via the portal circulation.

2.4.3 Toxicity

Mercury binds to metallothionein and substitutes for zinc, Cu and other trace metals reducing the effectiveness of metalloenzymes [54]. Mercury toxicity can cause hypertension, coronary heart disease, pulmonary embolism, myocardial infarction, blood vessel

obstruction, cardiac arrhythmias and atherosclerosis [54, 55]. Furthermore Hg has been linked to inflammation, vascular smooth muscle proliferation and migration, endothelial dysfunction, anaemia, haemolysis of erythrocytes and an increase in platelet aggregation by decreasing cyclic adenosine monophosphate (cAMP) [2, 54, 55, 60]. Mercury also increases coagulation and thrombosis by an increase in factor VIII, platelet factor IV; and thrombin and reduces protein C, inhibits endothelial cell formation and migration, inhibits prostaglandin E and induces platelet shape changes – from an inactivated round and flat discoid shape to a swollen state with projection of multiple pseudopods from the surface of the platelets, which enhances aggregation (Fig. 2.2) [54, 55, 61, 62]. Other toxic Hg effects also include: haemorrhage, damage to erythrocytes and inhibition of haemopoiesis, a decrease in endothelial repair, a decrease nitric oxide bio-availability, endothelial dysfunction and a decrease in tissue type plasminogen activator (t-PA) [2, 55, 56, 63]. An increase in pollution and thus Hg emissions is a rising concern all over the world.

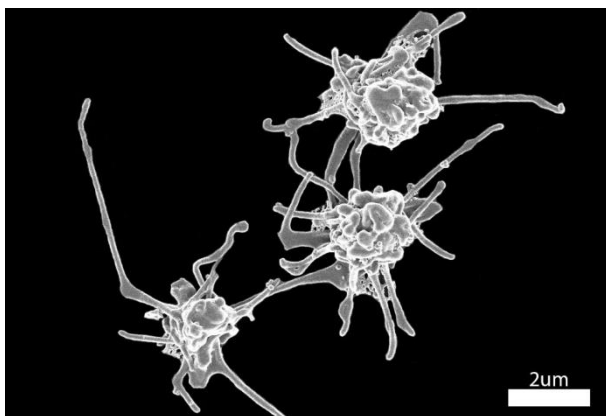


Figure 2.2: Induced platelets with multiple pseudopods and an increase in aggregation.

Prolonged exposure (1 – 48 hrs) to low doses of mercuric ions (0.25 – 5 μM) induces erythrocyte shape changes from discocytes (normal shape) to echinocytes and then to spherocytes/sphere-echinocytes (Fig. 2.3) accompanied by micro-vesicle generation [54]. It can be noted that Hg enhances coagulation by various alterations in the blood system.

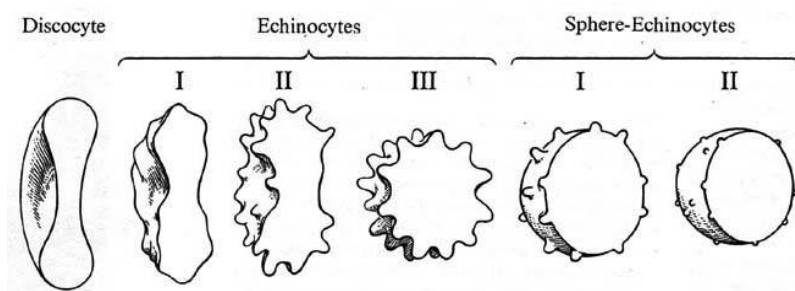


Figure 2.3: Discocyte, echinocyte and spherocyte shaped erythrocytes [64].

2.5 Specific metal targets

The CVS has been identified as a specific target of Cu, Mn and Hg toxicity. However the effect of these metals as part of mixtures, the most common type of exposure on the CVS is unknown. As the metals have specific modes of toxicity and targets (section 2.2 – 2.4), the effect of these metals would possibly be synergistic. The established WHO and South African safety limits in water of each metal is presented in Table 2.3. The low safety limit for Hg reflects the high toxicity of this metal. As this study focuses on the effect of these metals on erythrocytes and the coagulation system, both will be described in more detail.

Table 2.3: Safety limits of each metal under investigation [65].

	Cu	Mn	Hg
WHO limit	2 mg/L	500 ug/L	1 ug/L
WHO limit (molarity) *	31.47 μ M	9.1 μ M	0.004 μ M
South African limit	1 mg/L	100 ug/L	1 ug/L

* Concentrations used in this study are based on these limits.

2.5.1 Erythrocytes

In healthy individuals, erythrocytes are the predominant cell type with a cell count that can exceed 4×10^{12} cells/L of circulating blood [66]. The other major cell types within the blood include platelets and leukocytes. Platelets range between $2 \times 10^5 - 5 \times 10^5$ circulating cells/ μ L and leukocytes range between 4000 – 11000 circulating cells/ μ L of whole blood. Leukocytes, consisting of granulocytes, lymphocytes and monocytes, play an important role in cellular immunity [67]. In an individual with 5 L of blood more than 10^{11} erythrocytes are destroyed and removed daily. The average size of an erythrocyte is 8 μ m, but erythrocytes can deform or change their shape to be able to pass through capillaries where the size of the lumen ranges between 5 and 7 μ m. The deformability of the erythrocyte is due to a composite membrane that consists of a lipid bi-layer coupled to an actin/spectrin-based network, which gives the flexibility and integrity of the overall structure [66]. Erythrocytes have a lifespan ranging between 100 and 120 days, though this can be shortened when erythrocytes are damaged [43]. Due to the abundance of erythrocytes in the bloodstream, these cells represent a potential target for metal ions. Metal ions bind to the outer membrane surface of the erythrocytes and can induce eryptosis [33].

Erythrocytes do not contain nuclei or mitochondria and undergo their own type of apoptosis, known as eryptosis. Eryptosis removes defective erythrocytes before haemolysis or the rupturing of the erythrocyte membrane can occur and thus prevents the release of intracellular materials and that can lead to inflammation [43]. Eryptosis is stimulated by hyperosmotic shock, an increase in cytosolic Ca^{2+} , energy depletion, hyperthermia and

oxidative stress. [68]. Eryptosis has similar features to apoptosis, including cell shrinkage, cell blebbing and cell membrane scrambling leading to PS exposure on the cell surface. Morphological features of damaged erythrocytes are membrane alterations including spike formation and blebbing, size alterations including swelling, shape alterations including distortions, and haemolysis resulting in the loss of cell content (Figure 2.3). Eryptotic erythrocytes are recognised by macrophages and are subsequently engulfed and degraded. Eryptotic erythrocytes can adhere to the vascular wall and can cause a decrease in microcirculation. Excessive eryptosis can result in both anaemia and thrombosis [43].

Stimulators of eryptosis, such as oxidative stress cause Ca^{2+} to enter erythrocytes through Ca^{2+} channels. Prostaglandin E_2 causes the activation of these Ca^{2+} -permeable, non-selective, cation channels and ceramide increases the Ca^{2+} sensitivity of erythrocytes. The entry of Ca^{2+} into the erythrocytes results in several effects. Firstly, calpain – a cysteine endopeptidase – is activated which degrades membrane proteins resulting in membrane blebbing. Secondly, an increase in Ca^{2+} causes a translocation of PS from the inner membrane to the outer membrane causing PS exposure and resulting in cell membrane scrambling, which is recognised by macrophages. Lastly, an increase in Ca^{2+} within the cell causes activation of K^+ channels, causing hyperpolarisation of the cell membrane due to the an efflux of K^+ and chloride ions. The loss of K^+ and chloride ions results in osmotic water flow out of the erythrocytes resulting in cell shrinkage (although this is not seen with Hg exposure) [44].

2.5.2 The coagulation system

The coagulation system is maintained and controlled by various factors and plasma proteins. The coagulant state of blood requires interaction between the endothelium, platelets and the coagulant factors. Thrombosis can occur when the flow of blood decreases, if the walls of the blood vessels have sustained oxidative injury or when there is an imbalance between the pro-coagulant and anti-coagulant factors. The initiation of platelet adherence and aggregation is due to vessel wall injury. The coagulation pathway or cascade involves various factors, which leads to the eventual formation of a fibrin clot (Fig. 2.4) [69].

When vessel injury occurs, TF-bound to cell membranes are exposed to blood. Tissue factor and activated factor VII work together, to convert factor IX and X to their activated forms. Activated factor X causes the conversion of prothrombin (inactive factor II) to thrombin (active factor II). This reaction is accelerated by factor V. Thrombin converts fibrinogen in plasma to fibrin monomers, by cleavage. The fibrin monomers polymerise and link together

to form a stable fibrin clot. Thrombin has a positive feedback mechanism on factor V and factor VIII thereby amplifying the coagulation cascade (Fig. 2.4) [69].

The tissue-factor pathway inhibitor forms a complex with activated factor VII and activated factor X and the complex inhibits the extrinsic coagulation pathway from occurring. The thrombomodulin (acts as a thrombin receptor), protein C and protein S pathway converts activated factor V and activated factor VIII, to their inactive form. Anti-thrombin III converts the active forms of factor IX, X and XI to their inactive forms and this reaction is accelerated by the presence of heparan sulphate [69].

Activated platelets initiate the plug formation in the blood vessel and support the coagulation cascade by the various factors through acting as a scaffold. Platelets become activated when vascular endothelium is exposed by injury, if the vessels have abnormal walls or if fibrin deposition occurs. An increase in levels of platelet factor IV, beta-thrombomodulin and thromboxane A_2 has been observed to be associated with an increase in platelet aggregation [69].

The fibrinolytic system is comprised of the pro-enzyme plasminogen, which is converted to active plasmin by plasminogen activators, urokinase type plasminogen activator (u-PA) or t-PA. Vascular smooth muscle cells and fibroblasts have the capability of producing plasminogen activators and plasminogen activator inhibitor, which regulates fibrinolysis during haemostasis [63]. Plasminogen causes the breakdown of the fibrin networks within the formed clot to fibrin, resulting in the formation of degenerated products [4].

Alpha-2 anti-plasmin is the main human plasmin inhibitor and PAI-1 is the primary inhibitor of the plasminogen activators in human plasmin and is stabilised by S-protein [4]. The t-PA has fibrin specificity, whilst the u-PA does not [4, 63]. The u-PA activates fibrin-bound and circulating plasminogen and also causes the degradation of fibrin, factor V and factor VIII (these three components cause coagulation) [4]. Fibrinolysis can be inhibited at the level of the plasmin or at the level of the plasminogen activators, which are regulated by the various factors including the main factor, thrombin [4, 63].

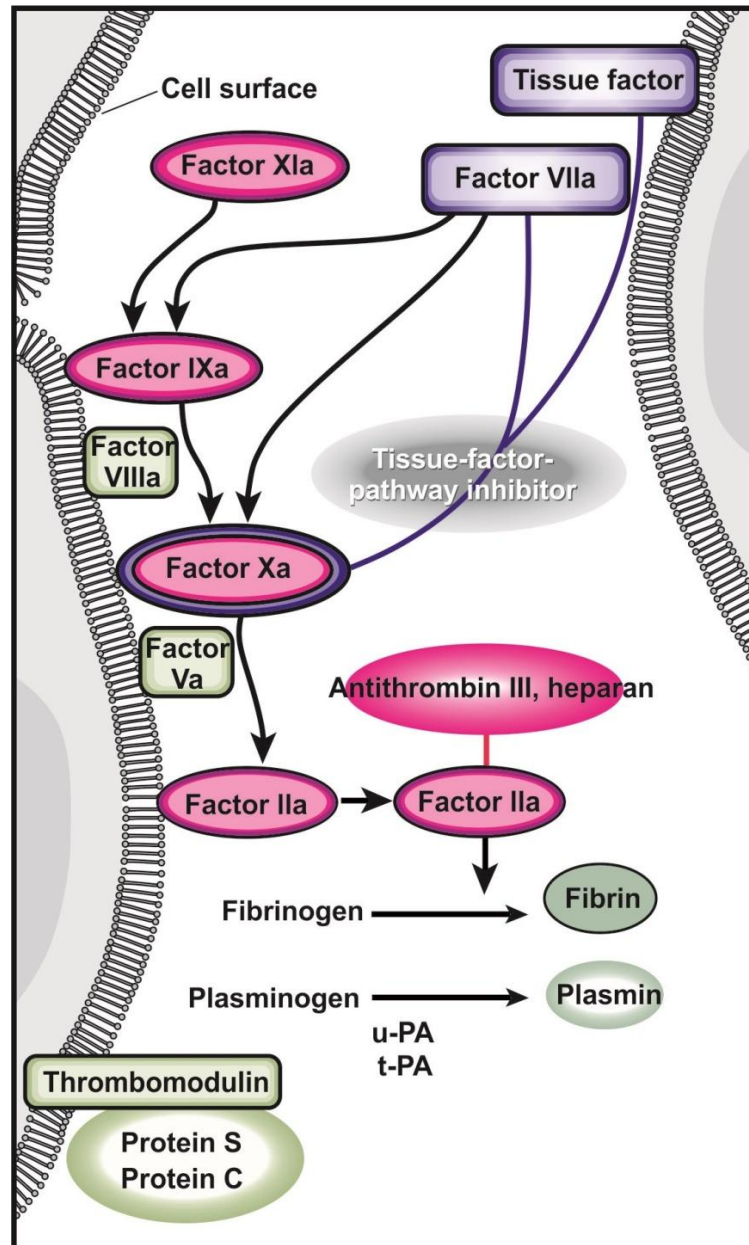


Figure 2.4: The factors that play a role in the coagulation pathway. Image adapted from [69].

As discussed, metals such as Cu, Mn or Hg can induce oxidative damage and inhibit enzymatic pathways. In the vascular system this can cause erythrocyte eryptosis and altered coagulation. Little is known regarding the effect of these metals in combination on erythrocyte structure, function and blood coagulation.

2.6 Aim

The aim of this study entailed the investigation of the potential toxicity of the metals Cu, Mn and Hg, alone and in combination, with regards to their effects on blood coagulation and thrombus formation, specifically on erythrocyte membrane rupturing; Hb precipitation and

distribution; erythrocyte, platelet and fibrin fibre morphological changes and coagulation property alterations.

2.7 Objectives

The aim of this study was achieved through the following research objectives:

1. Investigating the effect of the metals Cu, Mn and Hg, alone and in combinations, on the cell membranes of erythrocytes by using the haemolysis assay.
2. Investigating the effect of Cu, alone and in combination, on Hb precipitation and distribution by using the scan Hb methodology.
3. Investigating the effect of the metals Cu, Mn and Hg, alone and in combinations, on the morphology of platelets, fibrin networks and erythrocytes by using scanning electron microscopy (SEM).
4. Investigating the effect of the metals Cu, Mn and Hg, alone and in combinations, on parameters of coagulation over time, using thromboelastography[®] (TEG[®]).

The results obtained from the investigative analysis of these methods are presented in the chapters to follow (chapter 3 – 5).

2.8 Funding

This project was supported by an National Research Foundation (NRF) grant, grant number: 92768, to the supervisor Dr HM Oberholzer. All additional costs were covered by the Department of Anatomy, Faculty of Health Sciences of the University of Pretoria.

2.9 Ethical considerations

Human blood was used for which ethical clearance was obtained, from the Research Ethics Committee of the University of Pretoria, ethical clearance number: 244/2016. Blood was collected from volunteers after signed informed consent had been obtained. Methods were performed in the cell culture laboratory, in the section of histology, cell biology and embryology in the department of Anatomy as well as the Unit for Microscopy and Microanalysis at the University of Pretoria. Volunteer inclusion criteria included: male participants (avoidance of the implications that the female hormone oestrogen has on the vascular system) between the ages of 20 – 40 years. Volunteer exclusion criteria included: smoking individuals, individuals with medical conditions that have a possible effect on the CVS e.g. hypercholesterolemia, individuals that take medication (effect on CVS) and individuals that live close to mines (affected by metal exposure).

2.9.1 Volunteer recruitment

Volunteers were recruited via telephone or e-mail from friends or family living in Pretoria during which the purpose of the study was explained. Once they consented verbally, a written informed consent form was signed and blood was drawn, at the Prinshof Campus of the University of Pretoria. The specific inclusion and exclusion criteria of the study were applied to the voluntary participants.

2.10 Study design

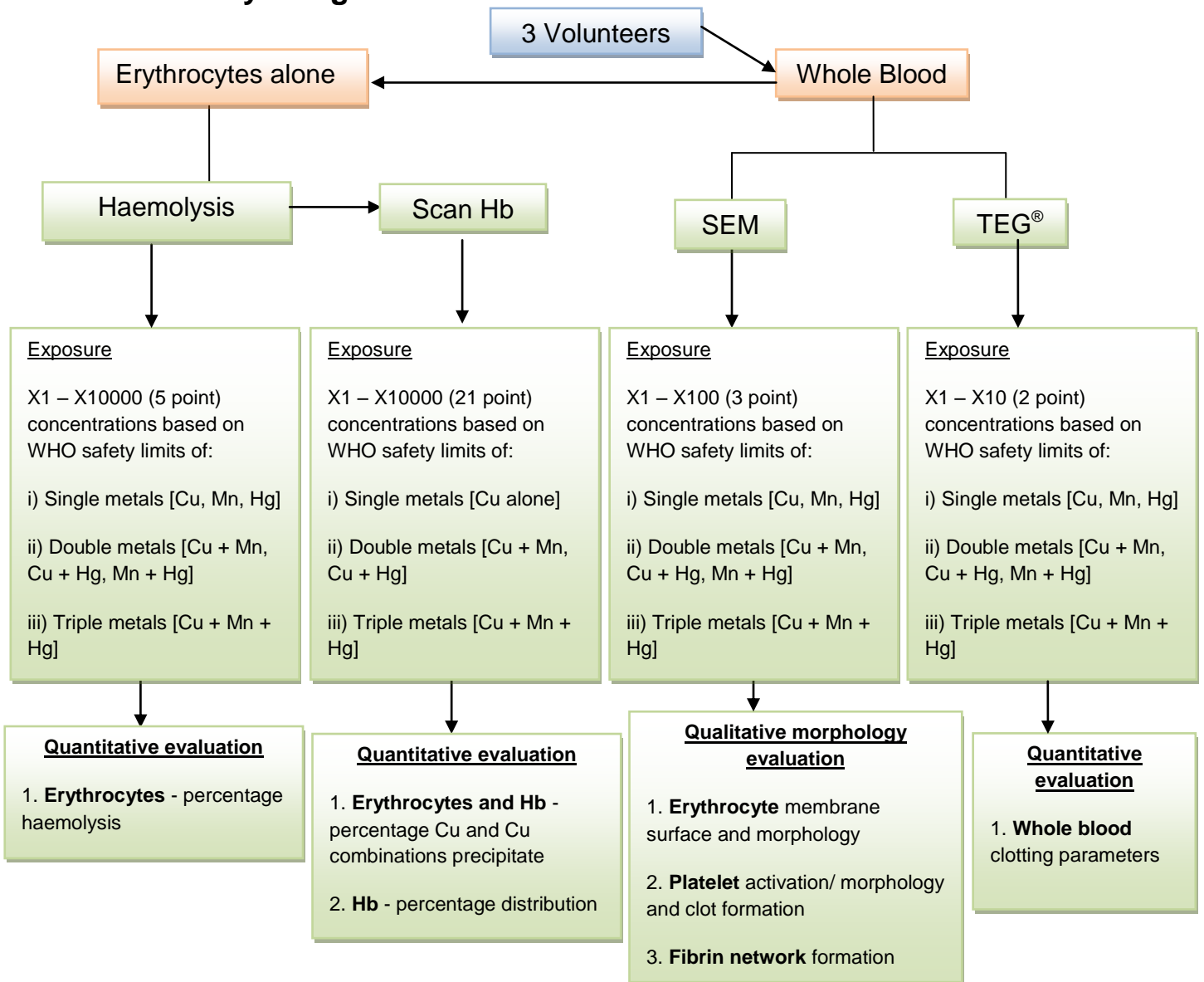


Figure 2.5: Flow diagram explaining the methodologies used for the different blood constituents being investigated.

CHAPTER 3: The haemolytic effects of copper, manganese and mercury, alone and in combination

3.1 Introduction

Erythrocytes are the most abundant blood cell type and these cells lack DNA and organelles and have a typical bi-layer lipid membrane [70, 71]. Haemoglobin is the most abundant protein present in erythrocytes and by binding to oxygen (O_2) it forms oxygenated haemoglobin (oxyHb), which transports O_2 from the lungs to the tissues. When Hb releases O_2 it is then known as deoxygenated haemoglobin (deoxyHb). Both oxyHb and deoxyHb are the major forms of normal Hb present in whole blood. Haemoglobin is made up of four globin chains, with each chain containing a centrally located heme molecule. Each heme molecule contains iron, which gives Hb and in turn erythrocytes their oxygen carrying function and red colour [72].

When erythrocytes encounter an excess of oxidants, the initial site of damage is the plasma membrane. The continuous peroxidation of membrane lipids contributes to progressive haemolysis and as the integrity of the plasma membrane is lost, Hb leaks out of the cell into the plasma [73, 74]. Clinically increased levels of Hb in the plasma are associated with diseases such as haemolytic anaemia [74]. Haemolysis can also occur as a result of improper handling, collection, processing and storage of blood or due to the blood donors having a membrane disorder or bacterial infections [70, 71, 74].

Erythrocyte plasma membrane damage leads to haemolysis and the amount of Hb released can be rapidly quantified spectrophotometrically [72]. This has led to the development of the haemolysis assay. In the laboratory human erythrocytes are exposed to different types and concentrations of drugs and toxins and the degree of Hb release is quantified. This assay has been widely used to evaluate the toxicity of medical drug carriers, bio-surfactants, medical devices, infective agents, herbal extracts and vitamins as well as known toxic substances such as palytoxin and lead [71, 75 – 82]. As human erythrocytes are important targets of metal toxicity (See 2.5.1) they are therefore physiologically relevant cellular models.

Besides oxyHb and deoxyHb, erythrocytes contain other forms of Hb which include MetHb and sulfhaemoglobin (SulfHb). When Fe^{2+} becomes converted to Fe^{3+} , normal Hb is converted to MetHb. Due to the altered state of Fe in MetHb, this form of Hb cannot transport O_2 and also causes the discolouration of blood from red to brown. Due to the

decreased O₂ carrying capabilities of MetHb, it is toxic. Methaemoglobin levels are normally between 0 – 2% of total Hb, but if this increases to 15% cyanosis is present, and at levels of 70% death occurs. Methaemoglobin poisoning is reversible following treatment with methylene blue, except if chlorate poisoning has occurred [83].

When a sulphur atom binds to Hb, it is converted to SulfHb and levels are 0 – 0.5% of the total Hb; levels greater than 10% have never been recorded [84]. Sulfhaemoglobin also cannot bind to O₂ and causes discolouration of blood from red to green [85, 86]. An increase in SulfHb is associated with an increase in cyanosis [84]. Unlike MetHb, SulfHb cannot be converted back to normal functioning Hb and is only removed when erythrocytes are destroyed by the spleen [84 – 86]. Sulfhaemoglobin is believed to form when intestinal bacteria release hydrogen sulphide, which then binds to Hb forming SulfHb and from the ingestion of drugs, such as sulfonamides [85].

Each Hb has unique absorption properties and maximal absorption peaks and these are 540 nm, 576 nm, 619 nm and 630 nm for oxyHb, deoxyHb, MetHb and SulfHb, respectively [87]. Quantification of these additional forms of Hb can also provide additional information related to the toxicity of heavy metals.

The aim of the research undertaken in this chapter was to investigate the haemolytic effects of Cu, Mn and Hg, alone and in combinations using the haemolysis assay and to further determine the extent of MetHb formation by Cu alone and in combination with Mn and Hg.

3.2 Materials and methods

3.2.1 Metal preparations

Stock solutions (concentrations are equal to X100000 the WHO values for each respective metal) for the various metals were made using: CuSO₄ [Sigma-Aldrich, St Louis, MO, USA], manganese chloride (MnCl₂) [Sigma-Aldrich, St Louis, MO, USA], HgCl₂ [Sigma-Aldrich, St Louis, MO, USA]. Working solutions were made from the stock solutions. The concentration ranges of these metals were X1, X10, X100, X1000 and X10000 the WHO safety level standards and were 31.47 µM for Cu, 9.1 µM for Mn and 0.004 µM for Hg. Each metal is in the ionic form as Cu²⁺, Mn²⁺ and Hg²⁺, but is abbreviated throughout as Cu, Mn and Hg. The double metal combinations contained each metal at the WHO limit concentration, e.g., for the combination X1 of Cu + Mn erythrocytes were exposed to 31.47 µM Cu and 9.1 µM Mn while the X10 double combination ratio contained 314.7 µM Cu and 91.0 µM Mn. All final volumes of the metal combinations were the same. The X1 triple combination contained 31.47 µM Cu : 9.1 µM Mn : 0.004 µM Hg. In the same ratios erythrocytes were exposed to X10 metal concentrations.

For the evaluation of the precipitation of protein and Hb and the possible formation of MetHb by Cu, the following metal solutions were also prepared from the stock solutions, in addition to X1 – X10000, X20 – X90 and X200 – X900, of the WHO safety level standards of Cu alone and in combinations with Mn and Hg as well as the triple combination of Cu, Mn and Hg was evaluated.

3.2.2 Blood collection

Approximately 16 mL of venous blood was drawn in four citrate tubes from each of the three healthy, human, male volunteers by a phlebotomist, using a sterile needle and vacuum extraction (EVAC) citrate tubes containing 3.2% sodium citrate. The experiments were conducted on the same day that the blood was drawn.

3.2.3 Sample preparation

Whole blood was centrifuged (Hermle Z300 centrifuge, Hamburg, Germany) at 2500 x g for 10 minutes, after which the plasma and buffy coat was removed. The erythrocytes were then washed with isotonic phosphate buffer saline (isoPBS) [0.137 M sodium chloride (NaCl) (Sigma-Aldrich, St Louis, MO, USA), 3 mM potassium chloride (KCl) (Sigma-Aldrich, St Louis, MO, USA), 1.9 mM monosodium phosphate (NaH_2PO_4) (Sigma-Aldrich, St Louis, MO, USA), 8.1 mM disodium phosphate (Na_2HPO_4) (Sigma-Aldrich, St Louis, MO, USA), pH 7.4] twice, by re-suspending the erythrocytes in the isoPBS and centrifuging between washes, at 1185 x g for 3 minutes. A 5% volume over volume (v/v) blood solution was made by diluting the packed erythrocytes in isoPBS. A positive control: 2% sodium dodecyl sulphate (SDS) solution was used to represent 100% haemolysis and a negative control: isoPBS was used to represent 0% haemolysis. The 5% blood solution was then exposed to a concentration series of the metals, alone and in combinations. All samples were then incubated (NuAire Autoflow NU-4750 water jacket CO_2 Incubator, Plymouth, NH, USA) for 16 hours, at 37°C. After the incubation period, the samples were centrifuged at 1185 x g for 2 minutes, transferred in triplicate to a 96-well plate, the absorbance was then measured at 570 nm with the FLUOstar Omega micro-plate reader (BMG LABTECH, Offenburg, Germany) and the results expressed as percentage haemolysis, using the following formula:

$$\% \text{ Haemolysis} = (A_{\text{sample}} - A_{0\%} / A_{100\%} - A_{0\%}) \times 100$$

Where A_{sample} = Absorbance of erythrocytes exposed to metals alone or in combination.

$A_{0\%}$ = Absorbance of erythrocytes exposed to isoPBS (0% haemolysis).

$A_{100\%}$ = Absorbance of erythrocytes exposed to 2 % SDS (100% haemolysis).

3.2.3.1 Evaluation of metal interactions

Metals in combination can have an antagonistic, additive or a synergistic effect. Many different methods have been reported to evaluate the interactions between drugs, chemical mixtures, metal mixtures and toxins such as insecticides [88 – 95]. For this study the model deviation ratio (MDR) method was used.

The MDR was calculated (Table 3.1) to determine whether the combination groups had an antagonistic, additive or synergistic effect. The formula used was:

$$\text{MDR} = \text{Ov}/\text{Ev}$$

Where Ov = the observed value (average % haemolysis) of the combination group

Ev = was the expected value (sum of the average % haemolysis of the single metal groups/number of groups).

Volume differences were taken into account by dividing the Ev by 2 for double metal combinations and 3 for the triple metal combinations. An additive effect is indicated where $0.5 < \text{MDR} < 2$, antagonism where $\text{MDR} < 0.5$ and synergism where $\text{MDR} > 2$ [96, 97].

Example: X1 Cu + Mn

$$\text{MDR} = \text{Ov}/\text{Ev}$$

$$= (1,349)/[(1,675 + 0.464) / 2]$$

$$= 1,262; \text{ Therefore additive effect.}$$

3.2.3.2 Precipitation and MetHb formation

Copper did not appear to cause any haemolysis but Cu-mediated precipitation was observed. To determine the extent of precipitation and the presence of toxic forms of Hb such as MetHb, and SulfHb, following the quantification of the amount of Hb in the supernatant, the pellets together with the remaining supernatant was resuspended and the erythrocytes were lysed with the addition of 100 μL of a 2% SDS solution. The SDS was found to lyse the erythrocyte plasma membrane but not the precipitate. The samples were vortexed well and then centrifuged at 1185 xg for 2 minutes to collect the precipitate and then the supernatant was transferred to a 96-well plate. The absorbance of the supernatant was measured at 540 nm. The effects of X1 – X10000 the WHO safety limit concentrations were determined. The percentage precipitate that formed was calculated as follows.

$$\% \text{ Precipitate} = 100 - [(A_{\text{Cu}} / A_{\text{NC}}) * 100]$$

Where A_{Cu} = Absorbance of the Cu-containing sample.

A_{NC} = Absorbance of the negative control (isoPBS)/no precipitation.

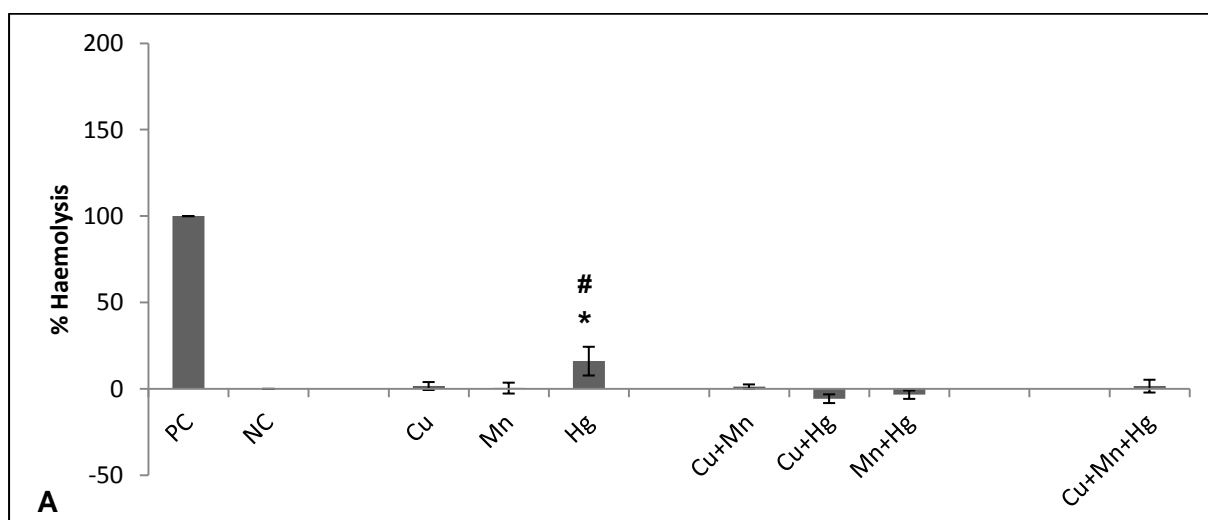
In all Cu samples where no or little precipitation occurred the absorbance of the lysed erythrocytes was measured at 540 nm, 576 nm, 619 nm and 630 nm for oxyHb, deoxyHb, MetHb and SulfHb, respectively. The relative percentages of the different Hb forms were calculated.

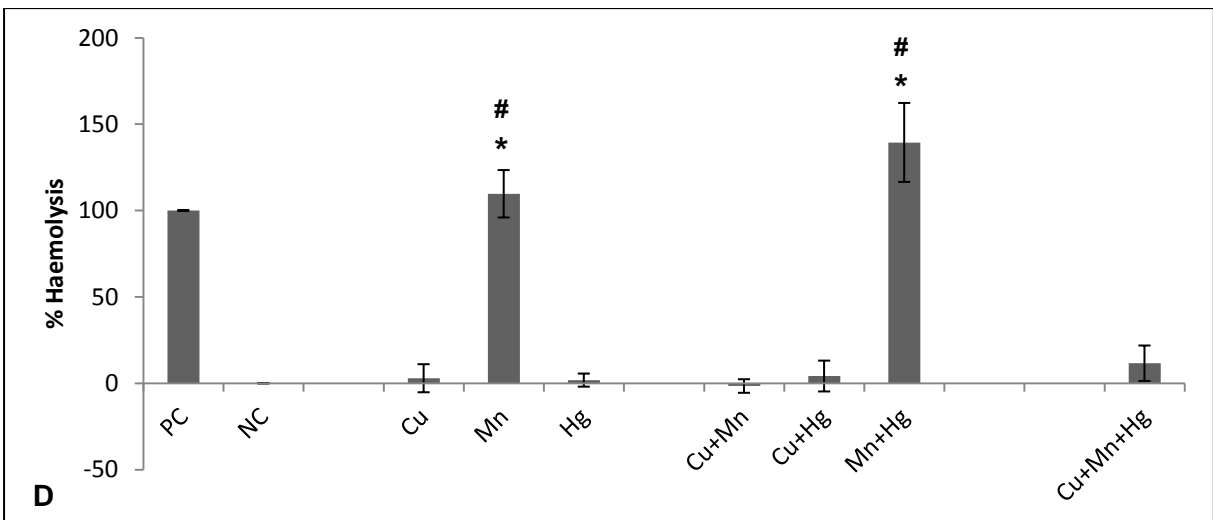
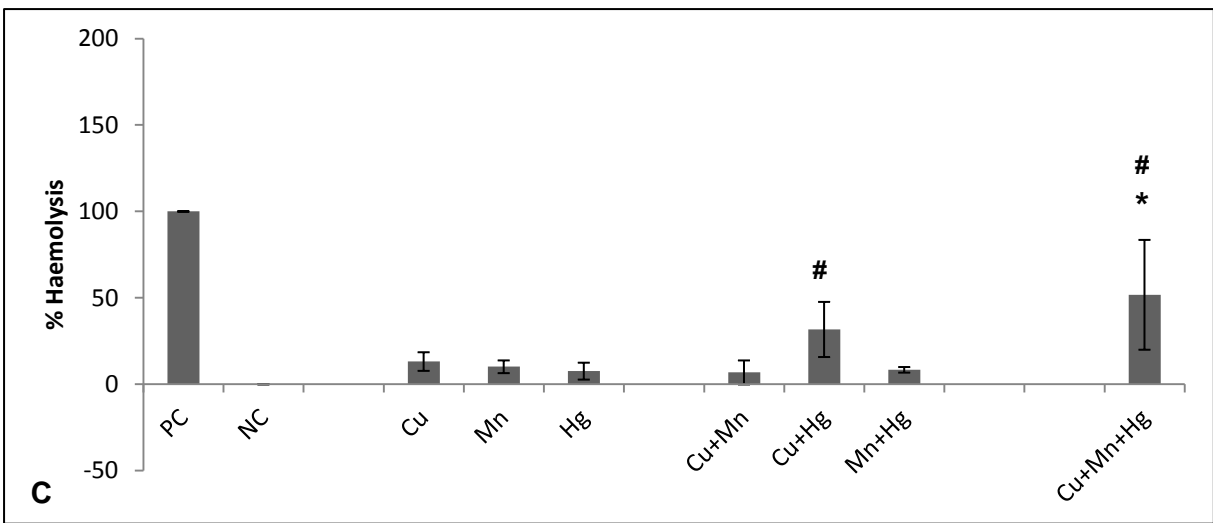
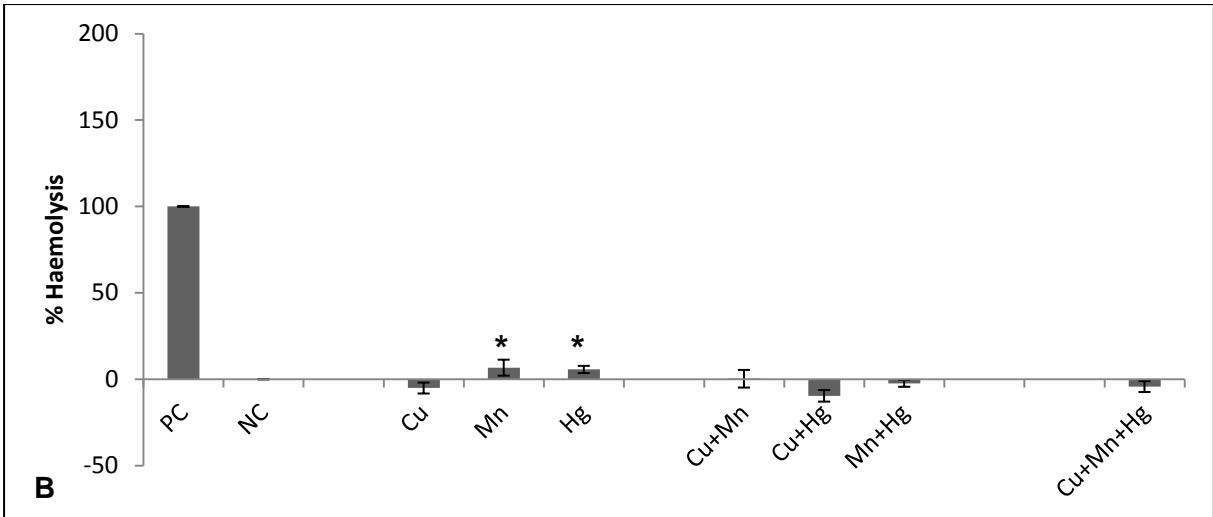
3.2.4 Statistical analyses

The paired t-test (Excel) and one way ANOVA methods (Graph Pad) were used to compare the significance of experimental groups to each other, for the haemolysis assay. Statistical analysis was performed with a 95% confidence interval and a p value < 0.05 considered significant. The one way ANOVA method was used to compare the significance of the % Hb distribution of the experimental groups, which did not precipitate, to each other. Statistical analysis was performed with a 95% confidence interval (p < 0.05). Statistical analyses was not needed for the % precipitation as this method was only used to determine which groups could be used to analyse the data of the % Hb distribution.

3.3 Results

The ability of Cu, Mn and Hg, alone and in combinations, to induce haemolysis at concentrations of X1 – X10000 the WHO safety limits was determined (Figure 3.1). At all concentrations evaluated, no Cu-induced haemolysis was observed. The Cu-containing groups – Cu + Hg and Cu + Mn + Hg – caused a significant increase in haemolysis at a X100 concentration. Manganese and Hg alone showed varied significance effects across concentrations. The Mn + Hg combination group showed significance at the highest concentrations – X1000 and X10000.





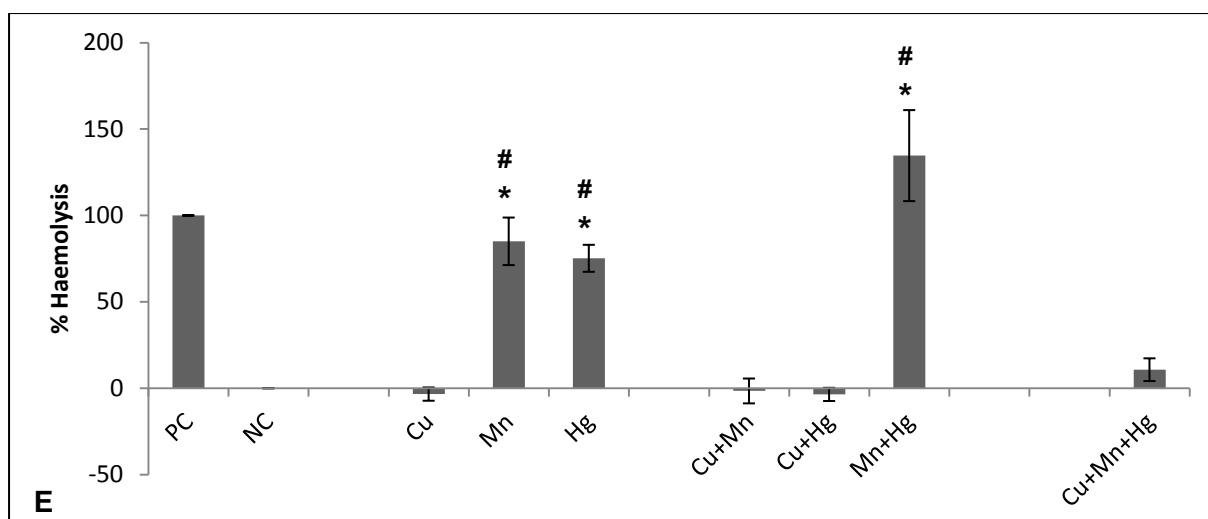


Figure 3.1: The haemolytic effects of Cu, Mn and Hg alone and in combinations evaluated at A) X1, B) X10, C) X100, D) X1000 and E) X 10000 the WHO safety level standards of each metal. Positive control (PC): 100% haemolysis induced by 2% SDS and negative control (NC): 0% haemolysis - isoPBS. Results express the average of eight experiments \pm standard error of mean, compared to a PC and NC. # Indicates significance compared to the NC and * indicates significance compared to other metal groups.

The haemolysis assay provides information on the effect of the metal mixtures but provides no information on whether the interactions between metals are antagonistic, additive or synergistic. An antagonistic interaction implies that two or more metals in combination reduce the toxicity of each single metal alone. Synergism represents a response that is higher than expected. Metal combinations that have synergism can pose a higher risk to population health. Table 3.1 describes the type of interactions that occurs between double and triple metal combinations containing Cu, Mn and Hg. Metal combinations that showed synergism were Cu + Hg (X100), Mn + Hg (X1000) and Cu + Mn + Hg (X100). Additive effects were found for Cu + Mn (X1 and X100), Cu + Hg (X1000) and Mn + Hg (X100 and X10000). Antagonistic effects were found for Cu + Mn (X10, X1000 and X10000), Cu + Hg (X1, X10 and X10000), Mn + Hg (X1 and X10) and Cu + Mn + Hg (X1, X10, X1000 and X10000).

Table 3.1: MDR values and the type of interactions between metal combinations.

Metal and metal combinations							
	Cu	Mn	Hg	Cu + Mn	Cu + Hg	Mn + Hg	Cu + Mn + Hg
X1 WHO limit							
Av % H	1,675	0,464	16,064	1,349	-5,672	-3,351	1,603
MDR				1,262	-0,639	-0,406	0,264
Interaction				Add ³	Ant ³	Ant	Ant
X10 WHO limit							
Av % H	-5,112	6,689	5,642	0,285	-9,606	-2,399	-4,239
MDR				0,361	-36,295	-0,389	-1,762
Interaction				Ant	Ant ¹	Ant	Ant ²
X100 WHO limit							
Av % H	13,135	10,110	7,585	6,828	31,709	8,346	51,758
MDR				0,587	3,061	0,943	5,036

Interaction				Add	Syn ²	Add	Syn ¹
X1000 WHO limit							
Av % H	2,926	109,682	1,829	-1,592	4,191	139,403	11,601
MDR				-0,028	1,763	2,500	0,304124
Interaction				Ant	Add ¹	Syn ³	Ant
X10000 WHO limit							
Av % H	-3,390	85,036	75,204	-1,572	-3,573	134,649	10,727
MDR				-0,039	-0,100	1,681	0,205
Interaction				Ant	Ant	Add ²	Ant

Ant indicates antagonistic, Add indicates additive and Syn indicates a synergistic effect. Numbers ¹⁻³ indicates combinations with the highest effects, with 1 being the highest.

The Cu alone and Cu-containing groups overall showed very little haemolysis. Due to the precipitation of Cu at higher concentrations, the data in Table 3.1 for Cu-containing combinations may not necessary reflect the type of interactions that do occur. However, at low concentrations where precipitation does not occur, the observed effects are antagonistic for X1 and X10 while for X100 these interactions are synergistic for Cu + Hg and Cu + Mn + Hg.

Copper causes no haemolysis at X1 and X10, while at a X20 concentration haemolysis occurs (Figure 3.2) whereas at a higher X100 concentration, less haemolysis occurs. Reduced levels of haemolysis at higher concentrations are associated with the formation of a brown coloured pellet (Figure 3.2).

Sample	Control (PBS)	Cu X1	Cu X10	Cu X20	Cu X100
Supernatant colour					
Precipitate formation					

Figure 3.2: The comparison of supernatant colours and precipitate formation of Cu samples at various concentrations compared to a control - PBS.

To quantify the amount of precipitated Hb, a novel approach was used. Treatment of a control (PBS) with SDS resulted in erythrocyte haemolysis and with centrifugation no pellet formation occurred i.e. all Hb is in solution. With the formation of an insoluble Cu-Hb pellet, treatment with SDS caused plasma membrane haemolysis without dissolution of the precipitate. With centrifugation an insoluble pellet formed and quantification of the amount of Hb in the supernatant provided an indirect method for quantification of the amount of precipitate. The results are presented in Figure 3.3. At X1 and X10 no precipitation was observed while at X20 52.90% precipitation occurred. At greater than X200, a 100% precipitation occurred.

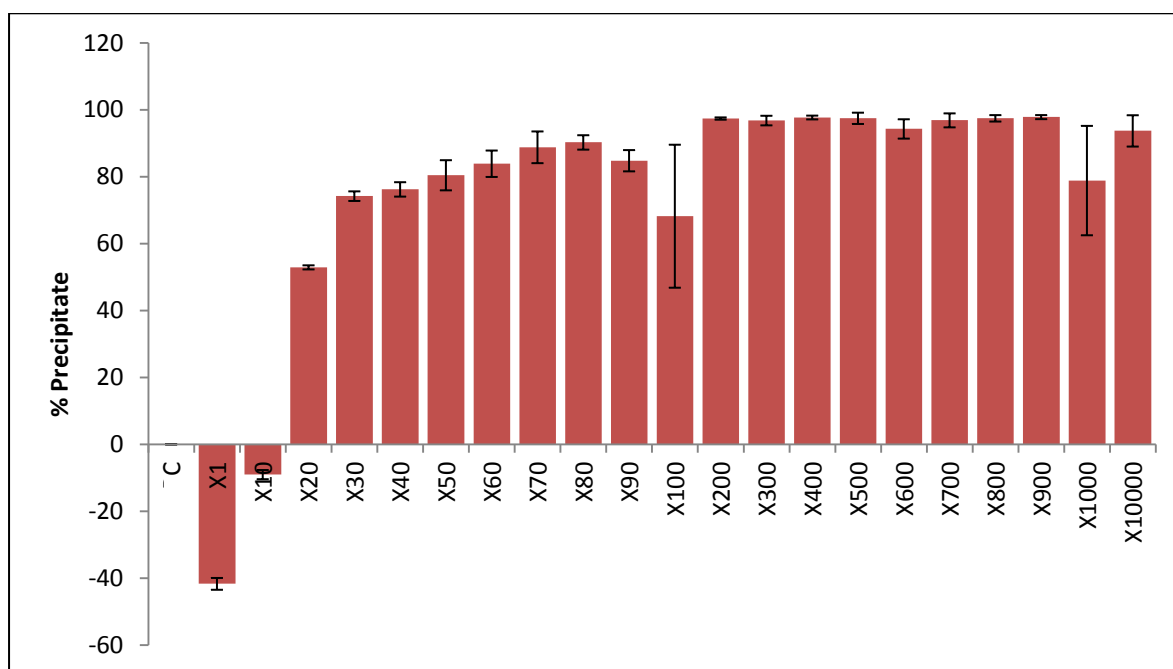
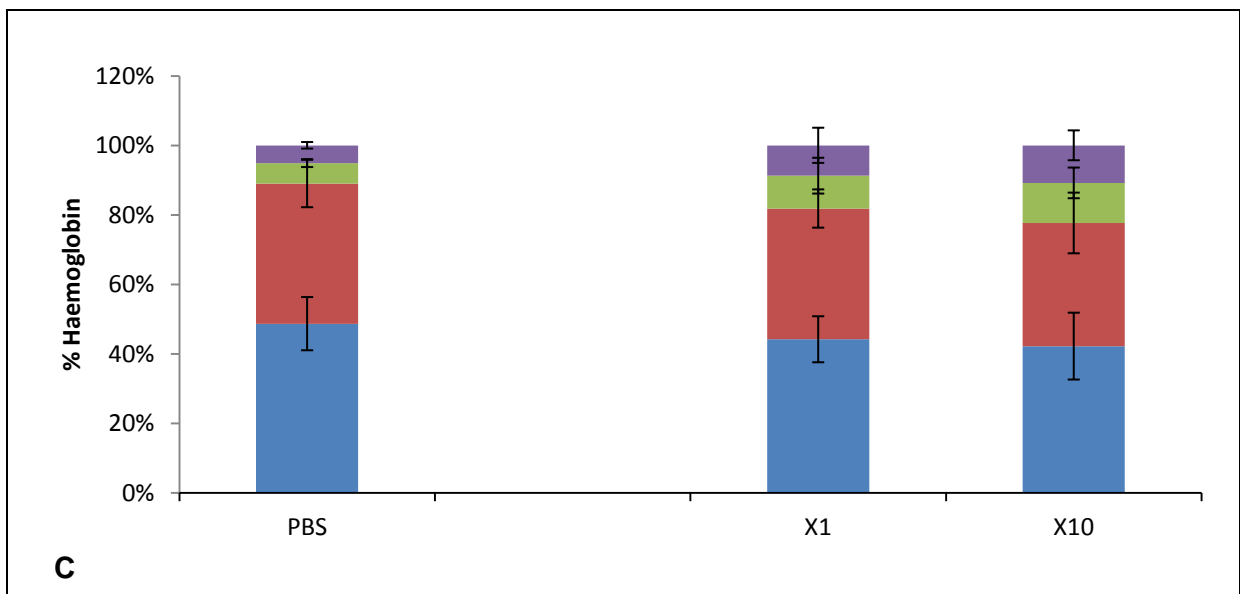
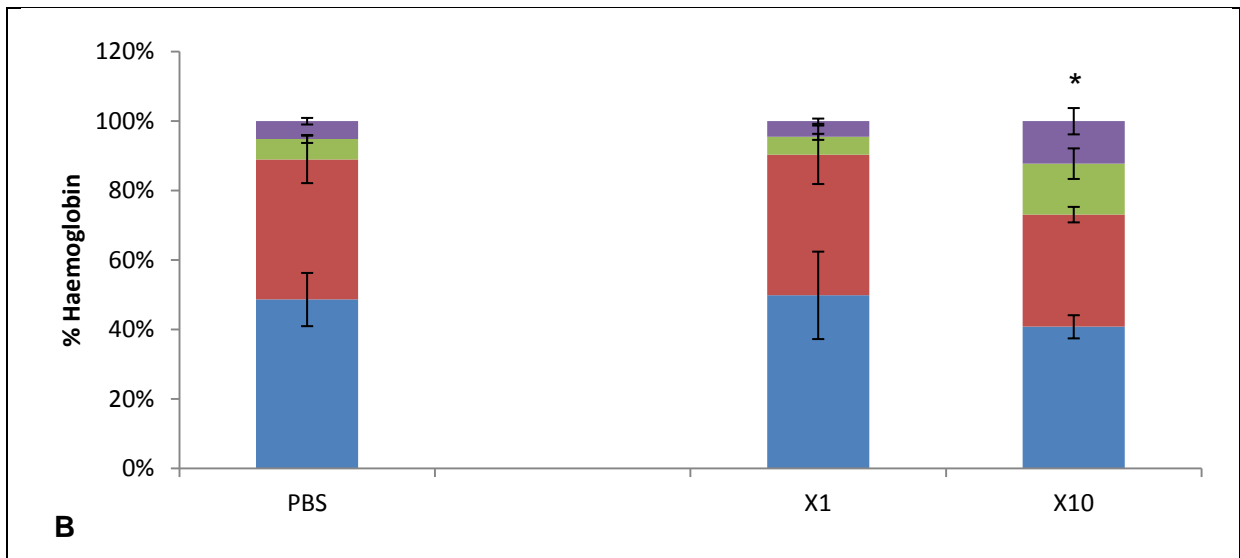
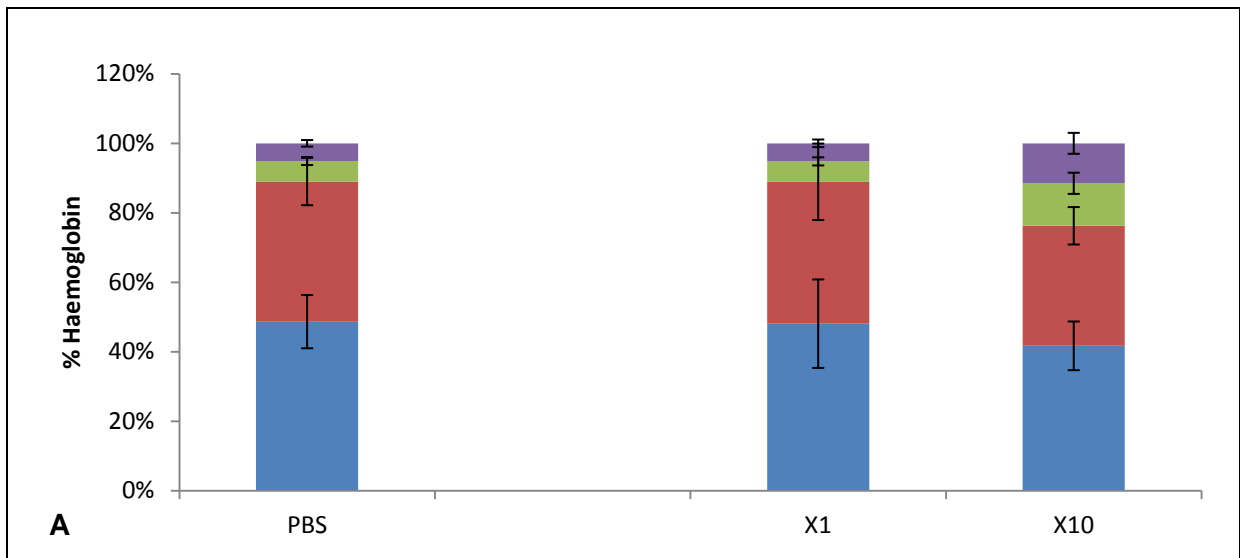


Figure 3.3: The % precipitation formed following exposure of erythrocytes to X1 – X10000 the WHO safety levels of Cu. Results express the average of three experiments \pm standard error of mean, compared to a control (C) – no added Cu.

In the control and the X1 and X10 concentrations, the percentage of the different types of Hb was determined and this included the percentage of normal oxyHb and deoxyHb and the toxic, MetHb and SulfHb. An increase in the toxic forms can pose a health risk. As shown in Figure 3.4 oxyHb and deoxyHb are the pre-dominant Hb types with MetHb and SulfHb being the less dominant types. The concentrations of MetHb and SulfHb in the control, not exposed to metals, were 0.12% and 0.136% respectively.



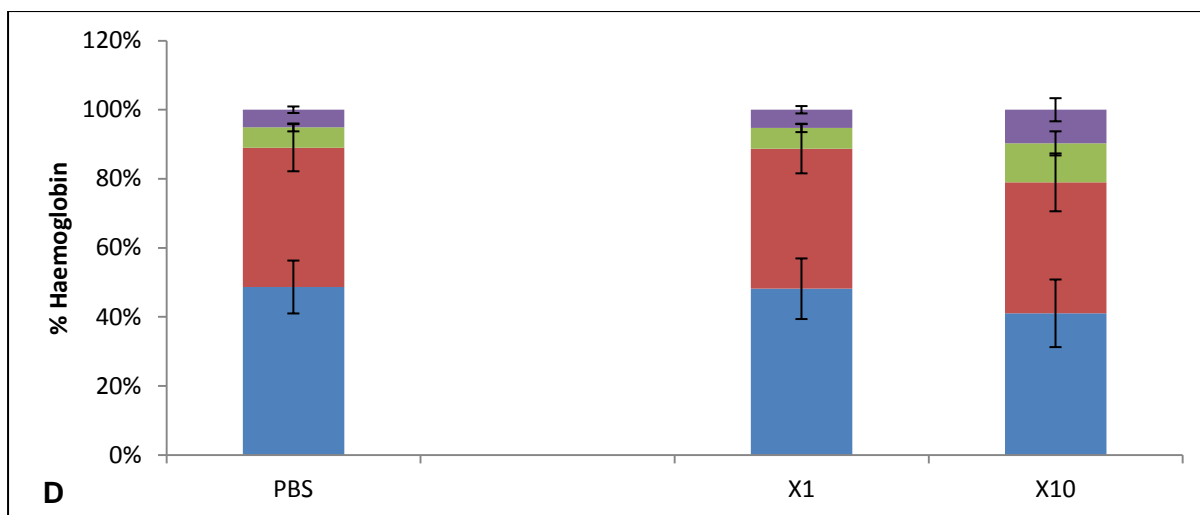


Figure 3.4: A comparison of Hb distribution (%) of various forms of Hb within erythrocytes. Erythrocytes were exposed to a X1 and X10 concentration, based on the WHO safety levels of A) Cu, B) Cu + Mn, C) Cu + Hg and D) Cu + Mn + Hg. Results express the average of three experiments \pm standard error of mean, compared to a control (PBS). * Indicates a significantly higher percentage of Sulf- and MetHb. OxyHb (blue), deoxyHb (red), MetHb (green) and SulfHb (purple).

The two toxic forms of Hb – MetHb and SulfHb – increased in the Cu-containing groups as compared to the control (PBS) as shown in Figure 3.4. The fold change in MetHb and SulfHb was calculated (Figure 3.5).

Copper at X1, did not cause a change compared to the control in MetHb levels while at X10 a 2.05-fold increase in MetHb was observed. Manganese in combination with Cu at X1 caused a 0.86-fold change and thus a decrease in MetHb, whilst at X10 a 2.45-fold increase was observed. Mercury in combination with Cu caused a 1.59-fold increase and a 1.93-fold increase for the X1 and X10 concentrations, respectively. For Cu in combination with Mn and Hg at X1, there was no change as compared to the control while at X10 there was a 1.89-fold increase. For all X10 combinations, MetHb formation was increased compared to the control and compared to the X1 concentrations. The only X1 combination that showed an increase in MetHb was Cu in combination with Hg.

The SulfHb results are very similar where Cu X1 and Cu in combination with Mn and Hg X1 showed no change as compared to the control. Copper in combination with Mn at X1 showed a decrease (0.89-fold change) in SulfHb whilst Cu in combination at X1 showed a fold increase (1.68-fold change). Copper alone at X10 had a 2.2-fold increase, Cu + Mn had a 2.45-fold increase, Cu + Hg had a 2.08-fold increase and the triple combination – Cu + Mn + Hg – had a 1.88-fold increase.

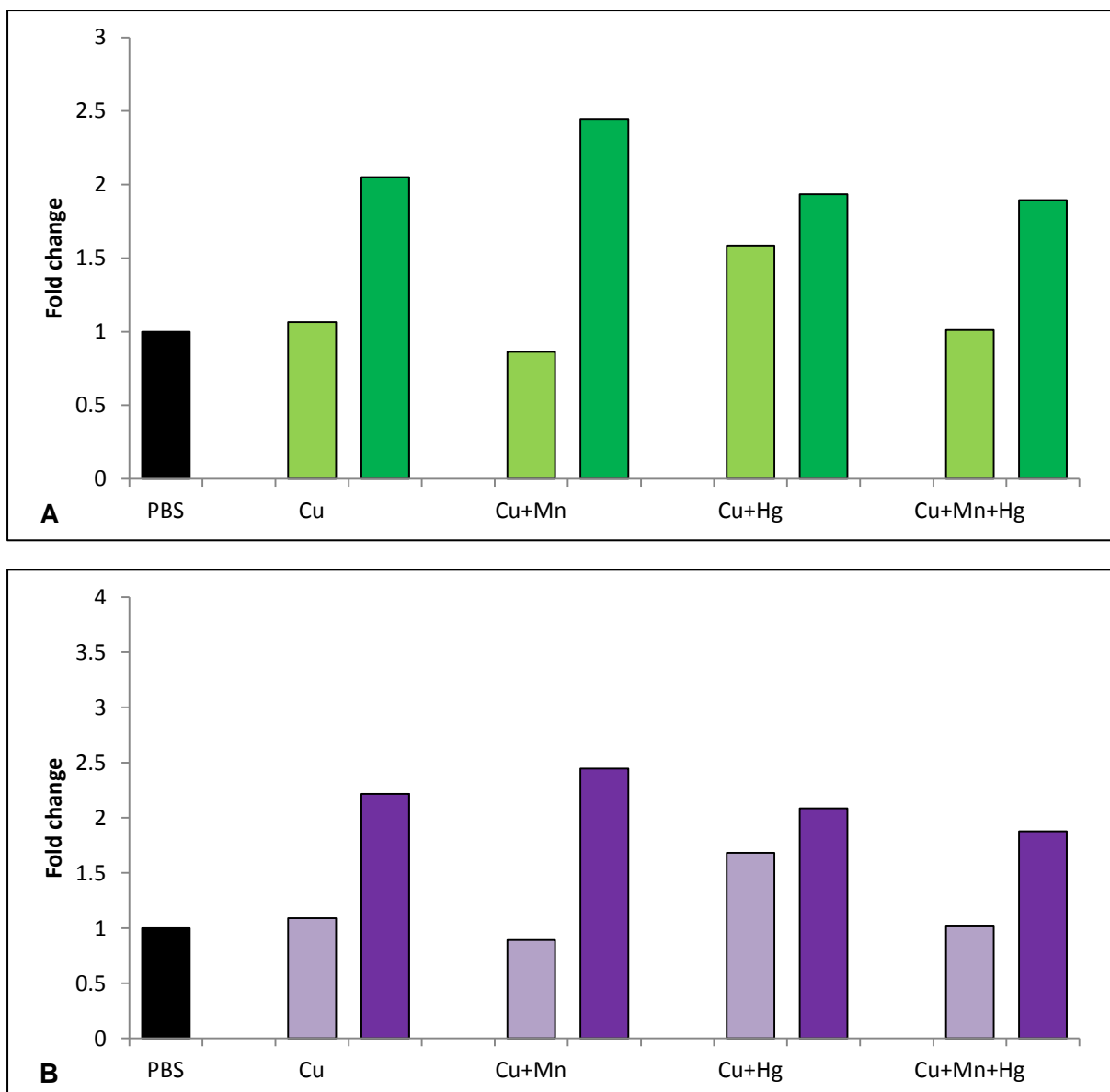


Figure 3.5: Representation of several fold change in A) MethHb and B) SulfHb of various Cu-containing samples at a X1 (lighter shade) and X10 (darker shade) concentration, based on the WHO safety levels of Cu, alone and in combinations with Mn and Hg compared to the control erythrocytes not exposed (PBS) (black).

3.4 Discussion

In this study the effect of Cu, Mn and Hg alone and in combinations, at concentrations of X1 – X10000 the WHO safety limits, of each metal, alone and in combination, on erythrocytes was evaluated. In the study of the toxicity of metals, especially in animal studies, arbitrary concentrations are selected. Findings of these studies are very difficult to correlate with environmental exposure. In this study, the limits of environmental exposure of each metal were selected and then toxicity was determined. Mercury is more toxic than Cu and Mn, where the WHO limit for Hg is 0.004 μM , Cu is 31.47 μM and Mn is 9 μM . The molar ratio for Hg:Cu is 1:7867 and the molar ratio for Hg:Mn is 1:2250 and this also reflects the high toxicity of Hg. With environmental exposure the absorption of each metal is different and

blood levels following exposure will be different between metals and will not be at the WHO limits, within blood. However by using the WHO limits, it can be determined which combinations may have synergistic effects related to increased toxicity.

3.4.1 Cu, Mn and Hg alone

Normal Cu levels are within the range of 640 – 1400 µg/L [98]. The WHO safety limit for Cu is 2000 µg/L [99]. If absorption is 40% blood levels are 800 µg/L [99]. A study conducted using Japanese workers, found an increase in blood Cu levels compared to control individuals. Cloisonné workers had an average blood level of 78.4 µg/L, silver plating workers a level of 88.8 µg/L and plant office workers a level of 78.8 µg/L compared to the control group with Cu levels of 74.6 µg/L. Differences between groups were not significant [11]. Copper levels in South African dam catchment areas showed increased Cu levels compared to worldwide levels and is possibly due to gold mines in the area [100]. Little is known about Cu blood levels of South African communities, living near gold mining and in heavily industrialised areas, although it can be proposed that Cu levels are increased.

Copper was found to bio-accumulate in fish in the Olifants River in South Africa. Natural Cu concentrations in water are 5 µg/L, however the Department of Water Affairs and Forestry has recorded Cu levels up to 12000 µg/L, in South Africa. Water analysis of the Olifants River at two different sites, within the Kruger National Park, reported Cu levels of 4 µg/L in the water samples collected in four different months. This increase in Cu contamination can be due to natural causes but also anthropogenic activity such as discharging of municipal and industrial sewage, production of fertilisers and algaecides, dumping of ash and also from mine dumps, all of which land up in the river. In fish Cu had bio-accumulated especially in the liver. The fish present in these waters did have high levels of accumulated Cu mainly in the liver indicating long term Cu exposure and the highest recorded concentration of 12000 µg/L is six times the WHO limit for Cu in water [101]. This implies that individuals living close to mines and drinking this river's water are exposed to toxic levels of Cu and bio-accumulation of Cu in exposed individuals is of concern.

An acute CuSO₄ poisoning case showed intravascular haemolysis with decreased haematocrit and Hb and the blood smear revealed anisocytosis, poikilocytosis (>10% abnormally shaped erythrocytes), echinocytes, microspherocytosis and degmacytes (bite and blister erythrocytes) [39]. In Wilson's disease, (discussed in detail in section 2.2.3), high levels of free Cu are released into the blood once liver Cu storage has reached capacity. One of the effects of increased Cu levels in blood is that Cu induces ROS formation and

inhibits the functioning of several enzymes and this leads to haemolysis. During this process Hb is oxidised resulting in MetHb formation [102].

Another congenital disease which can explain the possible effect of Cu ions on Hb is thalassemia. A clinical feature of this disease is haemolytic anaemia which occurs as the result of the precipitation of unstable Hb chains and consequently this may be the reason why these erythrocytes are being destroyed prematurely [103]. As found in this study higher concentrations of Cu > X20 WHO levels caused the precipitation of Cu. At X1 and X10, Cu induced an increase in MetHb and SulfHb formation.

Normal MetHb levels in blood are approximately 1% and an increase in MetHb results in methaemoglobinaemia. Naturally the low levels of MetHb are kept at homeostasis by the hexose monophosphate shunt pathway where glutathione (GSH) reduces oxidising agents and via the enzymes diaphorase I nicotinamide adenine dinucleotide (NADH) MetHb reductase and diaphorase II NADPH MetHb reductase, MetHb is reduced. When these pathways are overwhelmed with an excess of oxidants, MetHb levels increase. Only when MetHb levels reach 10% or greater, does it become clinically significant [104]. In the present study, at X1 and X10, Cu did increase MetHb levels although only significant for Cu + Mn X10.

Sulfhaemoglobin is also formed when Fe^{2+} becomes oxidised, but in addition a sulphur atom binds to the porphyrin ring of the Hb molecule. Some products known to cause MetHb can also form SulfHb and since they have similar absorption peaks it may be difficult to definitively distinguish between both Hb forms [84]. A case of sulfhaemoglobinaemia had SulfHb blood levels of 6%, after paint ingestion and this high level of SulfHb resulted in death [102]. In this study, X10 Cu-induced Met- and SulfHb formation was 2.05- and 2.22-fold greater than the controls, respectively. Although these differences are not statistically significant, small changes in Met- and Sulf-Hb are biologically relevant and can adversely impact on the health of an individual.

The WHO safety limit for Mn is 500 $\mu\text{g/L}$ and if maximal 5% absorbance occurs blood levels are 25 $\mu\text{g/L}$. The total Mn blood range in normal individuals is 4 – 15 $\mu\text{g/L}$, which makes the WHO safety limit slightly higher than normal blood ranges [45]. In Japan, Cloisonné workers had an average blood Mn level of 37.3 $\mu\text{g/L}$, silver plating workers a level of 36.1 $\mu\text{g/L}$ and plant office workers a level of 28.7 $\mu\text{g/L}$ compared to 14.5 $\mu\text{g/L}$ for the control group. Significant differences in Mn levels were found between the controls and Mn exposed workers. The worker's Mn blood levels exceed that of the normal ranges as well as the WHO safety limit [99]. In South African school children living within cities the average Mn blood levels were 9.8 $\mu\text{g/L}$ and 6.74 $\mu\text{g/L}$ for children living in Johannesburg and Cape Town,

respectively. The source of Mn came mainly from dust in classrooms and the school's soil. Even though these levels are within range it was shown that 12.5% of the Johannesburg and 4.2% of the Cape Town school children have Mn blood levels higher than that of normal blood values [12]. Another study found that in Durban school children the average Mn blood levels were 10 ug/L, where 8% of the sample children exceeded the 15 ug/L safety limit. These high Mn levels were attributed to increased pollution, especially due to the presence of Mn in motor fuel [13]. Levels of 6.74 – 15 µg/L is equivalent to normal Mn blood ranges, however a percentage of the children did exceed the normal ranges. This could be attributed to different susceptibility potentials of individuals. Although in the present study, no haemolysis was observed, the *ex vivo* model used does not take into account cumulative effects.

At X1 – X1000, Hg only caused low levels of haemolysis while at X10000, Hg caused 75.20% haemolysis. Kunimoto *et al.* (1985), found that slight haemolysis of rat erythrocytes occurred at concentrations of 0.1 mM Hg, when erythrocytes were incubated for 60 minutes, and no haemolysis occurred at lower concentrations [14]. This concentration is 250000 times greater than the WHO safety level and 25 times higher than the highest concentration evaluated in the present study. This indicates that Hg-induced haemolysis is a function of concentration and exposure time. The WHO safety limit for Hg is 1 ug/L and with absorbance of about 15%, blood levels are about 0.15 ug/L. The average non-occupational exposed blood levels are <10 µg/L and for occupationally exposed individuals it is 15 µg/L. [15].

Case reports on patients with Hg toxicity revealed some patients are asymptomatic even at toxic Hg blood levels. Acute blood level ranges were from 85 ug/L – 16000 ug/L and chronic ranges were 19 – 680 ug/L. Although the X10000 WHO safety limit concentration is possible, it is very rare and requires ingestion of over 1 g of Hg. Ingestion of 1.4 g of HgCl₂, by an elderly woman, resulted in a blood Hg concentration of 590 ug/L and a haematocrit drop from 47% to 27% within a 24 hour timeframe [59]. The haematocrit drop is indicative of erythrocyte haemolysis as was observed in the present study where at the X10000 concentration, 70.25% haemolysis was observed. Some patients exposed to Hg presented with mild to severe symptoms whilst others had developed rashes. The latter are individuals that eat a diet rich in seafood and sea mammals and in these cases blood levels ranged from 6 – 19 ug/L [59].

A study done on the Hg exposure of low-income communities in South Africa, found that the individuals living near ASGM and coal power stations, were exposed to Hg. Of this population 15% had higher blood Hg levels than the non-exposed individuals with blood

levels of < 10 µg/L. Only 20% of this study population used coal as a fuel source, while 63% ate fish from the river and 67% drank water from the river. Some individuals living in the area had also previously worked in the mine. One individual's blood Hg level was 24 µg/L, caused by 20 years of occupational exposure [15]. These results show that the X1 and X10 WHO safety limit concentrations are plausible for Hg exposed individuals. The main concern is with individuals living near gold mining and coal burning power stations where the water is contaminated and Hg has bio-accumulated in fish.

Exposure of erythrocytes to X1 and X10 WHO safety limit concentrations of Hg is relevant and probable amongst the population exposed to Hg, through contaminated water, exposure in the work environment and diet. The results of this study, based on the ability of Cu, Mn and Hg alone to induce haemolysis confirms that Hg is the most toxic, and in addition because Hg bio-accumulates within the food chain, there is an increased risk for associated diseases that occur later on in life.

3.4.2 Cu, Mn and Hg in combination

Synergistic interactions of chemicals and metals are of great concern to the general population. Metals that could be safe alone could be potentially toxic when synergistically interacting with other metals [96]. Exposure to a single metal is rare and will most likely only occur with accidental or deliberate poisoning. Usually environmental exposure is to a mixture of metals of different types and at different concentrations. Also the exposure time is a further confounding factor investigating the effects of environmental exposure.

Haemolysis induced by metals is due to lipid peroxidation or oxidative stress of unsaturated fatty acids in the erythrocyte membrane [105]. An increase in oxidative stress induces lipid peroxidation of lipid membranes and modification of protein structure and function. These modifications can lead to erythrocyte haemolysis and are also linked to CVD [106].

The mechanism whereby each metal in the present study induces haemolysis differs. Copper is a redox active metal and undergoes redox cycling reactions and can form ROS. Copper can cause direct oxidation of Hb via the reaction: $\text{Cu}^{2+} + \text{HbFe}^{2+} \rightarrow \text{Cu}^{+} + \text{HbFe}^{3+}$, where Cu^{+} can react with oxygen and form Cu^{2+} again, thus prolonging the oxidation cycle as well as ROS formation [107]. In addition, Cu can also form Cu^{3+} a strong oxidizing ion. The HbFe^{3+} which is MetHb has a reduced capacity to bind oxygen.

Manganese can enhance oxidative stress due to its ability to change between oxidation states and can also increase ROS production by interfering with mitochondrial oxidative respiration, although this is not relevant in erythrocytes [108]. Mercury also inhibits

antioxidant pathways through ROS formation and binding to GSH and N-acetylcysteine (NAC) due to Hg high binding affinity to the thiol groups of both molecules. The increase in binding of Hg to GSH results in a decrease in the total GSH content and other thiol-containing redox molecules. Not only does this cause the inhibition of enzyme activity and associated biochemical pathways but also results in an increase in ROS accumulation [109]. This depletion of cellular antioxidant mechanisms can lead to cell damage and consequently leading to the haemolysis of erythrocytes. Therefore, as these metals have different mechanisms generating ROS and/or inhibit antioxidant pathways, these metals in combination may have synergistic effects.

In this study the effects of Cu, Mn and Hg in double combinations (Cu + Mn, Cu + Hg and Mn + Hg) and as a triple combination (Cu + Mn + Hg) was investigated. For the double combination, Cu + Mn at X1 – X10000, no increase in haemolysis was observed and at all concentrations the interactions between Cu and Mn was either antagonistic or synergistic. Lack of haemolysis is related to the formation of Cu-induced Hb precipitation. At the X1 and X10 concentrations, there was a 0.86- and 2.45-fold change, respectively, as compared to the control for MetHb formation. For SulfHb formation there was a similar fold change compared to the control.

Few studies have been undertaken to investigate the toxicity of Cu and Mn in combination. The effects of Cu, Mn and aluminium on amphipods in South African waters have been investigated. In this study, the Cu and Mn concentrations used were 0.0175 mg/L and 13.993 mg/L respectively, which was ten times higher than the South African standard for aquatic ecosystems [16]. At these concentrations the Cu + Mn combination group had a synergistic interaction and proved to be the most toxic combination group, out of all the other combination groups evaluated, with the lowest percentage of amphipod survival compared to the other combination groups [16].

The effects of Cu + Mn on rat behaviour, memory and learning abilities, showed that Cu + Mn caused an impairment in learning ability and memory as well as an increase in dopamine and norepinephrine levels and a decrease in 5-hydroxytryptamine. Concentrations used were 1000 µg/mL MnCl₂ in water and 250 mg/kg Cu as part of a casein-based diet [17]. This study identified specific tissue and organ targets of toxicity, however concentrations used far exceed levels of environmental exposure.

For the combination of Cu and Hg, except for the X100 concentration where 30.70% haemolysis occurred; no haemolysis was observed for the X1, X10, X1000 and X10000 concentrations. No dosage dependent increase in haemolysis was observed. All interactions were either antagonistic or additive, except for the X100 concentration where the interaction

between Cu and Hg was synergistic. At the X1 and X10 concentrations, there was a 1.59 and 1.93-fold increase, respectively, as compared to the control for MetHb formation. For SulfHb formation there was a 1.68- and a 2.08-fold increase for the X1 and X10 concentrations, respectively.

Mercury has been found to replace metallothionein-bound Cu and oral HgCl₂ intoxication increased the retention of Cu in kidneys. A study conducted in Wistar rats investigated the effects of Hg and cadmium retention after Cu supplementation, at 50 µg/kg. After 28 days exposure, a decrease in Hg retention was observed. These researchers postulated that Cu supplementation releases the Hg-bound to the metallothionein proteins and consequently Hg is excreted. Therefore, Cu decreases the bio-availability of inorganic Hg in the GIT [18]. Metallothionein is found in erythrocytes and plasma and this may be a possible mechanism whereby Cu reduces the expected toxicity of Hg on erythrocytes and this may account for the antagonistic effects observed for several Cu, Mn and Hg combinations.

For Mn in combination with Hg no increase in haemolysis was observed for the X1, X10 and X100 concentrations and the interactions were either antagonistic or additive. At the X1000 and X10000 concentrations there was an increase in haemolysis (both over 100%) and the interactions were synergistic and additive, respectively. This group was not tested for MetHb or SulfHb as neither Mn nor Hg caused Hb precipitation.

The toxicity of Mn and Hg alone and in combination has been evaluated by Pathak *et al.* (1987). Mercury was found to be highly toxic alone and in combination with Mn was found to be toxic only at high concentrations. In combination low Mn concentrations reduced Hg toxicity, but at higher Mn concentrations the toxicity of Mn + Hg was higher than that of the individual metals alone. The concentrations used were 1, 10, 100 and 1000 mg/L [19]. These concentrations are equivalent to X2 the concentrations used for Mn and X1000 the concentrations used for Hg in the present study and observations – although different concentrations were used – were similar to that found with the haemolysis assay.

For the triple combination of Cu, Mn and Hg, except for the X100 concentration where 51.76% haemolysis occurred, no significant haemolysis was observed for the X1, X10, X1000 and X10000 concentrations. No dosage dependent increase in haemolysis was observed. All interactions were antagonistic, except for the X100 concentration where the interaction between Cu, Mn and Hg was synergistic. At the X1 concentration no change was seen in MetHb or SulfHb formation, as compared to the control and at the X10 concentration, there was a 1.89- and a 1.88-fold increase for MetHb and SulfHb, respectively.

Most metals in combination had an additive effect and these were Cu + Mn X1, Mn + Hg X100, Cu + Hg X1000 and Mn + Hg X10000. The groups that showed a synergistic effect were Cu + Hg X100, Cu + Mn + Hg X100 and Mn + Hg X1000 while remaining combinations had an antagonistic effect. However, there were no clear indications of the effects of Cu because, for the Cu combinations at the X100, X1000 and X10000 concentrations, Cu-induced sample precipitation. According to Cedergreen (2014) synergistic effects are rarely seen and are found in approximately 5% of tested mixture combinations [96]. In the present study, of the 20 combinations evaluated, only 3 combinations showed synergism which is 15% of all combinations.

At a X100, synergism was observed for Mn + Hg and Cu + Mn + Hg with MDR values of 3.06 and 5.04 respectively, which indicates that at this concentration there is an increase in toxicity and this may be related to the differences in the mechanisms of action. Haemolysis occurs as a consequence of cellular damage but in this study it does not appear to be a sensitive indicator of cellular effects. Future studies should focus on the various changes of the specific cellular targets such as changes in antioxidant enzyme activity, GSH levels, lipid peroxidation and PS exposure.

3.5 Conclusion

In conclusion, there is inter-variability amongst individuals regarding susceptibility to metal-induced haemolysis. The low concentrations of the metals Mn and Hg, showed little haemolytic effects on the erythrocytes while at higher concentrations toxic effects were noted. It was found that Mn and Hg both had high toxicity, but Hg is the more toxic metal and synergism was observed between Mn + Hg (X100), Cu + Mn + Hg (X100) and Cu + Mn (X1000). Copper caused Hb precipitation and at higher concentrations interactions could not be determined. At low concentrations Cu and combinations induced MetHb and SulfHb formation especially for the Cu + Mn X10 group where a significant increase in both the Sulf- and MetHb, of about 5 – 10% was observed. Although not lethal, these levels for MetHb can reduce the oxygen-carrying capacity of Hb and for SulfHb these levels can be lethal.

CHAPTER 4: The effects of copper, manganese and mercury, alone and in combinations, on erythrocyte, platelet and fibrin network morphology

4.1 Introduction

The vascular system requires smooth membranes for optimal functioning and when any membrane, whether blood vessel, platelet or erythrocyte undergoes damaging alterations it causes an increase in attachment of cells to the endothelium of blood vessels and activation of the coagulation pathways. Mannucci *et al.*, (1969) reported that an increase in haemolysis adversely affects the coagulation system as haemolysed erythrocytes can increase fibrinogen, factor V and factor VIII due to intravascular coagulation by an increase in thrombo-plastic material release by the haemolysed erythrocytes. The metals can also alter coagulation factors, as discussed previously (section 2.2.3, 2.3.3 and 2.4.3), possibly due to the metals affecting endothelial cells by oxidative stress [110]. Haemolysis has been noted to be a pro-coagulant condition and incidence of increased thrombosis has been noted in patients with haemolytic anaemia. Increased thrombosis is due to multiple factors including abnormal erythrocyte properties, an increase in Hb and micro-particles in plasma and endothelial dysfunction [111]. Although the levels of haemolysis identified for Cu, Mn and Hg alone and in combination in Chapter 3 were low, this may be sufficient to alter blood haemostasis.

In addition, ROS can also activate the coagulation pathway. A study performed using PC12 cells exposed to varying amounts of MnCl_2 revealed an increase in levels of oxidants. Concentrations of 38 – 300 μM caused metabolic distress, and concentrations higher than 300 μM caused an increase in production of the oxidant H_2O_2 . Copper²⁺ can catalyse the Fenton reaction with H_2O_2 as the substrate and the generated ROS can subsequently cause lipid peroxidation as well as MetHb formation [112]. Likewise in the present study, erythrocytes were exposed to 9.1 – 91 μM Mn which represents a X1 and X10 exposure and consequently this Mn can form H_2O_2 , which as a substrate for the Fenton reaction forms radicals. In addition Cu²⁺ can oxidize Fe²⁺ resulting in MetHb and radical formation. In a mixture of metals containing different cellular targets it is time consuming and expensive to measure changes in the levels and activity of specific coagulation factors. To determine if the consequence of these effects is physiologically relevant it is better to evaluate the

consequence of exposure such as the extent of platelet activation and the density of the clot that forms.

Scanning electron microscopy is ideal for this purpose as this technique produces high resolution images of surface cellular structure and was used in the present study to investigate the effect of the metals Cu, Mn and Hg, alone and in combinations, on platelets, fibrin networks and erythrocyte morphology [113].

4.2 Materials and methods

4.2.1 Metal preparations

All reagents are the same as those used in section 3.2.1, however, the concentration ranges of the various metals only included: X1, X10 and X100 (3-point) the WHO safety level standards for each respective metal, which are: 31.47 μM for Cu, 9.1 μM for Mn and 0.004 μM for Hg. Only a 3-point concentration range was used, as these levels were more probable exposure levels than the extreme levels.

4.2.2 Blood collection

The process of blood collection was the same as described in section 3.2.2.

4.2.3 Sample preparation

Whole blood was exposed to the different metals at the 3-point concentrations and then incubated for 30 minutes, at room temperature. This exposure time was determined to be the optimal time frame for exposure through a side time-based study comparing samples exposed for 10 minutes, 30 minutes and 16 hours. The standard SEM sample preparation procedures were then followed. Blood smears (whole blood only) were made on round glass cover slips (LASEC, South Africa), with and without the addition of human thrombin [20 U/mL (Sigma-Aldrich, St Louis, MO, USA)]. The cover slips were then dried for 10 minutes and washed in PBS for 20 minutes. The samples were then fixed in a 2.5% glutaraldehyde/formaldehyde (GA/FA) (Sigma-Aldrich, St Louis, MO, USA) – [5 mL buffer solution, 1 mL GA, 1 mL FA and 3 mL distilled water (dH_2O) solution in 0.075 M PBS (pH 7.4)] for 30 minutes and then washed three times in the same buffer. The samples then underwent secondary fixation in 1% osmium tetroxide (Sigma-Aldrich, St Louis, MO, USA) for 30 minutes and were washed again as explained in the previous step. The samples were then dehydrated using increasing serial dehydration with 30%, 50%, 70% and 90% ethanol (EtOH), followed by three changes of absolute EtOH. The 100% EtOH (Merck, Darmstadt, Germany) was removed and a 100% hexamethyldisilazane (HMDS) [Merck, Darmstadt,

Germany] was used to dry the sample. Once the samples were dry, the cover slips were then mounted on aluminium stubs, coated by carbon evaporation and viewed with the Zeiss Ultra Plus FEG SEM (Oberkochen, Germany) at 1 kV.

4.3 Results

The effects of Cu, Mn and Hg alone and in combination on erythrocyte morphology (Figure 4.1), platelet activation and aggregation (Figure 4.2) and fibrin network formation of whole blood (Figure 4.3) exposed to each metal group for 30 minutes was evaluated.

Figure 4.1 shows representative images of erythrocytes acquired from blood smears prepared from whole blood without the addition of thrombin. Figure 4.1A depicts the erythrocyte control group (isoPBS) and shows the typical structure of an erythrocyte with biconcave shape, a smooth membrane and diameter of approximately 8 μm . Figure 4.1B – V shows erythrocytes exposed to X1, X10 and X100, the WHO safety level concentrations, of the metals Cu, Mn and Hg, alone and in combinations. In figure 4.1B, erythrocytes from the Cu X1 exposed group have become deformed exhibiting a bulging appearance. In figure 4.1C, the erythrocytes from the Cu X10 exposed group appeared semi-spherical and slightly swollen. Matter deposition (pink arrow) can also be seen surrounding the cells. This might be due to the ability of Cu to precipitate proteins or the spontaneous deposit of fibrin might be another possibility. At these concentrations Cu seems to have a similar effect on the erythrocytes by causing a loss in membrane integrity (due to disruption of membrane proteins) and an increase in osmosis (due to an increase in permeability to cations), which first causes bulging then swelling. In figure 4.1D, the erythrocytes from the Cu X100 exposed group revealed the formation of primary echinocytes, as indicated by the nodule-like spicules (purple arrow), which is indicative of an increased loss of membrane integrity.

Figure 4.1E, the Mn X1 exposed group, shows erythrocytes that also have a bulging appearance. In figure 4.1F, the erythrocytes from the Mn X10 exposed group became primary echinocytes with nodule-like spicules (purple arrow) and they appeared larger than the Mn X1 group. In figure 4.1G, the Mn X100 exposed group revealed erythrocytes that have either undergone formation of primary echinocytes, as indicated by the nodule-like spicules (purple arrow) or increased swelling from the bulging appearance (as seen in X1 concentration – Figure 4.1E). The degree of nodule-like spicule formation was more apparent in the X100 concentration. In Figure 4.1H, the erythrocytes from the Hg X1 exposed group also have a bulging appearance, similar to what was seen in the Cu X1 and Mn X1 groups (Figures 4.1B and 4.1E respectively). In figure 4.1I, the Hg X10 exposed group revealed erythrocytes that either appeared swollen, resulting in a spherical shape

(increase in osmosis) or cells with increased diameters, resulting in the loss of the typical biconcavity (suggesting loss in integrity of membrane proteins). In Figure 4.1J, the erythrocytes from the Hg X100 exposed group have deformed, with an increase in swelling. A ghost erythrocyte (yellow arrow) was also seen in this group which was not seen in any of the other exposed groups. This cell indicates a ruptured erythrocyte with only a membrane as remnant.

Figure 4.1K, L and M are representative of erythrocytes from the Cu + Mn combination group at X1, X10 and X100 respectively. Erythrocytes in the X1 exposed group were deformed where those from the X10 and X100 groups appeared deformed with numerous primary echinocytes (purple arrows) present. In the Cu + Hg combination groups that can be seen in figure 4.1N, O and P, the erythrocytes appeared deformed having a bulging and swollen appearance with membrane projections starting to form at the X10 concentration. Only at the X100 concentration, did the presence of primary echinocytes become apparent with an increase in nodule-like spicule formation (purple arrows).

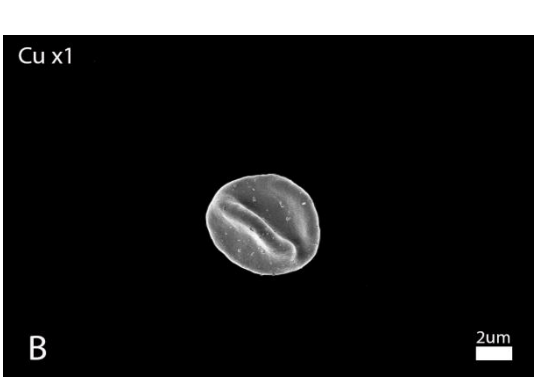
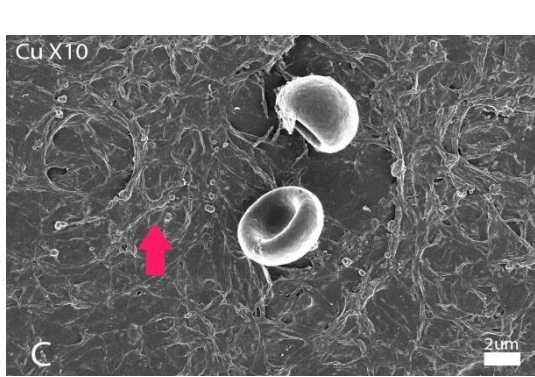
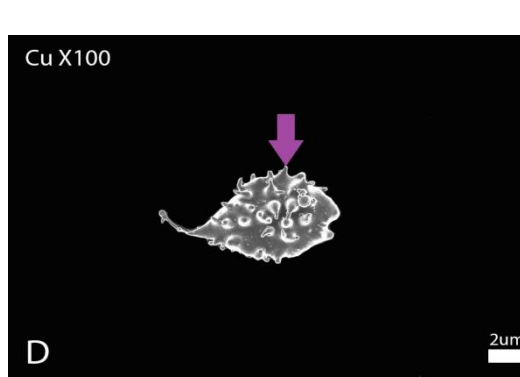
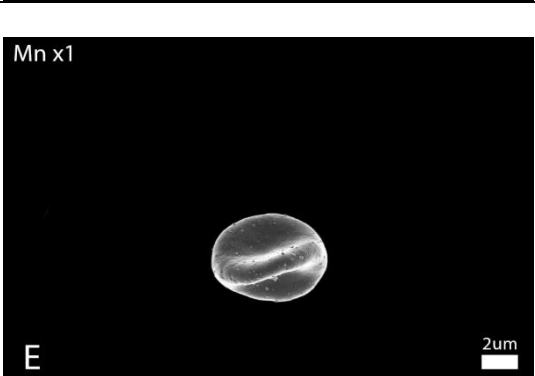
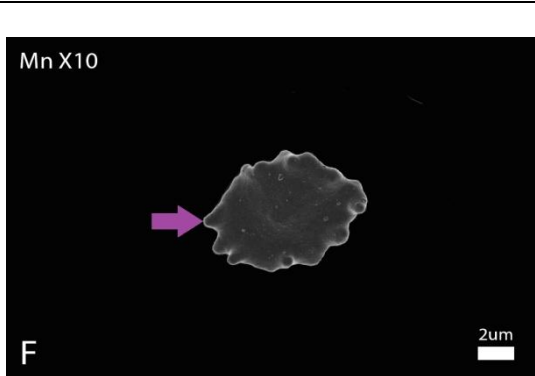
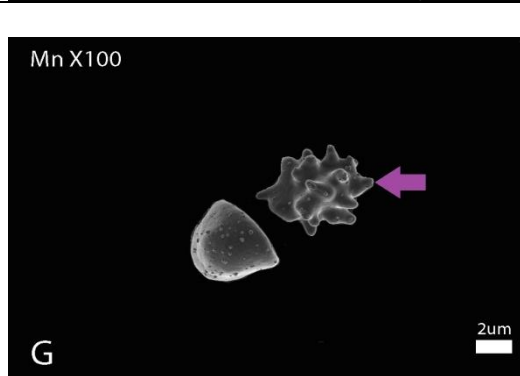
The Mn + Hg exposed groups at X1, X10 and X100 are shown in Figure 4.1Q, R and S respectively. The erythrocytes appeared deformed with some having a bulging appearance (X1) or were completely swollen (X10). The erythrocytes in the X100 exposed group had pointed extensions of the membrane, which gave them a pinched-off appearance. In Figure 4.1T, the triple combination (Cu + Mn + Hg) X1 exposed group revealed erythrocytes ranging in their deformation from slightly abnormal to bulging and swelling to nodule projections starting to form. In Figure 4.1U, the X10 exposed group shows erythrocytes that also have membrane deformation, similar to that of the X1 group. In figure 4.1V, the X100 exposed erythrocytes also have deformation with pointed extensions of the membranes. A summary of the findings on erythrocyte morphology is shown in Table 4.1.

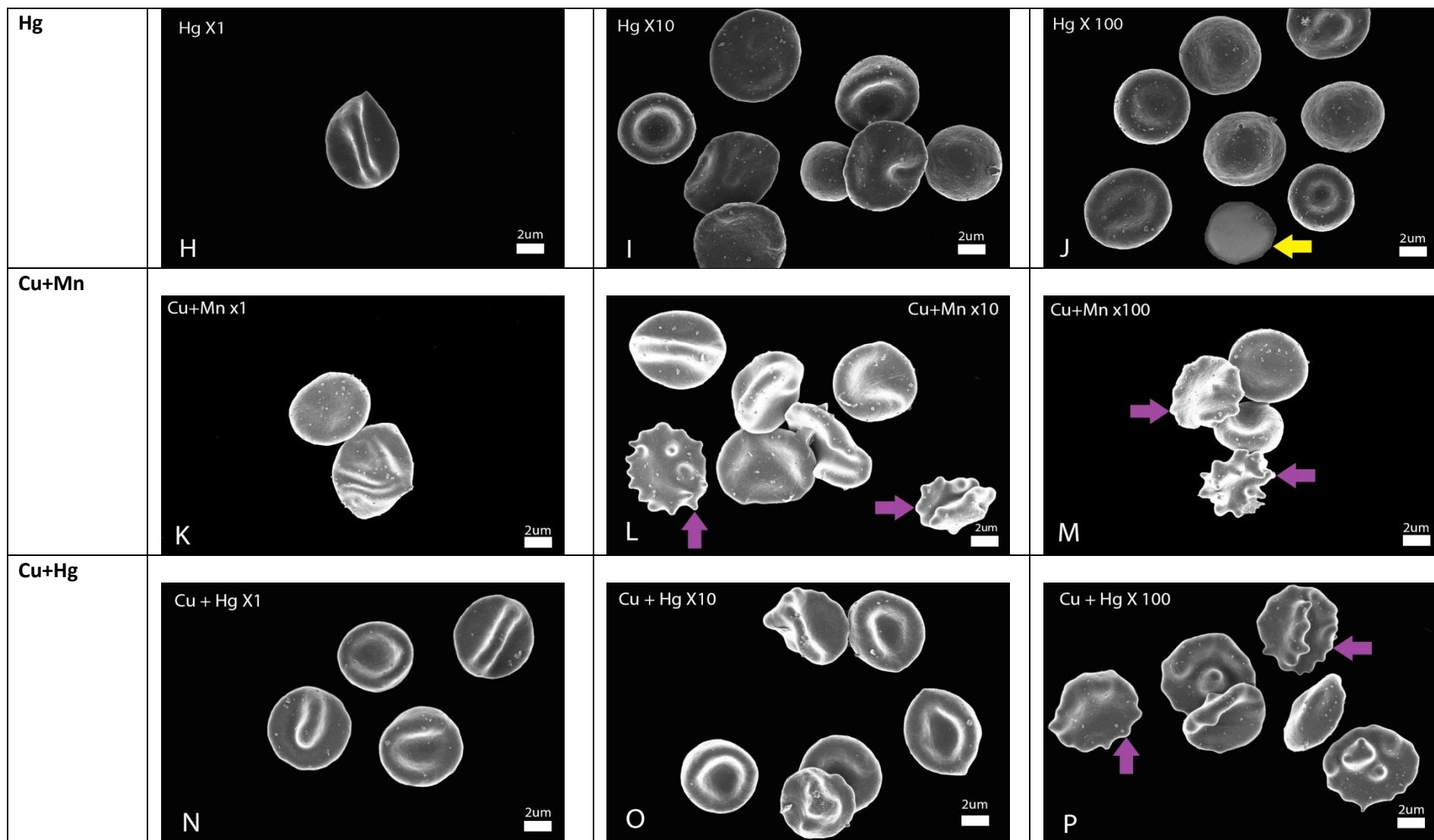
Table 4.1: Summary of morphological changes to erythrocytes exposed to metal combinations.

	Altered shape	Swollen or bulging	Echinocyte formation	Pointed extension or membrane projection	Matter deposition	Nodule-like spicules	Ghost cells
Cu							
X1	X	X	-	-	-	-	-
X10	X	X	-	-	X	-	-
X100	X	-	X	-	-	X	-
Mn							
X1	X	X	-	-	-	-	-
X10	X	-	X	-	-	X	-
X100	X	X	X	-	-	X	-
Hg							
X1	X	X	-	-	-	-	-
X10	X	X	-	-	-	-	-
X100	X	X	-	-	-	-	X

<u>Cu + Mn</u>							
X1	X	-	-	-	-	-	-
X10	X	X	X	-	-	X	-
X100	X	X	X	-	-	X	-
<u>Cu + Hg</u>							
X1	X	X	-	-	-	-	-
X10	X	X	-	X	-	-	-
X100	X	X	X	-	-	X	-
<u>Mn + Hg</u>							
X1	X	X	-	-	-	-	-
X10	X	X	-	-	-	-	-
X100	X	-	-	X	-	-	-
<u>Cu + Mn + Hg</u>							
X1	X	X	-	X	-	-	-
X10	X	X	-	X	-	-	-
X100	X	-	-	X	-	-	-

X indicates a presence of a particular feature whilst – indicates the absence of a particular feature.

Control	<div data-bbox="376 193 909 536"> <p>Control</p>  <p>A</p> <p>2um</p> </div>		
Group	1x	10x	100x
Cu	<div data-bbox="376 576 909 954"> <p>Cu x1</p>  <p>B</p> <p>2um</p> </div>	<div data-bbox="958 576 1491 954"> <p>Cu X10</p>  <p>C</p> <p>2um</p> </div>	<div data-bbox="1529 576 2047 954"> <p>Cu X100</p>  <p>D</p> <p>2um</p> </div>
Mn	<div data-bbox="376 954 909 1331"> <p>Mn x1</p>  <p>E</p> <p>2um</p> </div>	<div data-bbox="958 954 1491 1331"> <p>Mn X10</p>  <p>F</p> <p>2um</p> </div>	<div data-bbox="1529 954 2047 1331"> <p>Mn X100</p>  <p>G</p> <p>2um</p> </div>



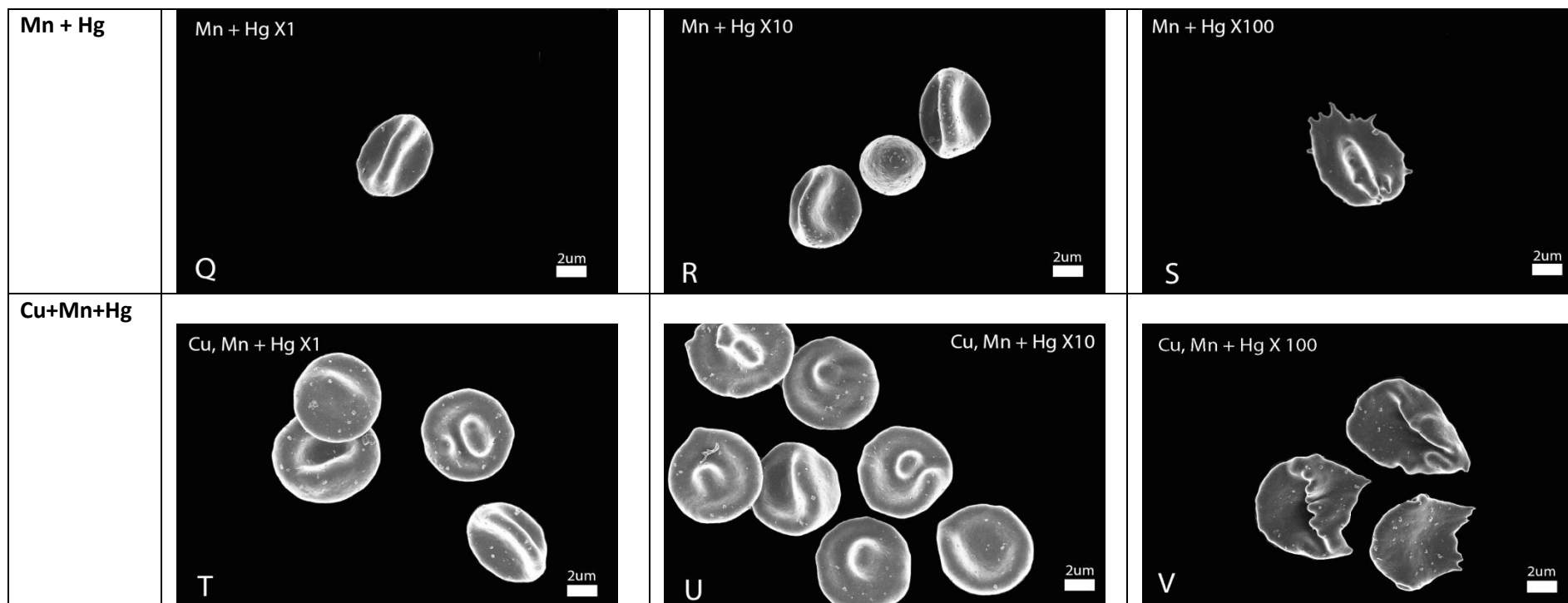


Figure 4.1: Scanning electron micrographs of whole blood without thrombin exposed to Cu, Mn and Hg, alone and in combination at concentrations of X1, X10 and X100 showing erythrocyte morphology; Scale bar = 2 μ m. **(A):** Control; **(B – D):** Cu X1, X10 and X100, **(E – G):** Mn X1, X10 and X100, **(H – J):** Hg X1, X10 and X100, **(K – M):** Cu + Mn X1, X10 and X100, **(N – P):** Cu + Hg X1, X10 and X100, **(Q – S):** Hg + Mn X1, X10 and X100, and **(T – V):** Cu + Mn + Hg X1, X10 and X100. **Pink arrows:** Deposition; **Purple arrows:** Nodule-like spicules and **Yellow arrows:** Ghost cells.

Figure 4.2A depicts the platelet control group (isoPBS) and shows normal morphology of a spherical platelet with few pseudopods. The open canalicular system (OCS) of the platelet can also be seen (indigo arrow). The OCS allows for the exit of granules from inside the platelet, when the platelet is activated. Inactivated platelets are generally discoid and flattened in shape with no pseudopods, but experimentally platelets can become slightly activated with few pseudopods due to contact activation [114].

Figure 4.2B, C and D are representative of platelets in the Cu X1, X10 and X100 exposed groups respectively. Platelets from the Cu X1 group showed an increase in platelet spreading (orange arrow) and platelet interaction was also visible (light yellow arrow). Platelets from the Cu X10 group also showed an increase in platelet spreading (orange arrow). In Figure 4.2D, the Cu X100 exposed group revealed platelets that aggregated (red arrow) as well as numerous pseudopodia present (green arrow) and membrane spreading (orange arrow), indicating clotting. Platelet interaction could also be seen (light yellow arrow). Figure 4.2E, F and G are representative of platelets in the Mn X1, X10 and X100 exposed groups respectively, where platelets showed an increase in platelet activation (early spread) that can be visualised as an increase in pseudopods (green arrow) in the Mn X1 group. An increase in spreading (orange arrow) can be seen in the Mn X10 exposed platelets, indicating an increase in activation and the Mn X100 group revealed an aggregation (red arrow) of multiple platelets, again with an increase in pseudopodia and spreading (orange arrow), indicating clotting.

The Hg exposed groups are represented in Figure 4.2H, I and J and shows an increase in activation with the presence of numerous pseudopods (green arrow) and platelet interaction (light yellow arrow) at the X1 concentration whereas at the X10 concentration a mass of aggregated platelets (red arrow) that appears necrotic can be seen. This effect is more severe in the X100 exposed group. In Figure 4.2K, platelets from the combination of Cu + Mn at a concentration of X1 the WHO, are shown where an increase in platelet pseudopodia (green arrows), and platelet interaction (light yellow arrow) can be seen. In the Cu + Mn X10 (Figure 4.2L) and X100 (Figure 4.2M) groups, an increase in platelet activation was observed by the presence of platelet aggregates (red arrow) and multiple pseudopodia (green arrow) in both concentration groups. However, this effect was more severe in the X100 exposed group where an increase in platelet spreading (orange arrows) was evident.

Figure 4.2N, O and P are representative of platelets in the Cu + Hg combination group at the three different concentrations respectively. Platelet spreading (orange arrow) was observed in the Cu + Hg X1 group, resulting in the 'fried egg' morphology. In Figure 4.2O, platelet spreading (orange arrow) and aggregation (red arrow) of multiple platelets with an increase

in pseudopodia was evident whereas in the Cu + Hg X100 exposed group the effect was more severe with an increase in platelet spreading (orange arrow) and aggregation (red arrow) with a necrotic appearance (membrane roughness) also visible. In Figure 4.2Q, platelets from the Mn + Hg X1 exposed group resulted in a mass of multiple aggregated platelets (red arrow) with an increased number of pseudopodia (green arrow). In the Mn + Hg X10 (Figure 4.2R), platelets have also formed an aggregate (red arrow) with the multiple platelets having increased pseudopodia (green arrow) and spreading (orange arrow) and those from the Mn + Hg X100 (Figure 4.2S) exposed group also showed a large aggregation as well as spreading (orange arrow).

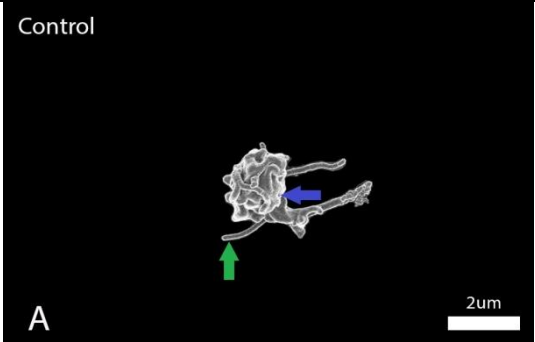
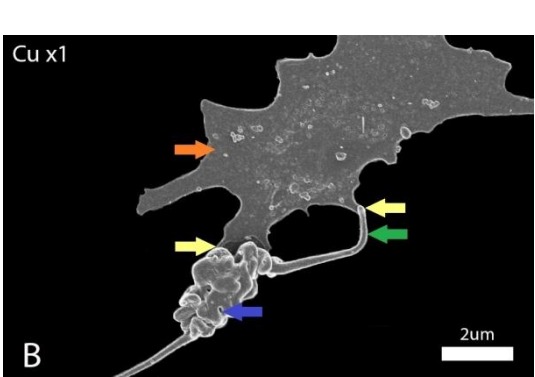
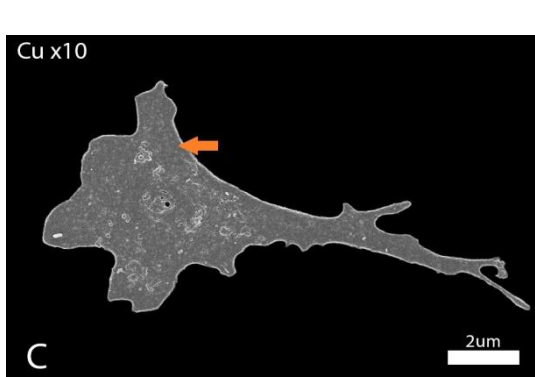
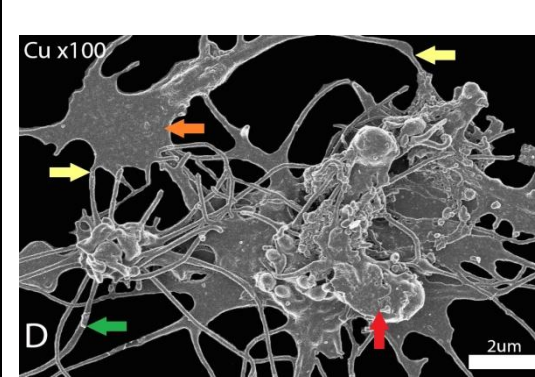
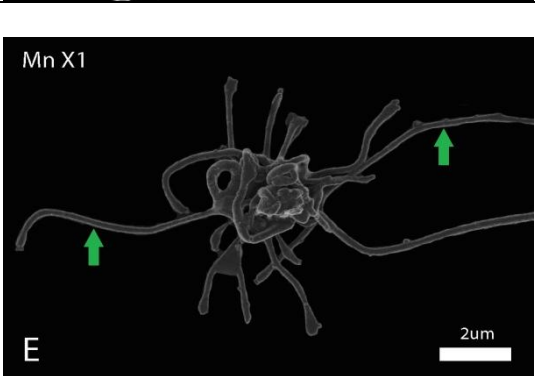
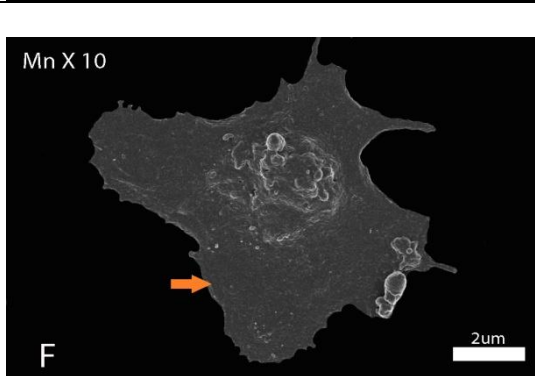
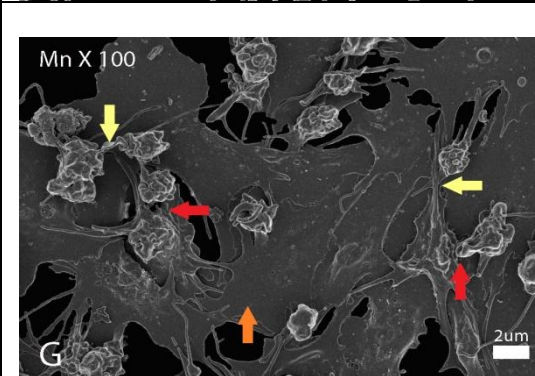
In the triple combination group represented in Figures 4.2T, U and V, an increase in platelet spreading (orange arrow) was observed in the X1 group with aggregates (red arrow) forming in the X10 group where numerous platelets had membrane spreading (orange arrow) as well. In Figure 4.2V, the platelets from the X100 exposed group revealed a large mass of aggregated platelets (red arrow) indicating clotting, however this mass of platelets appear to be necrotic or damaged, as indicated by an increase in membrane roughness. A summary of the findings on platelet morphology is shown in Table 4.2.

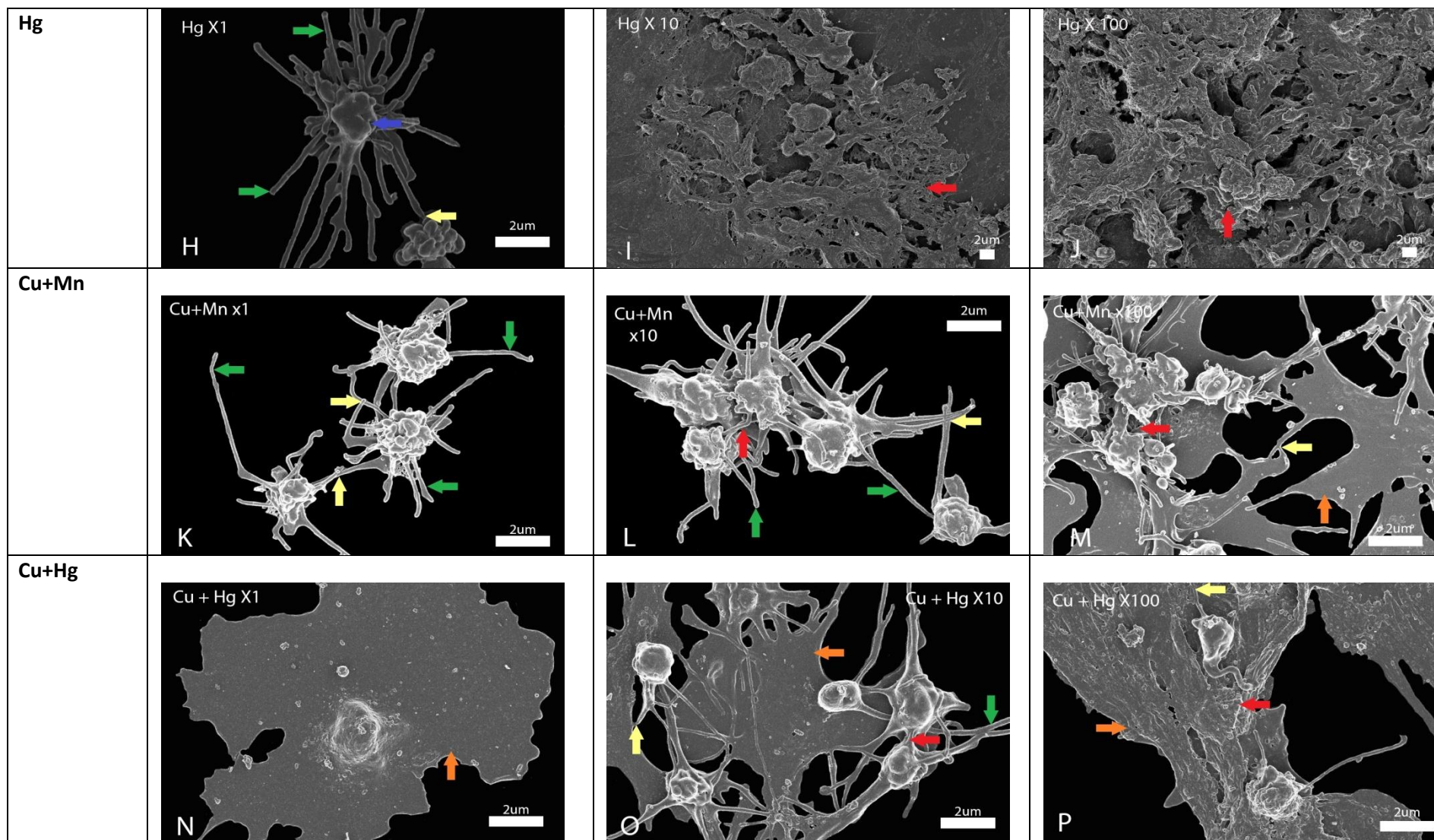
Table 4.2: Summary of morphological changes to platelets exposed to metal combinations.

	Visible OCS	Increased pseudopodia	Membrane spreading	Platelet interaction	Aggregation	Necrosis
<u>Cu</u>						
X1	X	-	X	X	-	-
X10	-	-	X	-	-	-
X100	-	X	X	X	X	-
<u>Mn</u>						
X1	-	X	-	-	-	-
X10	-	-	X	-	-	-
X100	-	-	X	X	X	-
<u>Hg</u>						
X1	-	X	-	X	-	-
X10	-	-	-	X	X	X
X100	-	-	-	X	X	X
<u>Cu + Mn</u>						
X1	-	X	-	X	-	-
X10	-	X	-	X	X	-
X100	-	-	X	X	X	-
<u>Cu + Hg</u>						
X1	-	-	X	-	-	-
X10	-	X	X	X	X	-
X100	-	-	X	X	X	-

<u>Mn + Hg</u>						
X1	-	X	-	X	X	-
X10	-	X	X	X	X	-
X100	-	X	X	X	X	-
<u>Cu + Mn + Hg</u>						
X1	-	-	X	-	-	-
X10	X	X	X	X	X	-
X100	-	-	-	X	X	X

X indicates a presence of a particular feature whilst – indicates the absence of a particular feature.

Control	<p>Control</p>  <p>A</p>		
Group	1x	10x	100x
Cu	<p>Cu x1</p>  <p>B</p>	<p>Cu x10</p>  <p>C</p>	<p>Cu x100</p>  <p>D</p>
Mn	<p>Mn X1</p>  <p>E</p>	<p>Mn X 10</p>  <p>F</p>	<p>Mn X 100</p>  <p>G</p>



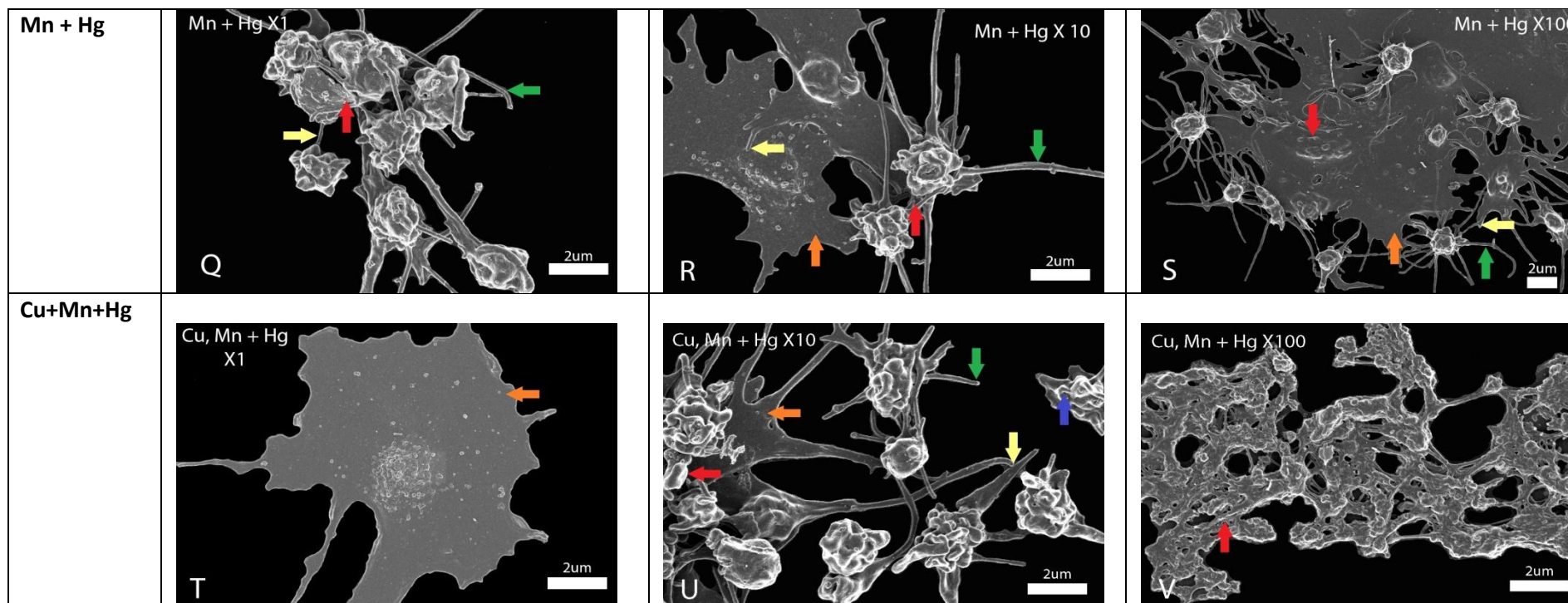


Figure 4.2: Scanning electron micrographs of whole blood without thrombin exposed to Cu, Mn and Hg, alone and in combination at concentrations of X1, X10 and X100 showing platelet morphology; Scale bar = 2 µm. **(A):** Control; **(B – D):** Cu X1, X10 and X100, **(E – G):** Mn X1, X10 and X100, **(H – J):** Hg X1, X10 and X100, **(K – M):** Cu + Mn X1, X10 and X100, **(N – P):** Cu + Hg X1, X10 and X100, **(Q – S):** Hg + Mn X1, X10 and X100, and **(T – V):** Cu + Mn + Hg X1, X10 and X100. **Green arrows:** Pseudopodia; **Indigo arrows:** Open canalicular system; **Light Yellow arrows:** Platelet interaction; **Orange arrows:** Platelet spreading and **Red arrows:** Platelet aggregates.

Thrombin was added to whole blood smears in order to form and visualise any alterations in the fibrin fibre networks, caused by metal exposure. Fibrin fibres that form clots are the thin minor fibres (light blue arrows) together with the thick major fibres (light green arrows). Alterations in the amount and prevalence of the two types of fibrin fibres can induce thrombosis through a decrease in clot lysis.

Figure 4.3A is representative of the control group and depicts whole blood with added thrombin where normal shaped erythrocytes can be seen with some fibres in between (normal thick and thin fibres indicated by the light green and blue arrows respectively).

Figure 4.3B – V shows representative images of whole blood with thrombin exposed to X1, X10 and X100, the WHO safety level concentrations, of the metals Cu, Mn and Hg, alone and in combinations. In Figure 4.3B, the Cu X1 exposed group, a fibrin network can be seen covering the erythrocytes showing thin (light blue arrow) and thick (light green arrow) fibrin fibres. Many of the thick fibres appeared bended or less taut (brown arrow). Some deformed erythrocytes can also be seen (pink arrow). In the Cu X10 group in Figure 4.3C, the fibres formed a well-defined network with numerous thick fibres (light green arrow) present. There are some less taut fibres (brown arrow) but overall the fibres looked taut and straight with some fibres forming sticky masses (maroon arrow) and also having a net-like covering appearance (peach arrow). When the erythrocytes become trapped in the fibrin network during clot formation, they can no longer hold their characteristic biconcave shape and thus deform (pink arrow). In Figure 4.3D, the Cu X100 exposed group, the fibrin networks appear less taut (brown arrow) overall and have increased sticky fibrin masses (maroon arrow) and less organisation of the fibrin fibres can be seen, as compared to the X10 concentration. Deformed erythrocytes are also visible (pink arrow).

In Figure 4.3E, the Mn X1 group revealed various areas of thin fibres forming net-like coverings (peach arrow) or fused fibrin fibres (light purple arrow) and the thick fibres forming sticky fibrin masses (maroon arrow). Some fibres appear less taut (brown arrow) and the erythrocytes also appear deformed (pink arrow). In Figure 4.3F, the Mn X10 group shows a large area of fused thin fibres (light purple arrow) forming a net-like covering (peach arrow). As with the X1 concentration, some fibres appear less taut (brown arrow) and the erythrocytes also appear deformed (pink arrow). In Figure 4.3G, the Mn X100 exposed fibrin networks have formed a fused area of fibres (light purple arrow) constituted of thin fibres and sticky fibrin masses (maroon arrow), presenting as disorganised fibrin formation. Individual fibres could not clearly be distinguished. Some fibres appear less taut (brown arrow) and the erythrocytes in this experimental group are also deformed (pink arrow).

In Figure 4.3H, the Hg X1 exposed group revealed fibrin networks with a fused area by thin fibres (light purple arrow), in which the deformed erythrocytes (pink arrow), become trapped. Some fibres appear less taut (brown arrow). In Figure 4.3I, the Hg X10 exposed group, the presence of less taut fibres (brown arrow), in which the deformed erythrocytes (pink arrow) become trapped, is more apparent as compared to the X1 concentration,. A worsened effect was seen in the Hg X100 exposed group represented by Figure 4.3J where a large amount of net-like coverings are formed by the thin fibres (peach arrows) with an underlying layer of fused fibrin fibres (light purple arrow) and less taut fibres (brown arrows) being more prominent. At all three concentrations the fibres have an unorganised, haphazard structure.

Figure 4.3K, L and M represent whole blood with added thrombin from the Cu + Mn exposed groups at the three various concentrations. In the X1 exposed group, indicated in Figure 4.3K, thin (light blue arrow) and thick (light green arrow) fibres, in which the deformed erythrocytes (pink arrow) become trapped, can be seen. Some less taut fibres (brown arrow) are also visible. In the X10 exposed group, figure 4.3L, the fibrin networks started to form net-like coverings (peach arrow) over the erythrocytes. There are some convoluted fibres but the majority are taut. The fibrin fibres, in which the deformed erythrocytes (pink arrow) become trapped, appear mesh-like. Some thick fibres have also started to stick together (maroon arrow). In Figure 4.3M, the Cu + Mn X100 exposed fibrin networks have fused together (light purple arrow) and formed a net-like covering (peach arrows), which appears necrotic as shown by the membrane roughness. Less fibres are present than what was seen in the X10 concentration with, again, deformed erythrocytes (pink arrow) and less taut fibres (brown arrow) present.

Figure 4.3N is representative of the Cu + Hg X1 exposed group, with fibrin networks showing fused areas of thick fibres (maroon arrow) and a net-like covering of thin fibres (peach arrow) with some areas having fused fibrin fibres (light purple arrow), in which the deformed erythrocytes (pink arrow) become trapped. Some less taut fibres (brown arrow) are also visible. In Figure 4.3O, the Cu + Hg X10 exposed group revealed fused thin fibrin fibres (light purple arrow) forming a net-like covering (peach arrow), which appeared as a thick layer over the regular fibres. Deformed erythrocytes (pink arrow) are also visible. This area appears to have precipitated proteins (Cu's ability) on top of it. In Figure 4.3P, the Cu + Hg X100 exposed fibrin networks appear less organised with more convoluted fibres (brown arrow) and the presence of fused fibrin areas (light purple arrow) can also be seen. The thick fibres appear to be forming clumps or sticky masses (maroon arrow). Deformed erythrocytes are also visible (pink arrow).

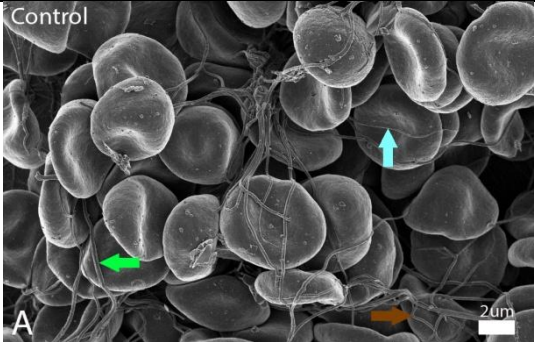
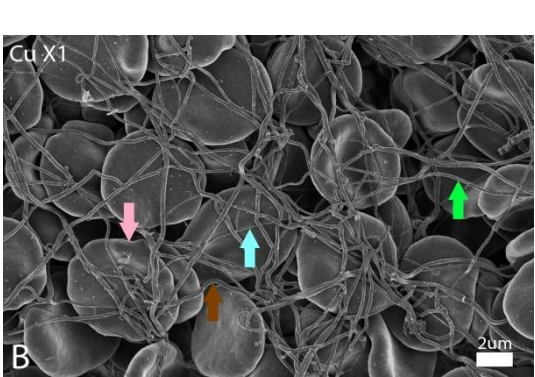
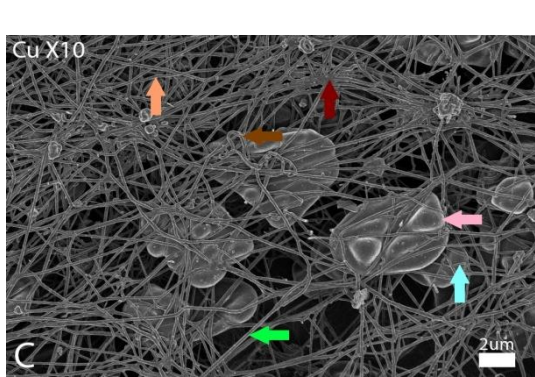
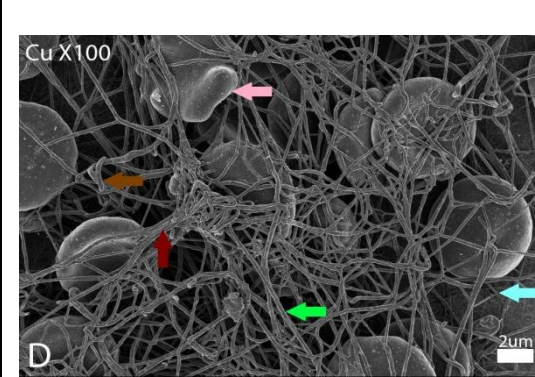
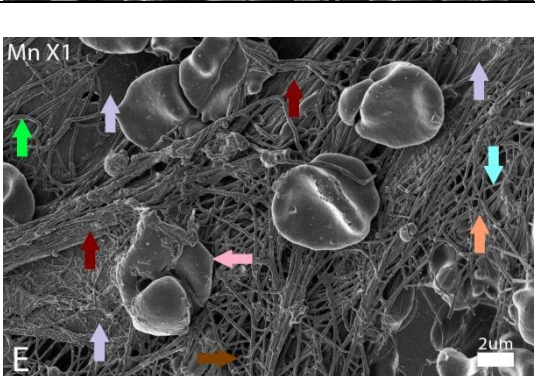
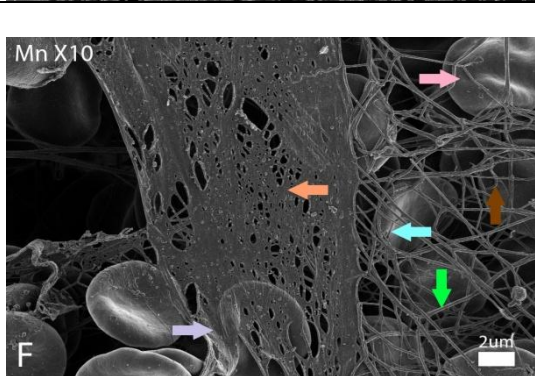
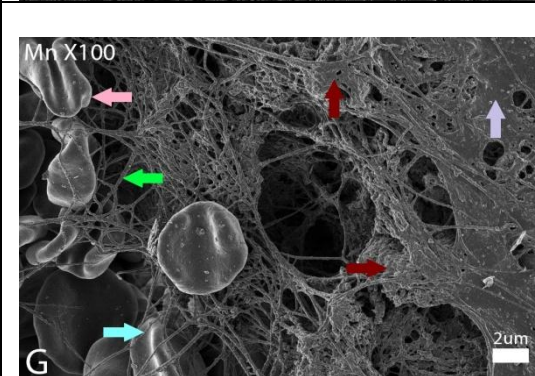
In Figure 4.3Q – S, the Mn + Hg X1, X10 and X100 respectively, exposed fibrin fibres appear to have a similar trend of less organised fibrin fibres that are less taut (brown arrow), in which the deformed erythrocytes (pink arrow) become trapped. These fibres are also starting to form sticky masses (maroon arrow). In Figure 4.3T, the triple combination group at X1 concentration shows fibrin networks that appear similar to the control with the presence of thin and thick fibrin fibres (light blue and light green arrow) with some less taut fibres (brown arrow). In Figure 4.3U, the X10 exposed group, some less taut fibres (brown arrow) and thick fibres sticking together (maroon arrow) can be seen. The fibres, in which the deformed erythrocytes (pink arrow) become trapped, appear unorganised. In Figure 4.3V, the X100 exposed group, net-like covering of thin fibres (peach arrow) is visible and the thick fibres are starting to form masses (maroon arrow), in which the deformed erythrocytes (pink arrow) become trapped. A summary of the findings observed in whole blood with added thrombin is shown in Table 4.3.

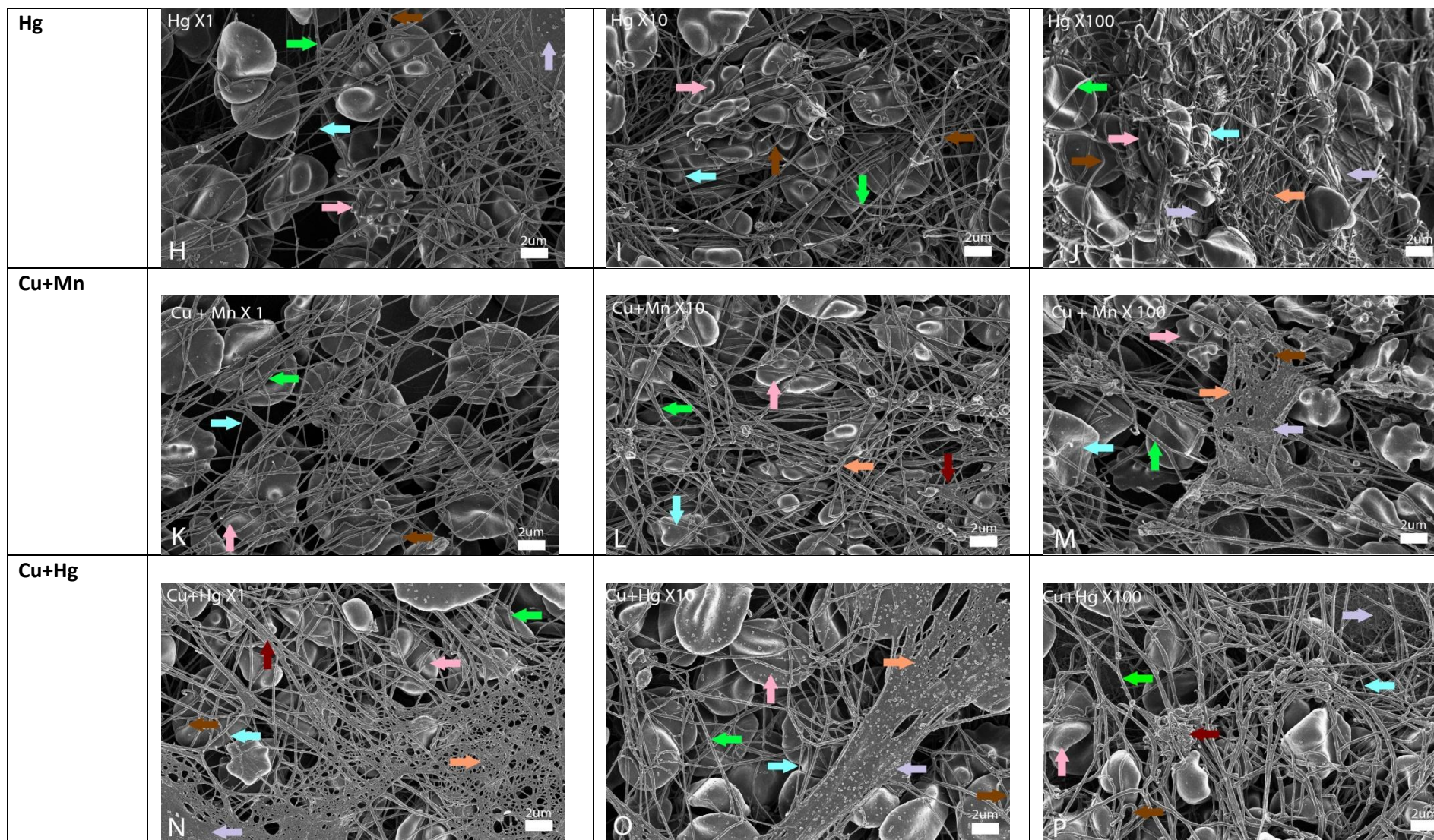
Table 4.3: Summary of changes observed in whole blood with added thrombin exposed to metal combinations.

	Deformed erythrocytes	Presence of major thick and minor thin fibres	Less taut fibres	Net-like covering of minor thin fibres	Sticky masses of thick fibres	Fused areas
<u>Cu</u>						
X1	X	X	X	-	-	-
X10	X	X	X	X	X	-
X100	X	X	X	-	X	-
<u>Mn</u>						
X1	X	X	X	X	X	X
X10	X	X	X	X	-	X
X100	X	X	X	-	X	X
<u>Hg</u>						
X1	X	X	X	-	-	X
X10	X	X	X	-	-	-
X100	X	X	X	X	-	X
<u>Cu + Mn</u>						
X1	X	X	X	-	-	-
X10	X	X	-	X	X	-
X100	X	X	X	X*	X	X
<u>Cu + Hg</u>						
X1	X	X	X	X	X	X
X10	X	X	-	X	-	X
X100	X	X	X	-	X	X
<u>Mn + Hg</u>						
X1	X	X	X	-	X	-
X10	X	X	X	-	X	-
X100	X	X	X	-	X	-

Cu + Mn + Hg						
X1	X	X	X	-	-	-
X10	X	X	X	-	X	-
X100	X	X	-	X	X	-

* Indicates with necrosis; X indicates a presence of a particular feature while – indicates the absence of a particular feature.

Control			
Group	1x	10x	100x
Cu			
Mn			



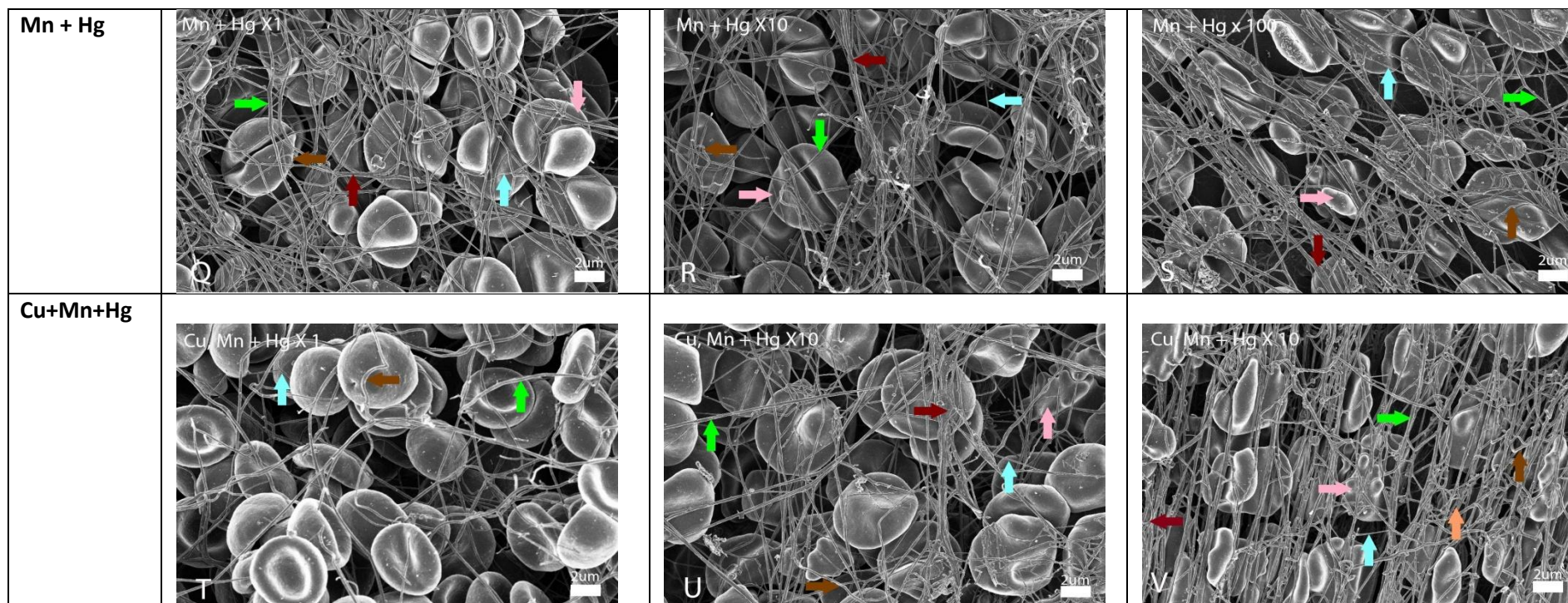


Figure 4.3: Scanning electron micrographs of whole blood with thrombin exposed to Cu, Mn and Hg, alone and in combination at concentrations of X1, X10 and X100 showing fibrin network formation together with erythrocytes; Scale bar = 2 μm . **(A):** Control; **(B – D):** Cu X1, X10 and X100, **(E – G):** Mn X1, X10 and X100, **(H – J):** Hg X1, X10 and X100, **(K – M):** Cu + Mn X1, X10 and X100, **(N – P):** Cu + Hg X1, X10 and X100, **(Q – S):** Hg + Mn X1, X10 and X100, and **(T – V):** Cu + Mn + Hg X1, X10 and X100. **Brown arrows:** Bending, less taut fibres; **Light Blue arrows:** Thin minor fibres; **Light Green arrows:** Thick major fibres; **Light Purple arrows:** Fused fibrin fibre areas; **Maroon arrows:** Sticky mass of fibrin fibres; **Peach arrows:** Net-like covering of thin fibres; and **Pink arrows:** Deformed erythrocytes.

4.4 Discussion

Due to the abundance of erythrocytes in the bloodstream, these cells represent a potential target for heavy metal ions. Heavy metal ions bind to the outer membrane surface of the erythrocytes and can induce echinocyte formation and other associated morphologies as shown in Figures 2.2 and 2.3 [115]. Overall the micrographs of the erythrocytes seem to depict that the different groups at different concentrations, all showed an increase in deformation of erythrocytes to a certain degree from swelling and bulging of the membrane to nodule projections and spike formation. Thus all erythrocytes were different to the control and showed a loss in membrane integrity due to the effects of the metal cations. All the X1 concentrations groups tended to show bulging in the membrane. Copper at X100 appeared to cause the highest degree of echinocyte formation, which may be due to Cu being a strong redox agent [32]. Also, the metal combinations with Cu tended to increase deformation as compared to the singular metals. Erythrocytes do not contain nuclei or mitochondria and undergo their own type of apoptosis, known as eryptosis. Eryptosis removes defective erythrocytes before haemolysis or the rupturing of the erythrocyte membrane can occur and thus prevents the release of intracellular materials [43]. Eryptosis is stimulated mainly through oxidative stress, for metal ions [68]. Eryptotic erythrocytes adhere to the vascular wall and can result in a decrease in microcirculation and contribution to thrombosis and anaemia [43].

The metal ions cause oxidative stress and thus PS exposure. PS exposed erythrocytes are able to adhere to the endothelium of blood vessels. Deformation of erythrocytes through micro-vesicle generation also contributes to an increase in the pro-coagulant state, by enhancing thrombin generation [43]. Micro-vesiculation occurs with an increase in intracellular Ca^{2+} concentrations, which induces shape change from discocytes to echinocytes and micro-vesicle budding off from the spicules or projections [116].

Platelets are an essential blood component that prevents continual blood loss following injury by forming a platelet plug which is crucial for haemostasis [114, 117]. When the coagulation cascade is activated, due to bleeding, platelets change shape and become activated in order to form a plug. *In vitro*, the coagulation cascade becomes activated by thrombin [114]. To determine if the metals, alone and in combination, induces coagulation, no thrombin was added to the whole blood smears. Thus any activation or change to platelet morphology would be a direct effect of metal exposure.

Platelet activation and morphological alterations including an increase in pseudopodia, spreading and aggregate formation which is indicative of the activation of the coagulation

cascade was seen in all the experimental groups. Thus all the metals at all concentrations evaluated have the potential to induce platelet activation. The experimental groups, at the X100 concentrations, showed aggregate formation. The Hg group appeared to be the most toxic as it formed necrotic aggregates at both the X10 and X100 concentrations. The combination metal groups appeared to be more potent than their singular metal counterparts, except for Hg, as the combination groups all formed aggregates even at the X10 concentration. The Cu + Mn and Mn + Hg combinations both showed aggregation at the lowest concentration (the WHO safety level). An increase in pseudopodia and membrane spreading is an indication for increased activation of platelets, which can increase the likelihood of clot formation [54].

Clotting of blood is highly dependent on the interaction between fibrinogen and thrombin. Clot formation is due to the interaction of platelets and erythrocytes together with fibrin fibres [114]. Thrombin is responsible for the conversion of fibrinogen to fibrin which then polymerises to form fibres. These fibrin fibre polymers cross-link longitudinally and transversely [117]. Fibrin fibres play a large role in the parameters of the clot as clots are in most part formed by fibrin fibres, but clots also contain erythrocytes and activated platelets as previously discussed [114]. The conversion of fibrinogen to fibrin, with thrombin catalysing this reaction, consists of three reversible steps. The first is the proteolysis of fibrinogen to fibrin monomers and fibrinopeptides (Fp) A and B. In the second step the fibrin monomers begin to polymerise through non-covalent bonding. Lastly, the polymers then aggregate to form a fibrin clot [118].

Thrombus formation is controlled through three pathways of the coagulation cascade. Firstly, enzyme inhibitors ensure homeostasis of coagulation enzymes. Secondly, once thrombin has been formed endothelial thrombomodulin-thrombin complexes activate protein C which inactivates factors Va and VIIIa, which results in the inhibition of thrombin formation. Lastly, the TF pathway inhibitor (TFPI) with protein S inhibits factor Xa resulting in inhibition of TF and factor VIIa (extrinsic pathway) [119]. This pathway is a negative feedback loop which ensures correct clotting and coagulation functioning [119]. Plasma TF can be found on and is enhanced by circulating micro-vesicles and both resting and activated platelets. Therefore, micro-vesicles and platelets are the main sites of active TF in human blood [120]. Any alteration to these mechanisms in the cascade can have an effect on coagulation through an imbalance of the enzymes thus resulting in a potential hypercoagulable state.

Platelet activation and echinocyte formation by all metals at most concentrations possibly indicates a common pathway of activation. This activation of a common pathway is most likely due to the ROS generation by the metals. With ROS-induced change in erythrocyte

morphology and membrane permeability, there is an increase in the uptake of Ca^{2+} , stimulation of scramblase leading to PS exposure. Consequent loss of K^+ leads to erythrocyte shrinkage. Cell shrinkage leads to the release of platelet activating factor (PAF), which further triggers cell shrinkage and PS exposure [121]. Platelet aggregation is then induced by PAF. Tissue factor coagulant activity can also be regulated with PS exposure on cell surfaces. Thus an increase in ROS, which results in an increase in PS exposure, can increase TF and therefore a proagulant state of blood [122]. The ROS can also cause alterations in the initial stages of the coagulation cascade.

Cimmino *et al.*, (2015) studied the effect of ROS on TFPI and found a degradation of TFPI with an increase in ROS formation. This means a decrease in the binding of TFPI to factor Xa and thus a decrease in the inhibition of the extrinsic pathway. A decrease in the inhibition will result in the continuous formation of fibrin polymers and thus a fibrin clot causing hypercoagulation or a proagulant state [119]. Activation of TF can also be induced by free heme as heme produces ROS and is highly toxic. The free heme can damage and activate endothelial cells in which TF is present and thus initiates clotting [123]. Therefore, the haemolysis inducing metals – Mn and Hg – would increase the free heme and thus ROS formation within the solution, which could result in a hypercoagulable state due to an increase in TF.

Crutchley and Que (1995) reported that THP-1 cells (monocytic) that were exposed to Cu^{2+} ions at a concentration of 5 – 10 $\mu\text{mol/L}$ had an increase in cellular damage, and TF expression was 70 times higher than that of the control. This was achieved with a lipophilic chelating agent in order to transport the Cu^{2+} ions intracellularly [124]. The increased expression of TF can result in a hypercoagulable state. Van den Besselaar (2002) reported that at a concentration of 0.5 mmol/L of Mn, the maximum shortening of TF-induced coagulation time was obtained [50]. Wierzbicki *et al.* (1983) reported that bovine fibrinogen binds Hg and following binding thrombin-mediated clotting was more than the control samples. In humans exposed to mercuric vapours, Wierzbicki *et al.* (2002) reported that there was an increase in thrombin-antithrombin complexes, β -thromboglobulin and a decrease in protein C activity in workers which indicated that in these workers there was a shift to a hypercoagulable state [125, 126].

Overall the micrographs of the whole blood with added thrombin showed that the different groups at different concentrations, except Cu + Mn + Hg X1, have an increase in the potential for clot formation. Less organised fibres as well as less taut fibres are present when clot retraction is inadequate. A decrease in clot retraction affects fibrinolysis, which ultimately lengthens the time of coagulation and thus increases the potential of thrombus formation.

Sticky thick fibres that mass together can also be indicative of a reduction in clot lysis time and therefore increase thrombus potential [114]. The combination with least toxic effect appeared to be the Cu + Mn and Hg X1 combination, whilst the most toxic group appeared to be Mn, as at the lowest concentration sticky masses and net-like coverings were formed while at the highest concentration necrosis was observed. The Hg and Cu + Hg groups also had a detrimental effect on coagulation with the lowest concentration also forming net-like coverings. Associated with the deformed erythrocytes are increased fibrin fibres, in which the deformed erythrocytes (pink arrow) become trapped.

The effects of Cu, Mn and Hg alone and in combination targets erythrocytes and platelets and the consequence of these effects is a hypercoagulable state with abnormal fibrin clot formation.

4.5 Conclusion

In conclusion, the various blood constituents revealed different sensitivities to different metal groups. Based on the ability of Cu, Mn and Hg to induce ROS via different pathways and mechanisms, ROS-induced echinocyte formation was the greatest for Mn. The combination of Mn and Cu had the greatest impact on erythrocyte morphology. Activation and necrosis of platelets were most evident at the highest Hg concentration. All double metal combinations caused platelet interactions and aggregation. Only at the X100 concentration for the Cu, Mn and Hg combination did activation of platelets and necrosis occur. Using whole blood the consequence of each of the above effects on clot formation was determined. Even at X1, Mn caused the formation of net like structures of thin fibres, sticky masses of thick fibres with fused areas. In combination with Cu and Hg, a similar effect was observed, although for Cu, Mn and Hg a lesser effect was observed since Mn content of this combination was lower. Novel findings were that even at X1 Mn adversely affected coagulation.

CHAPTER 5: The quantitative effects of copper, manganese and mercury, alone and in combinations, on coagulation parameters

5.1 Introduction

There is a limitation to morphological studies, as they provide qualitative data and not quantitative data. Therefore TEG[®] was used to provide this project with a method to accurately quantify the qualitative data generated in chapter 4. Thromboelastography[®] has been used to determine coagulation properties in trauma cases, patients that are undergoing heart surgery or liver transplantation, obstetric haemorrhage and in the development of new anti-coagulant drugs [127, 128]. In addition this will provide an indication whether TEG[®] can be used to evaluate the effect of exposure to Cu, Mn and Hg, alone and in combination, on clot formation in exposed populations.

Clot formation is achieved through platelet activation and signalling via the coagulation cascade (Figure 2.4) [69]. There are some methods that measure the functionality of clot formation through various parameters, however, these methodologies take time and also do not accurately represent the coagulation as a whole as they test these parameters individually. The TEG[®] is a method that combats the conventional limitations in order to test the efficiency of coagulation in blood as a whole. The TEG[®] is effective and convenient as it tests multiple parameters (Table 5.1) of whole blood by evaluating the elastic properties of blood [127]. The TEG[®] measures the properties of the blood using a pin, which is suspended in a cup via a torsion wire that is connected to a mechanical-electrical transducer. As the clot forms, the rotation of the pin changes and electrical signals are produced and converted by a computer into numerical and graphical (waveform as shown in Figure 5.1) data [129].

The advantages are that TEG[®] continually evaluates the coagulation process from clot formation to clot lysis. It is also a rapid, easy to use computerised process which generates useful qualitative data [127]. Disadvantages are that TEG[®] has never been standardised as has been done with conventional tests and a delay in the processing may alter the accuracy of the results. Thromboelastography[®] alone should not be used to express a hypercoagulable state [65]. The TEG[®] also requires daily calibration [129].

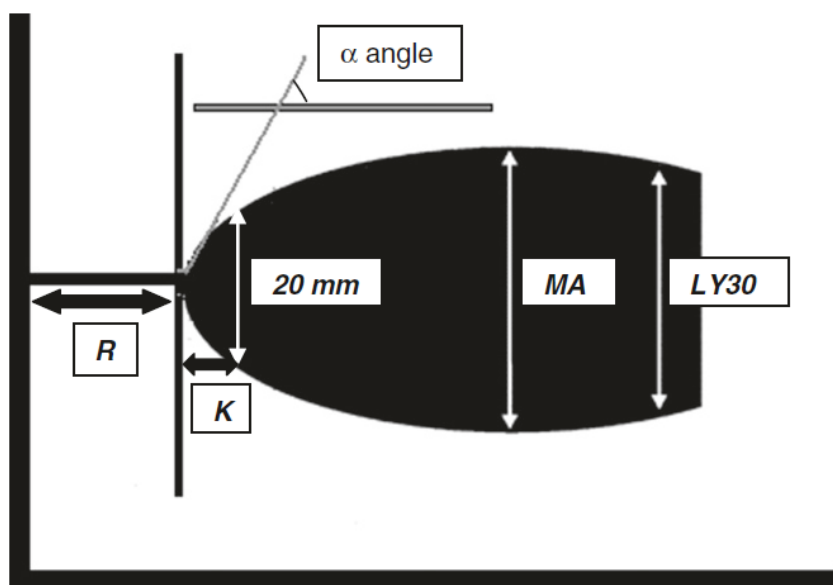


Figure 5.1: The graphical waveform representation of a normal signature TEG[®] tracing [129].

Table 5.1: Description of the various whole blood parameters measured by the TEG[®] [129, 130].

<u>Abbreviation</u>	<u>Parameter</u>	<u>SI Unit</u>	<u>Description</u>
R	Reaction time	min	Time taken from the start of the test to initial fibrin formation or the time it takes to reach an amplitude of 20 mm.
K	Clotting time	min	Time taken until the clot firmness is at a fixed level or the period between 2 and 20 mm amplitude.
α	Angle (slope between R and K)	degrees	Rate of clot formation (speed at which fibrin build up and cross linking occurs).
MA	Maximum amplitude	mm	Ultimate strength of the fibrin clot.
MRTG	Maximum rate of thrombus generation	dynes/cm ² /s or dcs	Velocity of thrombus formation.
TMRTG	Time to maximum rate of thrombus generation	min	Time to commencement of coagulation.
TTG	Clot strength	dynes/cm ² or dyn/cm ²	Final clot strength.

5.2 Materials and methods

5.2.1 Heavy metal preparations

All reagents are the same as those used in section 3.2.1, however, the concentration ranges of the various metals only included X1 and X10 (2-point), the WHO safety level standards for each respective metal, which are 31.47 μM for Cu, 9.1 μM for Mn and 0.004 μM for Hg. Only a 2-point concentration range was used as higher levels caused Cu precipitation, which would interfere with the sensitive readings of the TEG[®].

5.2.2 Blood collection

The process of blood collection was the same as in section 3.2.2

5.2.3 Sample preparation

Whole blood was exposed to the different metal groups at the 2-point concentration range and then incubated for 30 minutes, at room temperature. Two samples were run in the two channels of the TEG[®] (TEG[®] 5000 computer-controlled device, Haemoscope Corp., Niles, IL, USA), simultaneously. A volume of 340 μ L of whole blood was added to the oscillating cup of the TEG[®] and 20 μ L of calcium chloride (CaCl_2) was added to the sample in order to start the coagulation process. The process was run until MA was reached.

5.2.4 Statistical analyses

The Mann-Whitney U test (Graph Pad) was used to compare the significance of the various parameters of each individual experimental group to the control. Statistical analysis was performed with a 95% confidence interval where a p value < 0.05 was considered significant.

5.3 Results

For Cu, Mn and Hg alone and in combination, clot formation was determined following exposure of whole blood for 30 minutes to X1 and X10 concentrations. Figure 5.2 shows various TEG[®] tracings which demonstrate all the blood parameters in numerical and graphical form. Figure 5.2A and C are representative waveforms of typical control and metal exposed, whole blood parameters – R, K, α and MA. The numerical values shown underneath each of the parameters is the normal range for each specific parameter, which is denoted on the graph by a coloured dashed line. The solid coloured lines represent the sample's values. As seen in Figure 5.2C (metal), the purple solid line (MA value) is approaching the upper normal range, whilst in Figure 5.2A (control), the purple solid line is approaching the lower normal range. This would, as an example, indicate that the metal sample has a greater MA value as compared to the control. The same can be done for the other parameters: blue (α -angle), green (K) and orange (R). Figure 5.2B and D are representative thrombus velocity curves (V-curves) of typical control and metal exposed, respectively, whole blood parameters – MRTG, TMRTG and TTG. These parameters together form the green area within the curve. Figure 5.2D (metal) has a greater green area as compared to Figure 5.2B (control), which indicates the metals can increase coagulability. Figures 5.2E and G show all the representative tracings for each metal group, at the X1 concentration, and the control (white). All the metal groups at this concentration show a

potential to increase the coagulability of the whole blood, as they vary from the control's tracing. Figure 5.2F and H show all the representative tracings for each metal group, at the X10 concentration, and the control (white). All the metal groups at this concentration showed similar tracings to the control.

When performing statistical analyses on each individual experimental group versus the control, by the Mann-Whitney U test, no significance ($p > 0.05$) was observed for any of the groups for each parameter. This means that none of the metal groups showed significant difference to the control for any of the parameters and thus may not increase thrombus formation in a significant way. In Tables 5.2 – 5.4, it can be seen that all the metal groups, except Hg X1 and the triple combination group X1 and X10, show a decrease in R (min) as compared to the control. It was noted that Cu X1 showed the lowest R value as compared to the other X1 concentrations and Cu showed no effect on the other metals. The Mn + Hg combination showed a lower R value as compared to the metals individually. All the metal groups at the X10 concentration were all close in value to the control.

In Tables 5.2 – 5.4, it can be seen that all the metal groups, except Hg X10, show a decrease in K (min) as compared to the control. An overall trend could not be distinguished but it was noted that there was an increase in K (min) between Cu X1 and X10, but a decrease in K (min) between Mn X1 and X10, whilst the other groups stayed relatively similar. In Tables 5.2 – 5.4, it can be seen that all the metal groups, except Mn X1, Hg X10 and Cu + Hg X1, show an increase in α (deg) as compared to the control. It was noted that Cu X1 was the only metal group that stood out as not being similar to the control and having an increase in the α angle value. All the metal groups show an increase in MA (mm) as compared to the control. Although none of the metal groups had a significant increase in MA as compared to the control, it was noted that the Cu + Mn X10 group showed the largest MA value. All the metal groups show an increase in MRTG (dcs) as compared to the control. This was the general trend seen with the K and α value as well. It was noted that Cu X1 and Mn + Hg X1 showed the greatest increase in MRTG, as compared to the control. This means that the experimental groups showed an increase in the speed of clot formation. In Most of the metal groups also show an increase in TMRTG (min) as compared to the control. However, the groups: Cu X1, Mn X1, Mn X10, Cu + Mn X10, Cu + Hg X1 and Mn + Hg X1 show a decrease in TMRTG (min). Finally, all the metal groups show an increase in TTG (dyn/cm^2) as compared to the control and this corresponds with the overall increase in MA by all the experimental groups.

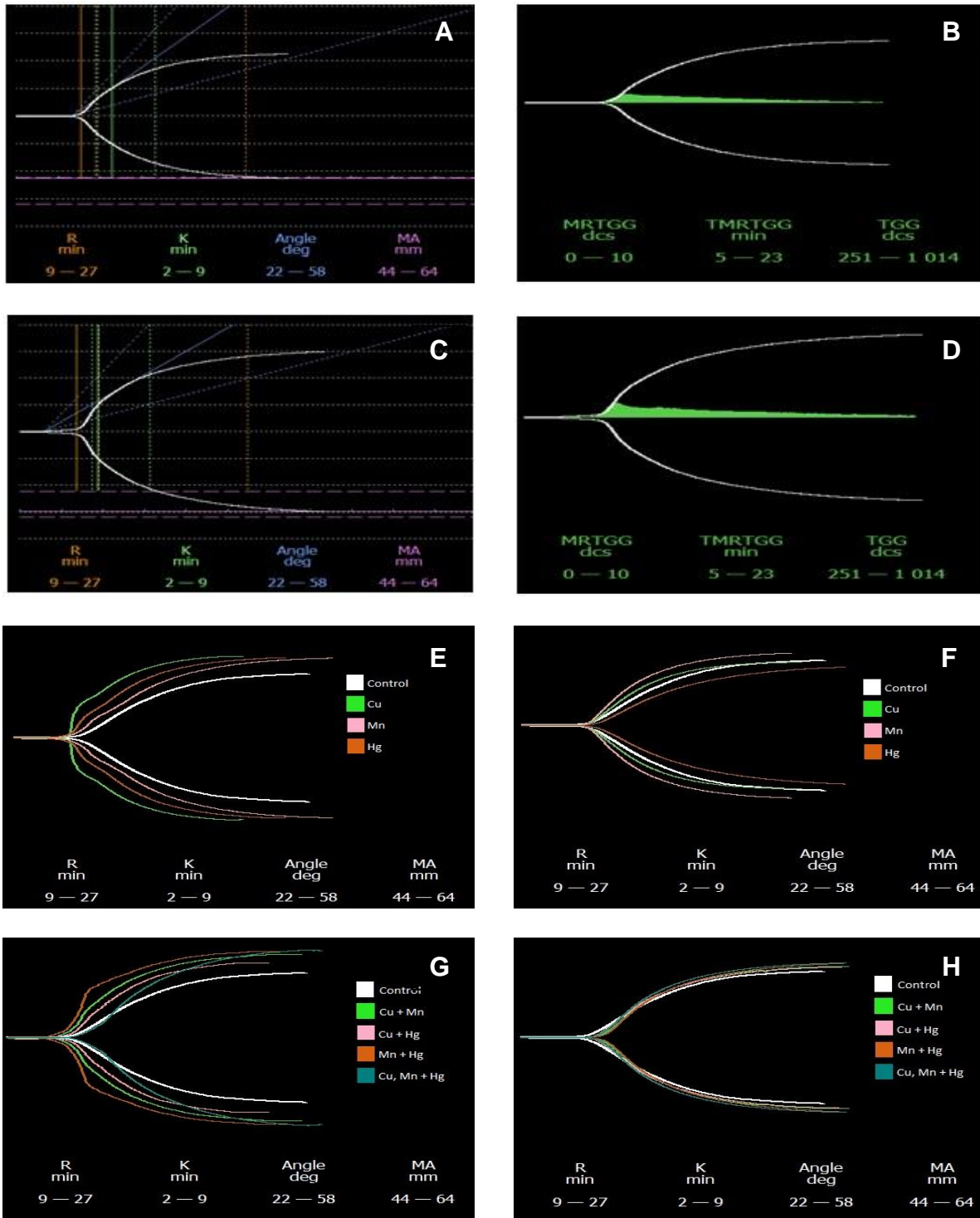


Figure 5.2: The graphical waveform representation of various TEG[®] tracings and V-curves (B & D). A & B: Representative waveforms for the control group; C & D: Representative waveforms for the metal groups; Representative tracings of the single metal groups, at X1 E and X10 F concentrations, vs the control; Representative tracings of the combination metal groups, at X1 G and X10 H concentrations vs the control.

Table 5.2: Summary of the effects of Cu, Mn and Hg, alone and in combinations, at the X1 concentration based on the WHO safety level standards of each respective metal, on the various parameters of whole blood.

Parameter	Normal ranges	Control		Cu		Mn		Hg	
		Mean ± SD	Range						
R (min)	9 – 27	7.8 ± 0.26	7.6 – 8.1	6.43 ± 0.35	6.1 – 6.8	7.3 ± 1.47	6.4 - 9	7.87 ± 2.4	5.8 – 10.5
K (min)	2 – 9	4.9 ± 1.04	3.7 – 5.7	2.33 ± 2.24	0.8 – 4.9	4.23 ± 1.36	2.7 – 5.3	4.17 ± 2.51	1.8 – 6.8
α (deg)	22 – 58	37.07 ± 10.19	26.4 – 46.7	66.4 ± 13.47	51.5 – 77.7	37.9 ± 2.41	35.4 – 40.2	46.6 ± 27.83	20.1 – 75.6
MA (mm)	44 – 64	42.17 ± 4.82	36.6 – 45	49.3 ± 8.5	40.8 – 57.8	50.23 ± 6.54	43.3 – 56.3	51.83 ± 6.83	44 – 56.6
MRTG (dcs)	0 – 10	2.45 ± 0.61	1.99 – 3.14	8 ± 4.86	2.61 – 12.05	3.04 ± 1.01	2.07 – 4.08	4.54 ± 2.83	1.85 – 7.49
TMRTG (min)	5 – 23	10.42 ± 1.88	9.25 – 12.58	7.47 ± 1.12	6.67 – 8.75	10.2 ± 2.64	8.67 – 13.25	10.66 ± 5.13	7.58 – 16.58
TTG (Dynes/cm ²)	251 – 1014	368.77 ± 69.98	287.97 – 410.04	506.14 ± 170.33	345.46 – 684.71	518.62 ± 132.13	382.49 – 646.35	548.21 ± 136.06	394.31 – 652.55
Parameter	Normal ranges	Cu + Mn		Cu + Hg		Mn + Hg		Cu + Mn + Hg	
		Mean ± SD	Range						
R (min)	9 – 27	7.4 ± 2.08	6.1 – 9.8	7.53 ± 1.36	6.7 – 9.1	6.73 ± 2	5.2 – 9	8.1 ± 2.7	5.4 – 10.8
K (min)	2 – 9	3.57 ± 1.72	2.2 – 5.5	4.13 ± 1.76	2.7 – 6.1	3.17 ± 0.8	2.4 – 4	4.1 ± 0.85	3.2 – 4.9
α (deg)	22 – 58	46.93 ± 11.72	33.3 – 55.6	37.67 ± 6.04	30.7 – 41.3	45.67 ± 6.2	41.6 – 52.8	45.43 ± 8.16	37.1 – 53.4
MA (mm)	44 – 64	52.9 ± 6.75	45.3 – 58.2	52.63 ± 6.62	46.3 – 59.5	53.87 ± 6.60	47.2 – 60.4	53.6 ± 8.09	45.1 – 61.2
MRTG (Dynes/cm ² /s)	0 – 10	4.23 ± 1.81	2.15 – 5.48	3.68 ± 1.58	2.07 – 5.22	7.31 ± 4.18	2.82 – 11.09	4.48 ± 2.59	2.25 – 7.32
TMRTG (min)	5 – 23	10.53 ± 4.04	7.75 – 15.17	11.47 ± 3.01	8.58 – 14.58	9.7 ± 1.93	8.42 – 11.92	12.67 ± 3.06	9.17 – 14.83
TTG (Dynes/cm ²)	251 – 1014	577.19 ± 145.68	414.73 – 696.19	571.14 ± 154.68	432.34 – 737.88	597.49 ± 155.27	448.3 – 758.2	600.48 ± 188	412.27 – 788.27

*Statistical significance: *p*-value of ≤0.05. SD: Standard deviation. R = reaction time; K = clotting time; α = angle; MA = maximum amplitude; MRTG = maximum rate of thrombus generation; TMRTG = time to maximum rate of thrombus generation; TTG = clot strength.

Table 5.3: Summary of the effects of Cu, Mn and Hg, alone and in combinations, at the X10 concentration based on the WHO safety level standards of each respective metal, on the various parameters of whole blood.

Parameter	Normal ranges	Control		Cu		Mn		Hg	
		Mean ± SD	Range	Mean ± SD	Range	Mean ± SD	Range	Mean ± SD	Range
R (min)	9 – 27	7.8 ± 0.26	7.6 – 8.1	7.63 ± 0.31	7.3 – 7.9	7.5 ± 0.66	6.9 – 8.2	7.27 ± 1.53	5.6 – 8.6
K (min)	2 – 9	4.9 ± 1.04	3.7 – 5.7	4.13 ± 1.07	3.2 – 5.3	3.13 ± 0.31	2.8 – 3.4	4.83 ± 1.42	3.3 – 6.1
α (deg)	22 – 58	37.07 ± 10.19	26.4 – 46.7	40.17 ± 11.7	26.8 – 48.6	50.8 ± 2.88	48.2 – 53.9	36 ± 10.56	28.1 – 48
MA (mm)	44 – 64	42.17 ± 4.82	36.6 – 45	45.5 ± 2.04	43.9 – 47.8	50.73 ± 4.54	46.6 – 55.6	43.17 ± 2.4	40.4 – 44.7
MRTG (Dynes/cm ² /s)	0 – 10	2.45 ± 0.61	1.99 – 3.14	2.72 ± 0.52	2.2 – 3.23	5.08 ± 3.01	3.15 – 8.55	2.7 ± 0.83	1.74 – 3.25
TMRTG (min)	5 – 23	10.42 ± 1.88	9.25 – 12.58	11.06 ± 1.49	9.47 – 12.33	10.16 ± 0.38	9.83 – 10.58	10.69 ± 2.25	9 – 13.25
TTG (Dynes/cm ²)	251 – 1014	368.77 ± 69.98	287.97 – 410.04	420.02 ± 35.36	391.89 – 459.72	522.8 ± 96.91	437.34 – 628.09	382.42 ± 36.83	339.97 – 405.88
Parameter	Normal ranges	Cu + Mn		Cu + Hg		Mn + Hg		Cu + Mn + Hg	
		Mean ± SD	Range	Mean ± SD	Range	Mean ± SD	Range	Mean ± SD	Range
R (min)	9 – 27	7.17 ± 3.8	2.8 – 9.7	7.67 ± 1.27	6.2 – 8.5	7.7 ± 1.55	6.1 – 9.2	7.87 ± 1.99	5.6 – 9.3
K (min)	2 – 9	3.4 ± 0.87	2.4 – 4	3.83 ± 0.15	3.7 – 4	3.4 ± 0.26	3.2 – 3.7	3.37 ± 1.17	2.1 – 4.4
α (deg)	22 – 58	43.9 ± 2.47	41.2 – 46	43.5 ± 4.35	39.6 – 48.2	47.4 ± 3.32	43.6 – 49.7	43.3 ± 3.12	39.7 – 45.2
MA (mm)	44 – 64	55.1 ± 5.89	48.6 – 60.1	51.03 ± 8.01	48.1 – 60.1	53.63 ± 9.42	46.1 – 64.2	52.77 ± 2.48	51 – 55.6
MRTG (Dynes/cm ² /s)	0 – 10	3.89 ± 1.42	2.98 – 5.53	3.05 ± 0.42	2.75 – 3.53	3.79 ± 1.19	3.02 – 5.16	3.96 ± 1.69	2.75 – 5.89
TMRTG (min)	5 – 23	10.03 ± 4.8	4.5 – 13.08	11.36 ± 0.86	10.67 – 12.33	10.94 ± 1.23	10 – 12.33	12.06 ± 5.79	6.17 – 17.75
TTG (Dynes/cm ²)	251 – 1014	628.33 ± 143.72	473.15 – 756.86	543.73 ± 187.51	408.95 – 757.87	611.11 ± 252.77	421.49 – 898.08	562.39 ± 58.46	520.83 – 629.23

*Statistical significance: *p*-value of ≤0.05. SD: Standard deviation. R = reaction time; K = clotting time; α = angle; MA = maximum amplitude; MRTG = maximum rate of thrombus generation; TMRTG = time to maximum rate of thrombus generation; TTG = clot strength.

Table 5.4: Data representing the changes of the various parameters measured of the metal exposed whole blood, as compared to the control. Data represents the average of three volunteers. ↑ = increase in value; ↓ = decrease in value and ↔ = similar value, as compared to the control values. The **○ encircled symbols = does not follow the trend of the majority groups.**

Metal groups	Cu X1	Cu X10	Mn X1	Mn X10	Hg X1	Hg X10	Cu+Mn X1	Cu+Mn X10	Cu+Hg X1	Cu+Hg X10	Mn+Hg X1	Mn+Hg X10	All X1	All X10
R (min)														
Average	↓	↓	↓	↓	↔	↓	↓	↓	↓	↓	↓	↓	↑	↔
K (min)														
Average	↓	↓	↓	↓	↓	↔	↓	↓	↓	↓	↓	↓	↓	↓
α (deg)														
Average	↑	↑	↔	↑	↑	↓	↑	↑	↔	↑	↑	↑	↑	↑
MA (mm)														
Average	↑	↑	↑	↑	↑	↑	↑	↑	↑	↑	↑	↑	↑	↑
MRTG (dsc)														
Average	↑	↑	↑	↑	↑	↑	↑	↑	↑	↑	↑	↑	↑	↑
TMRTG (min)														
Average	↓	↑	↓	↓	↑	↑	↑	↓	↓	↑	↓	↑	↑	↑
TTG (dynes/cm²)														
Average	↑	↑	↑	↑	↑	↑	↑	↑	↑	↑	↑	↑	↑	↑

R = reaction time; K = clotting time; α = angle; MA = maximum amplitude; MRTG = maximum rate of thrombus generation; TMRTG = time to maximum rate of thrombus generation; TTG = clot strength.

5.4 Discussion

Platelet activation together with the coagulation cascade results in clot formation. This process can be quantified using tests that measure parameters such as: prothrombin time, thrombin time and partial thromboplastin time. However, these tests are not accurate in describing the full coagulation cascade and the changes in various blood parameters as they are isolated tests. The TEG[®] is a method that was developed in order to combat the problem of isolating different blood parameters. It monitors and measures whole blood coagulation in an effective and convenient way. It assesses elastic properties of whole blood and gives an overall measurement on haemostatic functioning, which can be used to accurately predict possible probability of excessive bleeding, clot lysis and thrombosis [127]. The functioning of the clot is due to all elements – coagulation proteins and cellular elements – working together thus providing the kinetics and physical properties of the entire clot being formed. Since TEG[®] measures the functioning of the clot it directly measures the functionality of the cellular components involved in forming the clot through variations in the different parameters [117]. No significant differences were observed between any of the parameters measured. Changes in these parameters were then evaluated.

However, these experiments explain acute exposures for a short period of time. The reality is that the general population is exposed to these metals in a chronic setting, over a long period of time. Thus, there may be no significance but the potential to cause thrombus formation will still be discussed through the individual parameters that the TEG[®] measures. A slight increase in the probability in thrombus formation can be indicative of a potential health hazard which includes other factors such as lifestyle, genetics and exposure to heavy metals. The following parameters discussed are the four main parameters used on the TEG[®] tracings, to deduce a normal or hypo- or hypercoaguable state.

The time it takes for the initiation of the clot development, through fibrin formation, is the reaction time or R value. The rate of activation of TF (coagulation initiator) and in turn factor VII, within the coagulation cascade, is responsible for a decreased or increased R value, as clot formation starts through the activation of these factors [117]. A decrease in the R value and thus a decrease in the time it takes for a clot to start forming would suggest an increase in activation of platelets, leading to clot formation. An increase in platelet activation can potentially result in a hypercoaguable state of blood and therefore thrombosis [117]. It is not possible to determine the exact mechanisms of the metals effect the enzymatic pathway coagulation factors through the methodologies used in this study. However, it can be deduced that an increase in platelet activation occurs with an increase in both Ca²⁺ and ROS. The groups that did not decrease the R value potentially did not increase Ca²⁺ or ROS production considerably and thus had less platelet activation.

The time it takes for the clot formation to amplify from the start of its development (R) to a fixed amplitude level of 20 mm represents the kinetics of the clot or the K value [127, 129]. The interactions of platelet functioning and fibrinogen levels are responsible for amplifying the clot formation [117, 131]. Fibrinogen levels would increase in response to an increase in thrombin [117]. A decrease in the K value and thus a decrease in the time it takes for the clot to amplify would suggest an increase in thrombin and thus an increase in fibrinogen levels and also an increase in platelet functioning resulting in platelet activation [117]. A considerable increase in thrombin and platelet activation could lead to a hypercoaguable state and therefore thrombosis, as thrombin cleaves fibrinogen to form fibrin which polymerises to form fibrin fibres and together with activated platelets they form the clot. When analysing the scanning electron micrographs (chapter 4) of the platelets of all the experimental groups, it was noted that they all showed some degree of platelet activation from increased amount of pseudopodia to platelet spreading and even aggregate formation. It is interesting to note that in the SEM micrographs, Hg X10 showed aggregation but with necrosis. Due to the Hg damaging the platelets in the time frame given (30 min incubation

period), it is possible that the TEG[®] measurement may have missed the window period in which the Hg increased platelet activation before damaging the platelets.

The kinetics of the clot development or the propagation of continual fibrin formation and cross-linking is measured by the angle or α of the clot [117, 127]. The α value is related to the K value as they both measure the rate at which the fibrin is polymerised to form the clot. The α value is more inclusive than the K value as it can be used as a good measure for some hypocoagulable states, where K cannot be used if the clot's amplitude never reaches the fixed level of 20 mm [117]. As with the K value, α is also affected by the fibrinogen levels and platelet functioning. An increase in the α value suggests an increase in fibrinogen levels, through an increase in thrombin, and an increase in platelet activation. An increase in these factors can result in thrombosis. The groups: Mn X1 and Cu + Hg X1 had similar α values to the control, even though their scanning electron micrographs of platelets showed platelet activation. They also showed considerable fibrin formation (net-like coverings and sticky masses formed), when looking at the scanning electron micrographs of the whole blood with added thrombin. The Hg X10 group, as discussed for the K value, showed necrotic platelets, but when looking at the thrombin-induced scanning electron micrographs it did show less net-like coverings as compared to the Hg X1 group. The amplification (K value) and propagation (α -angle) of the clot development is determined more by the fibrinogen levels and less by platelet activation.

The maximum level of the constantly activated fibrin and platelets, which represents the maximum strength or stiffness of the clot, is the maximum amplitude or MA of the developed clot [117]. This clot strength is determined mainly by platelet functioning (80%) and slightly by the involvement of fibrin (20%) [127]. An increase in clot strength can represent a hypercoagulable state [117]. The increase in MA for all the experimental groups correlates with the scanning electron micrographs showing a form of platelet activation for all the groups. It can be noted in Figure 5.3D that Hg X10 showed the smallest MA compared to other experimental groups. This factor, again, can be due to Hg's rapid damaging effects on the platelets.

The speed or calculated velocity of the propagation of the clot is the maximum rate of thrombus generation or MRTG [128]. Thus MRTG is related to K and α . An increase in the speed at which the clot forms can result in thrombus formation as coagulation speed could be faster than fibrinolysis speed and so haemostasis would not be achieved and the clot would continually propagate. This implies that all the experimental groups that showed an increase in MRTG, K or α could cause thrombus formation.

The time it takes to reach the maximum velocity at which the thrombus is formed is the TMRTG or time to MRTG [128]. It is unclear why these groups go against the general trend of the experimental groups. Recent studies have shown a correlation between TMRTG and thrombin/anti-thrombin levels. It is also hypothesised that a hypercoagulable state can be determined to be enzymatic or due to platelet functioning, through TMRTG [132]. Although most of the groups show an increase in TMRTG, the groups that show a decrease in TMRTG represent a hypercoagulable state [133]. It can be noted that the main inducers of the decrease in TMRTG appear to be the metals Cu and Mn, with Cu X1 having a considerable decrease in TMRTG as compared to the control, as seen in Figure 5.3F. In chapter 4, qualitative morphological assessment noted that Mn had the greatest influence in increasing fibrin formation, even at the lowest concentrations.

The final clot strength or stability of the clot, from the initial fibrin formation to fibrinolysis, is the total thrombus generation or TTG [129, 130]. This parameter is related to MA, but TTG is the better measurement when discussing clot strength as it is a measure or unit of force and takes into account both platelet and enzymatic roles in clot formation [129, 132]. Therefore, all the metal groups can produce a stronger and more stable clot, as compared to the control, and this factor can contribute to thrombosis. However, in Figure 5.3G the Cu X10 and Hg X10 groups showed less of an increase in TTG as compared the other experimental groups versus the control.

Although not significant, it can be noted that overall Cu X1 stood out above all other groups. It had a reduced R value, K value and TMRTG value with an increased α value and MRTG. However, no considerable trends could be seen for MA and TTG. This could mean that Cu X1 can produce a large clot quickly but the strength or stability of the clot is not great enough that this clot could succumb to fibrinolysis easily.

All the metal groups at the X10 concentration showed similar overall whole blood parameters to the control. This phenomenon can be seen in Figures 5.2F and 5.2H, whereby the TEG[®] tracings for the X10 concentrations showed the experimental groups to have similar tracings as the control group. This factor may be due to the 'window period' effect whereby the time in which the metals exerted the highest effect on the whole blood, was missed. A shorter exposure time for higher concentrations can be done to determine if this is the case.

5.5 Conclusion

In conclusion, no statistically significant changes were observed in the measured coagulation parameters, however, trends were observed compared to the control. These were a decrease in R, a decrease in K, an increase in α , an increase in MA, an increase in MRTG, an increase in TTG and either increased or reduced TMRTG. These trends indicate a more hypercoagulable state of blood in the presence of the metals Cu, Mn and Hg.

CHAPTER 6: Concluding Discussion

6.1 Summarised results

An increase in pollution and exposure to pollution is a concern and can potentiate many harmful health effects in the general population, including CVD due to alterations in the coagulation system. The adverse effects associated with metal exposure; in particular Cu, Mn and Hg, to components of the blood coagulation system, i.e. erythrocytes, Hb, platelets, fibrin networks and whole blood parameters, have been reported. The results obtained in this study might lead to an increase in awareness by the general population and implementation of methods by higher authorities to prevent an increase in and exposure to pollution and excessive amounts of these metals. There is data surrounding metal exposure and potential effects, but more data is needed regarding Cu, Mn and Hg exposure, specifically in South Africa's general population and populations living close to mining and power plant areas, in order to understand the possible effect they have on the coagulation system. Also, very little to no information is available on the regarding the combined effect of these metals, at different concentrations. Therefore, the aim of this study was to investigate the potential toxic effects of Cu, Mn and Hg, alone and in combinations, on the coagulation system.

To attain these aims, the haemolysis assay, scan Hb, SEM and TEG[®] methods were used. Blood was obtained from healthy male volunteers, under consent and with ethical clearance. To assess erythrocyte membrane damage by the metals, the haemolysis assay was used. Results obtained showed that Hg and Mn, at the higher concentrations (X1000 and X10000) were the main inducers of haemolysis and in combination had an even greater effect. The Cu groups showed no effects unless in combination with the other metals, at the X100 concentration. These higher concentrations are not highly probable in an environmentally-exposed setting. Unfortunately, Cu precipitated the Hb and so no results could be accepted at face value and another method had to be used. An increase in haemolysis is an indication for possible thrombus formation.

Although, some experimental groups showed significant percentage haemolysis at certain concentrations, the interaction between metals in the combination groups could not be explained through significance. Thus the MDR was calculated to investigate the synergy or interactions of the various metals in the combination groups. The only group found to have definitive synergy was the Mn + Hg combination group at the X1000 concentration. This result reiterated the notion that Hg potentiates the harmful effects of other metals.

The next method utilised, due to Cu's precipitating effect, was the scan Hb methodology. This methodology measured the point at which Cu forms precipitates and the formation of toxic forms of Hb – Sulf- and MetHb. Results obtained showed that only at the X1 and X10 concentrations did Cu not precipitate any Hb. At these concentrations, it was determined if Cu, alone and in combinations, formed Sulf- or MetHb. It was found that the Cu + Mn combination, at the X10 concentration, was the only group that significantly converted the oxy- and deoxyHb to the Sulf- and MetHb types by about 5 – 10%. For MetHb this is not lethal but reduces oxygen carrying capacity, which can have a hazardous effect on individuals already suffering from CVD. On the other hand an increase in SulfHb can be lethal.

Upon investigation of changes in the morphology of erythrocytes, platelets and fibrin networks, different findings were obtained. Erythrocytes altered morphology in different forms for the various experimental groups, but Cu showed the highest prevalence of echinocyte formation. Platelets also showed altered morphology and became more activated for all experimental groups. Increasing activation was illustrated with an increase in pseudopodia, platelet spreading and aggregation. Mercury had the highest toxicity by causing necrosis at the X10 and X100 concentrations. In the experimental groups fibrin fibres, in which the deformed erythrocytes (pink arrow) become trapped, became thicker and less organised. Manganese formed more net-like coverings and sticky fibrin masses than any other group, even at the X1 concentration. This might imply that the fibrin networks are a target of Mn toxicity and this contribute to CVD.

Scanning electron microscopy is a qualitative methodology, so TEG[®] was used in combination with SEM in order to provide quantitative data on whole blood parameters which could possibly explain what was seen with SEM. Seven different parameters of whole blood were measured. The overall trend for all the experimental groups, as compared to the control, showed a decrease in R, decrease in K, an increase in α , an increase in MA, an increase in MRTG, and an increase in TTG and TMRTG did not show a common trend. The Cu X1 group stood out as compared to the other experimental groups with decreased R, K and TMRTG and an increased α and MRTG, but did not have a considerable change in MA and TTG as compared to the control. This might imply that Cu X1 can produce a large clot quickly but the strength or stability of the clot is not great enough that this clot could succumb to fibrinolysis easily.

All these morphological alterations had a possible common pathway of toxicity due to ROS production, PS exposure and an increase in Ca^{2+} . All these factors together can induce thrombus formation, which can result in CVD, including myocardial infarction, angina,

venous thrombo-emboli and stroke. Cardiovascular disease is becoming one of the greatest causes of deaths in the world and affects many individuals.

6.2 Limitations and future prospective

A limitation of this study is that a concentration range of X1 – X10000 based on the WHO water safety limit was used. This does not take into account the absorption and distribution of each metal. There are two strategies that can be followed to address this limitation. Evaluations using an *ex vivo* study on the effects of reported metal levels in South African waters on erythrocyte, platelets and coagulation properties can be used. Future studies can also include an animal study (*in vivo*) which reflects a chronic exposure to X1 and X10 Cu, Mn and Hg levels.

In this study only the formation of the clot was investigated. In the future the use of the clot lysis assay can be used to evaluate the lysis of the clot. Atomic force microscopy can also be used to evaluate the elasticity of erythrocytes and fibrin networks exposed to Cu, Mn and Hg, alone and in combination.

Morphological studies provide information on the final outcome of Cu, Mn and Hg exposure, alone and in combination, but this does not provide any information on the effect of ROS on TF and TFPI activity. This can be evaluated by the 1-stage clotting assay, TF staining, immunohistochemistry, cell culture in conjunction with an activity assay, reverse transcription-polymerase chain reaction (RT-PCR) analysis, Western blotting and ligand dot blotting. The same methodology can also be used to evaluate the effect of ROS on other coagulation proteins mentioned in Figure 2.4.

Increased ROS is the result of these metals catalysing the Fenton reaction, inhibiting GR, GSH and NAC. It is unknown for each metal and their combination the actual source of ROS. To address these limitations, quantification and enzymatic assays can be used to determine the changes in these factors.

CHAPTER 7: References

- [1]: Department of Water Affairs and Forestry. Water for Growth and Development in South Africa Framework: Version 6 (2009). [Internet]. [Cited July 2017]. Available from: <http://www.dwa.gov.za/WFGD/documents.aspx>.
- [2]: Kampa M & Castanas E. Human health effects of air pollution. *Environmental Pollution*. 2008; 151: 362 – 367.
- [3]: Brook RD. Cardiovascular effects of air pollution. *Clinical Science*. 2008; 115: 175 – 187.
- [4]: Collen D & Lijnen HR. Basic and clinical aspects of fibrinolysis and thrombolysis. *Blood Journal*. 1991; 78 (12): 3114 – 3124.
- [5]: Gaziano TA. Cardiovascular disease in the developing world and its cost-effective management. *Circulation*. 2005; 112: 3547 – 3553.
- [6]: Pacyna EG, Pacyna JM, Sundseth K, Munthe J, Kindbom K, Wilson S, Steenhuisen F & Maxson P. Global emission of mercury to the atmosphere from anthropogenic sources in 2005 and projections to 2010. *Atmospheric Environment*. 2010; 44 (10): 2487 – 2499.
- [7]: Alo BI & Olanipekun A. Heavy metal pollution in different environmental media in Africa: problems and prospects (with case studies from Nigeria). [Internet]. [Cited October 2015]. Available from: http://www.who.int/ifcs/documents/forums/forum5/olanipekun_alo.pdf.
- [8]: Masekoameng K, Leaner J & Dabrowski J. Trends in anthropogenic mercury emissions estimated for South Africa during 2000 – 2006. *Atmospheric Environment*. 2010; 44 (25): 3007 – 3014.
- [9]: Dabrowski JM, Ashton PJ, Murray K, Leaner JJ & Mason RP. Anthropogenic mercury emissions in South Africa: Coal combustion in power plants. *Atmospheric Environment*. 2008; 42 (27): 6620 – 6626.
- [10]: Wagner N & Hlatshwayo B. The occurrence of potentially hazardous trace elements in five Highveld coals, South Africa. *International Journal of Coal Geology*. 2005; 63 (3 – 4): 228 – 246
- [11]: Arai F, Yamamura Y, Yoshida M & Kishimoto T. Blood and urinary levels of metals (Pb, Cr, Cd, Mn, Sb, Co and Cu) in Cloisonne workers. *Industrial Health*. 1994; 32: 67 – 78.
- [12]: Röllin H, Mathee A, Levin J, Theodorou P & Wewers F. Blood manganese concentrations among first-grade schoolchildren in two South African cities. *Environmental Research*. 2005; 97 (1): 93 – 99.
- [13]: Batterman S, Su F-C, Jia C, Naidoo RN, Robins T & Naik I. Manganese and lead in children's blood and airborne particulate matter in Durban, South Africa. *Science of the Total Environment*. 2011; 409 (6): 1058 – 1068.
- [14]: Kunimoto M, Miura T & Kubota K. An apparent acceleration of age-related changes of rat red blood cells by cadmium. *Toxicology and Applied Pharmacology*. 1985; 77: 451 – 457.
- [15]: Oosthuizen MA, John J & Somerset V. Mercury exposure in a low-income community in South Africa. *The South African Medical Journal*. 2010; 100 (6): 366 – 371.

- [16]: Musibono, D-A.E.A-E.A. 1998. Toxicological studies of the combined effects of aluminium, copper and manganese on a freshwater amphipod in acidic waters. PhD thesis. University of Cape Town.
- [17]: Murthy RC, Lal S, Saxena DK, Shukla GS, Ali MM & Chandra SV. Effect of manganese and copper interaction on behavior and biogenic amines in rats fed 10% casein diet. *Chemico-Biological Interactions*. 1981; 37 (3): 299 – 308.
- [18]: Grosicki A. Cadmium and mercury rat body burden following copper supplements. *Proceedings of ECOpole*. 2010; 4 (2): 257 – 261.
- [19]: Pathak SM, Mukhiya YK & Singh VP. Mercury, manganese interaction studies on barely: germination and phytotoxicity. *Indian Journal of Plant Physiology*. 1987; 30 (1): 13 – 19.
- [20]: Stern BR. Essentiality and toxicity in copper health risk assessment: overview, update and regulatory considerations. *Journal of Toxicology and Environmental Health – Part A*. 2010; 73 (2): 114 – 127.
- [21]: Crisponi G, Nurchi VM, Fanni D, Gerosa C, Nemolato S & Faa G. Copper-related diseases: From chemistry to molecular pathology. *Coordination Chemistry Reviews*. 2010; 254 (7 – 8): 879 – 889.
- [22]: Angelova M, Asenova S & Nedkova V. Copper in the human organism. *Trakia Journal of Sciences*. 2011; 9 (1): 88 – 98.
- [23]: Jomova K & Valko M. Advances in metal-induced oxidative stress and human disease. *Toxicology*. 2011; 283 (2 – 3): 65 – 87.
- [24]: World Health Organisation. Copper in drinking-water (2004). [Internet]. [Cited Feb 2016]. Available from: http://www.who.int/water_sanitation_health/dwq/chemicals/copper.pdf.
- [25]: Wapnir RA. Copper absorption and bioavailability. *The American Society for Clinical Nutrition*. 1998; 67 (5): 1054 – 1060.
- [26]: Stern BR, Solioz M, Krewski D, Aggetti P, Aw T-C, Baker S, Crump K, Dourson M, Haber L, Hertzberg R, Keen C, Meek B, Rudenko L, Schoeny R, Slob W & Starr T. Copper and human health: biochemistry, genetics, and strategies for modelling dose-response relationships. *Journal of Toxicology and Environmental Health, Part B*. 2007; 10: 157 – 222.
- [27]: Linder MC, Wooten L, Cerveza P, Cotton S, Shulze R & Lomeli N. Copper transport. *The American Society for Clinical Nutrition*. 1998; 67 (5): 9655 – 9715.
- [28]: Osredkar J & Sustar N. Copper and zinc, biological role and significance of copper/zinc imbalance. *Journal of Clinical Toxicology*. 2011; 3: 1 – 18.
- [29]: Permyakov EA. *Metalloproteomics*. 1st Ed. John Wiley and Sons, 2009. pg 368 – 370.
- [30]: Lemire JA, Harrison JJ & Turner RJ. The Fenton reaction, free radical chemistry and metal poisoning. *Nature Reviews Microbiology*. 2013; 11: 371 – 384.
- [31]: Das TK, Wati MR & Fatima-Shad K. Oxidative stress gated by Fenton and Haber Weiss reaction and its association with Alzheimer's disease. *Archives of Neuroscience*. 2014; 2 (3): 1 – 8.

- [32]: Pham AN, Xing G, Miller CJ & Waite TD. Fenton-like copper redox chemistry revisited: Hydrogen peroxide and superoxide mediation of copper-catalyzed oxidation production. *Journal of Catalysis*. 2013; 301: 54 – 64.
- [33]: Pretorius E, Swanepoel AC, Buys AV, Vermeulen N, Duim W & Kell DB. Eryptosis as a marker of Parkinson's disease. *Aging*. 2014; 6 (10): 1 – 32.
- [34]: Raicu V & Feldman Y. *Dielectric Relaxation in Biological systems: Physical Principles, Methods and Applications*. 1st Ed. Oxford University Press, 2015. pg 364.
- [35]: Vos MJ, Martens D, van de Leur SJ & van Wijk R. Neonatal haemolytic anaemia due to pyknoctosis. *European Journal of Padiatrics*. 2014; 173: 1711 – 1714.
- [36]: Zhang B, Lee AI & Podoltsev N. Tumor lysis syndrome and acute anaemia in an African-American man with chronic lymphocytic leukemia. *Oxford Medical Case Reports*. 2014; 11 (8): 138 – 140.
- [37]: Yoo D & Lessin LS. Drug-associated 'bite cell' hemolytic anemia. *The American Journal of Medicine*. 1992; 92 (3): 243 – 248.
- [38]: Tkachuk DC.; Hirschmann JV & Wintrobe MM. *Wintrobe's Atlas of Clinical Hematology*. 1st Ed. Lippincott Williams & Wilkins, 2007. pg 30.
- [39]: Valsami S, Stamoulis K, Lydataki E & Fountoulaki-Paparizos L. Acute copper sulphate poisoning: A forgotten case of severe intravascular haemolysis. *British Journal of Haematology*. 2012; 156 (3): 294.
- [40]: Aster J, Kumar V, Robbins SL, Abbas AK, Fausto N & Cotran RS. *Robbins and Cotran Pathologic Basis of Disease*. 8th Ed. Saunders/Elsevier, 2010. pg 724 – 725.
- [41]: Wang YP, Zhou LS, Zhao YZ, Wang SW, Chen LL, Liu LX, Ling ZQ, Hu FJ, Sun YP, Zhang JY, Yang C, Yang Y, Xiong Y, Guan KL & Ye D. Regulation of G6PD acetylation by SIRT2 and KAT9 modulates NADPH homeostasis and cell survival during oxidative stress. *The European Molecular Biology Organisation Journal*. 2014; 33 (12): 1304 – 1320.
- [42]: Walshe JM. The acute haemolytic syndrome in Wilson's disease-a review of 22 patients. *The Quarterly Journal of Medicine*. 2013; 106 (11): 1003 – 1008.
- [43]: Zhu E, Qadri SM & Lang F. Killing me softly – suicidal erythrocyte death. *The International Journal of Biochemistry & Cell Biology*. 2012; 44: 1236 – 1243
- [44]: Lupescu A, Jilani K, Zelenak C, Zbidah M, Qadri SM & Lang F. Hexavalent chromium-induced erythrocyte membrane phospholipid asymmetry. *Biometals*. 2012; 25: 309 – 318.
- [45]: O'Neal SL & Zheng W. Manganese Toxicity upon overexposure: a decade in review. *Current Environmental Health Reports*. 2015; 2 (3): 315 – 328.
- [46]: Crossgrove J & Zheng W. Manganese toxicity upon overexposure. *Nuclear Magnetic Resonance in Biomedicine*. 2004; 17 (8): 544 – 553.
- [47]: Watts DL. The nutritional relationships of manganese. *Journal of Orthomolecular Medicine*. 1990; 5 (4): 219 – 222

- [48]: Finley JW. Manganese absorption and retention by young women is associated with serum ferritin concentration. *The American Journal of Clinical Nutrition*. 1999; 70: 37 – 43.
- [49]: Hunt C. Proceedings of the VIIIth Conference of the International Society for Trace Element Research in Humans (ISTERH), the IXth Conference of the Nordic Trace Element Society (NTES), and the VIth Conference of the Hellenic Trace Element Society (HTES), 2007. 1st Ed. Springer, 2009. pg 5 – 7.
- [50]: Van den Besselaar A. Magnesium and manganese ions accelerate tissue factor-induced coagulation independently of factor IX. *Blood Coagulation and Fibrinolysis*. 2002; 13 (1) 19 – 23.
- [51]: Thompson LC, Goswami S, Ginsber DS, Day DE, Verhamme IM & Peterson CB. Metals affect the structure and activity of human plasminogen activator inhibitor-1. I. Modulation of stability and protease inhibition. *Protein Science*. 2011; 20 (2): 353 – 365.
- [52]: Rossander-Hulten L, Brune M, Sandstrom B, Lonnerdal B & Hallberg L. Competitive inhibition of iron absorption by manganese and zinc in humans. *American Journal of Clinical Nutrition*. 1991; 54 (1): 152 – 156.
- [53]: Kadikoylu G, Yavasoglu I, Bolaman Z & Senturk T. Platelet parameters in women with iron deficiency anaemia. *Journal of the National Medical Association*. 2006; 98 (3): 398 – 402.
- [54]: Lim KM, Kim S, Noh JY, Kim K, Jang WH, Bae ON, Chung SM & Chung JH. Low-level mercury can enhance proagulant activity of erythrocytes: A new contributing factor for mercury-related thrombotic disease. *Environmental Health Perspectives*. 2010; 118 (7): 928 – 935.
- [55]: Houston MC. Role of mercury toxicity in hypertension, cardiovascular disease and stroke. *Wiley Periodicals*. 2011; 13: 621 – 627.
- [56]: El-Demerdash FM. Effects of selenium and mercury on the enzymatic activities and lipid peroxidation in brain, liver, and blood of rats. *Journal of Environmental Science and Health, B36*. 2001; 4: 489 – 499.
- [57]: Salonen JT, Seppänen K, Nyyssönen K, Korpela H, Kauhanen J, Kantola M, Tuomilehto J, Esterbauer H, Tatzber F & Salonen R. Intake of mercury from fish, lipid peroxidation and the risk of myocardial infarction and coronary, cardiovascular and any death in eastern Finnish men. *Circulation*. 1995; 91 (3): 645 – 655.
- [58]: Park JD. Human exposure and health effects of inorganic and elemental mercury. *Journal of Preventative Medicine and Public Health*. 2012; 45: 344 – 352.
- [59]: Nuttall KL. Review: Interpreting mercury in blood and urine of individual patients. *Annals of Clinical and Laboratory Science*. 2004; 34 (3): 235 – 250.
- [60]: Kumar SV & Bhattacharya S. *In vitro* toxicity of mercury, cadmium and arsenic to platelet aggregation: influence of adenylate cyclase and phosphodiesterase activity. *In Vitro and Molecular Toxicology*. 2000; 13 (2): 137 – 144.
- [61]: Macfarlane DE. The effects of methyl mercury on platelets – induction of aggregation and release via activation of the prostaglandin synthesis pathway. *Molecular Pharmacology*. 1981; 19 (3): 470 – 476.
- [62]: White JG & Krivitt W. An ultrastructural basis for the shape changes induced in platelets by chilling. *Blood Journal*. 1967; 30 (5): 625 – 635.

- [63]: Yamamoto C, Kaji T, Sakamoto M & Kozuka H. Cadmium stimulation of plasminogen activator inhibitor-1 release from human vascular endothelial cells in culture. *Toxicology*. 1993; 83: 215 – 223.
- [64]: Bessis M. *Blood Smears Reinterpreted*. 1st Ed. Springer, 1977.
- [65]: Mamba BB, Rietveld LC & Verberk JQJC. SA drinking water standards under the microscope. *Water Wheel*. 2008; 7: 24 – 27.
- [66]: Zhu Q, Vera C, Asaro RJ, Sche P & Sung LA. A hybrid model for erythrocyte membrane: A single unit of protein network coupled with lipid bilayer. *Biophysical Journal*. 2007; 93: 386 – 400.
- [67]: Barrett K, Brooks H, Boitano S, Barman S. *Ganong's Review of Medical Physiology*. 23rd Edition. McGraw-Hill Book Company, 2010. pg 522 – 523.
- [68]: Lang F, Lang E & Foller M. Physiology and pathophysiology of Eryptosis. *Transfusion Medicine and Hemotherapy*. 2012; 39: 308 – 314.
- [69]: Biousse V. The coagulation system. *Journal of Neuro-Ophthalmology*. 2003; 23 (1): 50 – 62.
- [70]: Han V, Serrano K & Devine DV. A comparative study of common techniques used to measure haemolysis in stored red cell concentrates. *The International Society of Blood Transfusion*. 2009; 1 – 8.
- [71]: Evans BC, Nelson CE, Yu SS, Beavers KR, Kim AJ, Li H, Nelson HM, Giorgio TD, Duvall CL. Ex vivo red blood cell hemolysis assay for the evaluation of pH-responsive endosomolytic agents for cytosolic delivery of biomacromolecular drugs. *Journal of Visualized Experiments*. 2013; 73: 1 – 5.
- [72]: Doshi R & Panditrao A. Optical sensor system for hemoglobin measurement. *International Journal of Computational Engineering Research*. 2013; 3 (7): 41 – 45.
- [73]: May JM, Qu Z & Mendiratta S. Protection and recycling of α -tocopherol in human erythrocytes by intracellular ascorbic acid. *Archives of Biochemistry and Biophysics*. 1998; 349 (2): 281 – 289.
- [74]: Sowemimo-Coker SO. Red blood cell haemolysis during processing. *Transfusion Medicine Reviews*. 2002; 16 (1): 46 – 60.
- [75]: Colonna WJ, Marti ME, Nyman JA, Green C & Glatz CE. Haemolysis as a rapid screening technique for assessing the toxicity of native surfactin and a genetically engineered derivative. *Environmental Progress & Sustainable Energy*. 2016; 36 (2): 505 – 510.
- [76]: Choi J, Reipa V, Hitchins VM, Goering PL & Malinauskas RA. Physicochemical characterization and *in vitro* hemolysis evaluation of silver nanoparticles. *Toxicological Sciences*. 2011; 123 (1): 133 – 143.
- [77]: Nemani KV, Moodie KL, Brennick JB, Su A & Gimi B. *In vitro* and *in vivo* evaluation of SU-8 biocompatibility. *Materials Science and Engineering C: Materials for Biological Applications*. 2013; 33 (7): 4453 – 4459.
- [78]: Kemp MW, Ahmed S, Beeton ML, Payne MS, Saito M, Miura Y, Usuda H, Kallapur SG, Kramer BW, Stock SJ, Jobe AH, Newnham JP & Spillar OB. Foetal *Ureaplasma parvum* bacteraemia as a function of gestation-dependant complement insufficiency: evidence from a sheep model of pregnancy. *American Journal of Reproductive Immunology*. 2016; 77 (1): 1 – 9.

- [79]: Zohra M & Fawzia A. Hemolytic activity of different herbal extracts used in Algeria. *International Journal of Pharma Sciences and Research*. 2014; 5 (8): 495 – 500.
- [80]: Ibrahim IH, Sallam SM, Omar H & Rizk M. Oxidative hemolysis of erythrocytes induced by various vitamins. *International Journal of Biomedical Science*. 2006; 2 (3): 295 – 298.
- [81]: Brovedani V, Sosa Silvio, Poli M, Forino M, Varello K, Tubaro A & Pelin M. A revisited haemolytic assay for palytoxin detection: limitations for its quantitation in mussels. *Toxicon*. 2016; 119: 225 – 233.
- [82]: Mrugesh T, Dipa L & Manishika G. Effect of lead on human erythrocytes: an *in vitro* study. *Polish Pharmaceutical – Drug Research*. 2011; 68 (5): 653 – 656.
- [83]: Hall AH, Kulig KW & Rumack BH. Drug- and chemical-induced methaemoglobinaemia. *Medical Toxicology*. 1986; 1 (4): 253 – 260.
- [84]: Gharahbaghian L, Massoudian B & DiMassa G. Methemoglobinaemia and sulfhemoglobinaemia in two pediatric patients after ingestion of hydroxylamine sulphate. *Western Journal of Emergency Medicine*. 2009; 10 (3): 197 – 201.
- [85]: Wu C & Kenney MA. A case of sulfhemoglobinemia and emergency measurement of sulfhemoglobin with an OSM3 CO-oximeter. *Clinical Chemistry*. 1997; 43 (1): 162 – 166.
- [86]: Beutler E: In *Hematology: Methemoglobinemia and other causes of cyanosis*. 6th edition. McGraw-Hill Book Company, 2001. pg 611 – 614.
- [87]: Reza DM, Akbar M-M A, Parviz N, Ghourchian, Hedayat-Olah & Shahrokh S. Inhibition of human hemoglobin autoxidation by sodium n-dodecyl sulphate. *Journal of Biochemistry and Molecular Biology*. 2002; 35 (4): 364 – 370.
- [88]: Tallarida RJ. Quantitative methods for assessing drug synergism. *Genes & Cancer*. 2011; 2 (11): 1003 – 1008.
- [89]: Zhao Y, Gao J-L, Ji, J-W, Gao M, Yin, Q-S, Qui Q-L, Wang C, Chen S-Z, Xu J, Liang R-S, Cai Y-Z & Wang X-F. Cytotoxicity enhancement in MDA-MB-231 cells by the combination treatment of tetrahydropalmatine and berberine derived from *Corydalis yanhusuo* W.T. Wang. *Journal of Intercultural Ethnopharmacology*. 2014; 3 (2): 68 – 72.
- [90]: Jonker MJ, Svendsen C, Bedaux JJM, Bongers M & Kammenga JE. Significance testing of synergistic/ antagonistic, dose level-dependant, or dose ratio-dependant effects in mixture dose-response analysis. *Environmental Toxicology and Chemistry*. 2005; 24 (10): 2701 – 2713.
- [91]: Chu KW & Chow KL. Synergistic toxicity of multiple heavy metals is revealed by a biological assay using a nematode and its transgenic derivative. *Aquatic Toxicology*. 2002; 61: 53 – 64.
- [92]: Fouquier J & Guedj M. Analysis of drug combinations: current methodological landscape. *Pharmacology Research & Perspectives*. 2015; 3: (3): 1 – 11.
- [93]: Balistrieri LS & Mebane CA. Predicting the toxicity of metal mixtures. *Science of the Total Environment*. 2014; 466 – 467 (788 – 799): 1 – 29.
- [94]: Chou T-C. Theoretical basis, experimental design, and computerized simulation of synergism and antagonism in drug combination studies. *Pharmacological Reviews*. 2006; 58 (3): 621 – 681.

- [95]: Pennetier C, Corbel V, Boko P, Odjo A, N'Guessan R, Lapied B & Hougard J-M. Synergy between repellents and non-pyrethroid insecticides strongly extends the efficacy of treated nets against *Anopheles gambiae*. *Malaria Journal*. 2007; 6 (38): 1 – 7.
- [96]: Cedergreen N. Quantifying synergy: A systematic review of mixture toxicity studies within environmental toxicology. *Public Library of Science ONE*. 2014; 9 (5): 1 – 12.
- [97]: Belden JB, Gilliom RJ & Lydy MJ. How well can we predict the toxicity of pesticide mixtures to aquatic life? *Integrated Environmental Assessment and Management*. 2007; 3: 364 – 372.
- [98]: Houston MC. Role of mercury toxicity in hypertension, cardiovascular disease and stroke. *Wiley Periodicals*. 2011; 13: 621 – 627.
- [99]: Murray RK, Jacob M & Varghese J. *Harper's Illustrated Biochemistry: Plasma proteins and immunoglobulins*. 29th Ed. MacGraw-Hill Book Company, 2011. Chapter 50.
- [100]: Van Aardt WJ & Erdmann R. Water SA – Heavy metals (Cd, Pb, Cu, Zn) in mudfish and sediments from three hard-water dams of the Mooi river catchment, South Africa. *Water South Africa*. 2004; 30 (2): 211 – 218.
- [101]: Avenant-Oldewage A & Marx HM. Bioaccumulation of chromium, copper and iron in the organs and tissues of *Clarius gariepinus* in the Olifants River, Kruger National Park. *Water South Africa*. 2000; 26 (4): 569 – 582.
- [102]: Santra G, Paul R, Choudhury PS, Ghosh SK, De D & Das S. Haemolytic anemia as first manifestation of Wilson's disease: a report of two cases. *Journal of the Association of the Physicians of India*. 2014; 62: 55 – 57.
- [103]: Akram H & Mahboob T. Red cell Na-K-ATPase activity and electrolyte homeostasis in Thalassemia. *Journal of Medical Sciences*. 2004; 4 (1): 19-23.
- [104]: Gupta A, Jain N, Agrawal A, Khanna A & Gutch M. A fatal case of severe methaemoglobinaemia due to nitrobenzene poisoning. *Emergency Medical Journal*. 2012; 29 (1): 70 – 71.
- [105]: Ribarov SR & Benov LC. Relationship between the haemolytic action of heavy metals and lipid peroxidation. *Biochimica et Biophysica Acta*. 1981; 640: 721 – 726.
- [106]: Jomova K & Valko M. Advances in metal-induced oxidative stress and human disease. *Toxicology*. 2011; 283: 65 -87.
- [107]: Bradberry SM, Aw T-C, Williams NR & Vale JA. Occupational methaemoglobinaemia. *Occupational and Environmental Medicine*. 2001; 68: 611 – 616.
- [108]: Farina M, Avila DS, da Rocha JBT & Aschner M. Metals, oxidative stress and neurodegeneration: A focus on iron, manganese and mercury. *Neurochemistry International*. 2013; 62: 575 – 594.
- [109]: Becker A & Soliman KFA. The role of intracellular glutathione in inorganic mercury-induced toxicity in neuroblastoma cells. *Neurochemical Research*. 2009; 34 (9): 1677 – 1684.
- [110]: Mannucci PM, Lobina GF, Caocci L & Dioguardi N. Effect on blood coagulation of massive intravascular haemolysis. *Blood Journal*. 1969; 33: 207 – 213.

- [111]: Cappellini MD. Coagulation in the pathophysiology of haemolytic anaemias. *American Society of Haematology*. 2007; 74 – 78.
- [112]: Taka E, Mazzi E, Soliman KF & Reams RR. Microarray genomic profile of mitochondrial and oxidant response in manganese chloride treated PC12 cells. *Neurotoxicology*. 2012; 33 (2): 162 – 168.
- [113]: Goldstein JI, Newbury DE, Echlin P, Joy DC, Romig Jr. AD, Lyma CE, Fiori C & Lifshin E. Scanning electron microscopy and X-ray microanalysis: a text for biologists, material scientists and geologists. 2nd Ed. Springer Science and Business Media, 2012. pg 149 – 151.
- [114]: Van Rooy MJ, Duim W, Ehlers R, Buys AV & Pretorius E. Platelet hyperactivity and fibrin clot structure in transient ischemic attack individuals in the presence of metabolic syndrome: a microscopy and thromboelastography[®] study. *Cardiovascular Diabetology*. 2015; 14 (86): 1 – 13.
- [115]: Le MT, Hassanin M, Mahadeo M, Gailer J & Prenner EJ. Hg- and Cd-induced modulation of lipid packing and monolayer fluidity in biomimetic erythrocyte model systems. *Chemistry and Physics of Lipids*. 2013; 170 – 171: 46 – 54.
- [116]: Greenwalt TJ. The how and why of exocytic vesicles. *Transfusion*. 2006; 46: 143 – 152.
- [117]: Ruttman T. Coagulation for the clinician. *South African Journal of Science*. 2006; 44 (1): 22 – 37.
- [118]: Scheraga HA. The thrombin-fibrinogen interaction. *Biophysical Chemistry*. 2004; 112: 117 – 130.
- [119]: Cimmino G, Cirillo P, Ragni M, Conte S, Uccello G, Golino P. Reactive oxygen species induce a procoagulant state in endothelial cells by inhibiting tissue factor pathway inhibitor. *Journal of Thrombosis and Thrombolysis*. 2015; 40: 186 – 192.
- [120]: Muller I, Klocke A, Alex M, Kotzsh M, Luther T, Morgenstern E, Ziesenis S, Zahler S, Preissner K, Engelmann B. Intravascular tissue factor initiates coagulation via circulating microvesicles and platelets. *The Federation of American Societies for Experimental Biology Journal*. 2017; 17 (3): 476 – 478.
- [121]: Lang PA, Kempe DS, Tanneur V, Eisele K, Klarl BA, Myssina S, Jendrossek V, Ishii S, Shimizu T, Waidmann M, Hessler G, Huber SM, Lang F, Wieder T. Stimulation of erythrocyte ceramide formation by platelet-activating factor. *Journal of Cell Science*. 2005; 118 (6): 1233 – 1243.
- [122]: Rao LVM & Pendurthi UR. Regulation of tissue factor coagulant activity on cell surfaces. *The Journal of Thrombosis and Haemostasis*. 2012; 10 (11): 2242 – 2253.
- [123]: Sparkenbaugh EM, Chantrathamchart P, Wang S, Jonas W, Kirchhofer D, Gailani D, Gruber A, Kasthuri R, Key NS, Mackman N, Pawlinski R. Excess of heme induces tissue factor-dependant activation of coagulation in mice. *Haematologica*. 2015; 100 (3): 308 – 314.
- [124]: Crutchley DJ & Que BG. Copper-induced tissue factor expression in human monocytic THP-1 cells and its inhibition by antioxidants. *Circulation*. 1995; 92 (2): 238 – 243.
- [125]: Wierzbicki R, Michalska M, Ciemiewski CS. Interaction of fibrinogen with mercury. *Thrombosis Research*. 1983; 30 (6): 579 – 585.
- [126]: Wierzbicki R, Prazanowski M, Michalska M, Krajewska U, Mielicki WP. Disorders in blood coagulation in humans occupationally exposed to mercuric vapours. *The Journal of Trace Elements in Experimental Medicine*. 2002; 15 (1): 21 – 29.

- [127]: Thakur M & Ahmed A. A review of thromboelastography[®]. *International Journal of Perioperative Ultrasound and Applied Technologies*. 2012; 1 (1): 25 – 29.
- [128]: Dias JD, Norem K, Doorneweerd DD, Thurer RL, Popovsky MA & Omert LA. Use of Thromboelastography[®] (TEG[®]) for detection of new oral anticoagulants. *Archives of Pathological and Laboratory Medicine*. 2015; 139: 665 – 673.
- [129]: da Luz LT, Nascimento B & Rizoli S. Thromboelastography[®] (TEG[®]): practical consideration on its clinical use in trauma resuscitation. *Scandinavian Journal of Trauma, Resuscitation and Emergency Medicine*. 2013; 21 (29): 1 – 8.
- [130]: de Villiers S, Swanepoel A, Bester J & Pretorius E. Novel diagnostic and monitoring tool in stroke: an individualised patient-centred precision medicine approach. *Journal of Atherosclerosis and Thrombosis*. 2015; 23 (5): 493 – 504.
- [131]: Scarpelini S, Rhind SG, Nascimento B, Tien H, Shek PN, Peng HT, Huang H, Pinto R, Speers V, Reis M & Rizoli SB. Normal range values for thromboelastography[®] in healthy adult volunteers. *Brazilian Journal of Medical and Biological Research*. 2009; 42 (12): 1210 – 1217.
- [132]: Gonzalez E, Kashuk JL, Moore EE & Silliman CC. Differentiation of enzymatic from platelet hypercoagulability using the novel thromboelastography[®] parameter delta (▲). *Journal of Surgical Research*. 2010; 163 (1): 96 – 101.
- [133]: Wilson AJ, Martin DS, Maddox V, Rattenbury S, Bland D, Bhagani S, Cropley I, Hopkins S, Mephram S, Rodger A, Warren S, Chowdary P & Jacobs M. Thromboelastography[®] in the management of coagulopathy associated with Ebola virus disease. *Clinical Infectious Diseases*. 2016; 62 (5): 610 – 612.

Appendix

Ethical clearance

Patient informed consent form

Declaration of originality

Ethical Clearance

The Research Ethics Committee, Faculty Health Sciences, University of Pretoria complies with ICH-GCP guidelines and has US Federal wide Assurance.

- FWA 00002567, Approved dd 22 May 2002 and Expires 20 Oct 2016.
- IRB 0000 2235 IORG0001762 Approved dd 22/04/2014 and Expires 22/04/2017.



UNIVERSITEIT VAN PRETORIA
UNIVERSITY OF PRETORIA
YUNIBESITHI YA PRETORIA

Faculty of Health Sciences Research Ethics Committee

30/06/2016

Approval Certificate New Application

Ethics Reference No.: 244/2016

Title: The effects of copper, manganese and mercury, alone and in combinations, in an ex vivo model of coagulation

Dear Maxine Janse van Rensburg

The **New Application** as supported by documents specified in your cover letter dated 27/06/2016 for your research received on the 27/06/2016, was approved by the Faculty of Health Sciences Research Ethics Committee on its quorate meeting of 29/06/2016.

Please note the following about your ethics approval:

- Ethics Approval is valid for 2 years
- Please remember to use your protocol number (**244/2016**) on any documents or correspondence with the Research Ethics Committee regarding your research.
- Please note that the Research Ethics Committee may ask further questions, seek additional information, require further modification, or monitor the conduct of your research.

Ethics approval is subject to the following:

- The ethics approval is conditional on the receipt of **6 monthly written Progress Reports**, and
- The ethics approval is conditional on the research being conducted as stipulated by the details of all documents submitted to the Committee. In the event that a further need arises to change who the investigators are, the methods or any other aspect, such changes must be submitted as an Amendment for approval by the Committee.

We wish you the best with your research.

Yours sincerely

Dr R Sommers; MBChB; MMed (Int); MPharMed, PhD
Deputy Chairperson of the Faculty of Health Sciences Research Ethics Committee, University of Pretoria

The Faculty of Health Sciences Research Ethics Committee complies with the SA National Act 61 of 2003 as it pertains to health research and the United States Code of Federal Regulations Title 45 and 46. This committee abides by the ethical norms and principles for research, established by the Declaration of Helsinki, the South African Medical Research Council Guidelines as well as the Guidelines for Ethical Research: Principles Structures and Processes 2004 (Department of Health).

☎ 012 356 3085 ✉ fnsethics@up.ac.za 🌐 <http://www.up.ac.za/healthethics>
✉ Private Bag X323, Arcadia, 0007 - Tswelopele Building, Level 4-59, Gezina, Pretoria

Participant information leaflet and consent form

INFORMATION LEAFLET AND INFORMED CONSENT FOR NON-CLINICAL RESEARCH (e.g. educational, health systems or non- clinical operational research)

TITLE OF STUDY: *The effects of copper, manganese and mercury, alone and in combinations, on the ex vivo model of coagulation*

Dear Participant

You responded to the invitation to participate in a research study. This information leaflet will help you to decide if you want to participate. Before you agree to take part you should fully understand what is involved. If you have any questions that this leaflet does not fully explain, please do not hesitate to ask the investigator.

2) THE NATURE AND PURPOSE OF THIS STUDY

The red blood cell or erythrocyte is the main type of cell found in blood. These cells can be isolated in the laboratory and be used to determine the effect of different compounds on cell functioning and structure. The aim of this study is to identify the effect of heavy metals, copper, manganese and mercury on the erythrocytes. At the same time in the same sample, we can also determine the effect of these metals on the coagulation system by employing various laboratory techniques.

3) EXPLANATION OF PROCEDURES TO BE FOLLOWED

You have volunteered for this study; we would like to confirm the following:

<u>Question</u>	<u>Answer</u>	
	Yes	No
Are you older than 18?		
Are you taking any medication?		
Do you smoke?		

If you are older than 18, are not taking any medication and are a non-smoker we would like to collect 16 mL (four citrate tubes), or about one tablespoon of blood. The tubes of blood will not be labelled with your name but a number will be assigned. This is done to ensure

anonymity. In the laboratory the blood components will be separated from each other and the red blood cells will be exposed to different concentrations of each metal, alone and in combination. The effect on the cells and the coagulation system will then be measured.

4) RISK AND DISCOMFORT INVOLVED

Sampling of the blood may cause some discomfort.

5) POSSIBLE BENEFITS OF THIS STUDY

Although you will not benefit directly from the study, the results of the study will tell us how dangerous are the heavy metals that we might be exposed to on a daily basis.

6) WHAT ARE YOUR RIGHTS AS A PARTICIPANT

Your participation in this study is entirely voluntary. You can refuse to participate or stop at any time during the study without giving any reason. Your withdrawal will not affect you in any way.

7) HAS THE STUDY RECEIVED ETHICAL APPROVAL

This study has received written approval from the Research Ethics Committee of the Faculty of Health Sciences at the University of Pretoria. A copy of the approval letter is available if you wish to have one.

8) INFORMATION AND CONTACT PERSON

Any questions regarding the study can be directed to Ms Maxine Janse van Rensburg on 083 289 2167 or Dr Nanette Oberholzer on 012 319 2533.

9) COMPENSATION

Your participation is voluntary. No compensation will be given for your participation.

10) CONFIDENTIALITY

All information that you give will be kept strictly confidential. Once we have analysed the information no one will be able to identify you. Research reports and articles in scientific journals will not include any information that may identify you.

CONSENT TO PARTICIPATE IN THIS STUDY

I confirm that the person asking my consent to take part in this study has told me about nature, process, risks, discomforts and benefits of the study. I have also received, read and understood the above written information (Information Leaflet and Informed Consent) regarding the study. I am aware that the results of the study, including personal details, will be anonymously processed into research reports. I am participating willingly. I have had time to ask questions and have no objection to participate in the study. I understand that there is no penalty should I wish to discontinue with the study and my withdrawal will not affect me in any way.

I have received a signed copy of this informed consent agreement.

Participant's name (Please print):

Participant's signature: Date:.....

Investigator's name (Please print):

Investigator's signature: Date:.....

Witness's name (Please print):

Witness's signature:..... Date:.....

Declaration of originality

UNIVERSITY OF PRETORIA

FACULTY Health Sciences

DEPARTMENT Anatomy

The Department of Anatomy places specific emphasis on integrity and ethical behaviour with regard to the preparation of all written work to be submitted for academic evaluation.

Although academic personnel will provide you with information regarding reference techniques as well as ways to avoid plagiarism, you also have a responsibility to fulfil in this regard. Should you at any time feel unsure about the requirements, you must consult the lecturer concerned before you submit any written work.

You are guilty of plagiarism when you extract information from a book, article or web page without acknowledging the source and pretend that it is your own work. In truth, you are stealing someone else's property. This doesn't only apply to cases where you quote verbatim, but also when you present someone else's work in a somewhat amended format (paraphrase), or even when you use someone else's deliberation without the necessary acknowledgement. You are not allowed to use another student's previous work. You are furthermore not allowed to let anyone copy or use your work with the intention of presenting it as his/her own.

Students who are guilty of plagiarism will forfeit all credit for the work concerned. In addition, the matter can also be referred to the Committee for Discipline (Students) for a ruling to be made. Plagiarism is considered a serious violation of the University's regulations and may lead to suspension from the University.

For the period that you are a student at the Department of Anatomy, the under-mentioned declaration must accompany all written work to be submitted. No written work will be accepted unless the declaration has been completed and attached.

I (full names) Maxine Janse van Rensburg
Student number 11107139
Subject of the work The effects of copper, manganese and mercury, alone and in combinations, in an ex vivo model of coagulation.

Declaration

1. I understand what plagiarism entails and am aware of the University's policy in this regard.
2. I declare that this dissertation (e.g. essay, report, project, assignment, dissertation, thesis etc) is my own, original work. Where someone else's work was used (whether from a printed source, the internet or any other source) due acknowledgement was given and reference was made according to departmental requirements.
3. I did not make use of another student's previous work and submitted it as my own.
4. I did not allow and will not allow anyone to copy my work with the intention of presenting it as his or her own work.

Signature

